

# **The Synthesis of New Comb Shaped Amphiphilic Polymers**

**Selin Temürlü**

Submitted to the  
Institute of Graduate Studies and Research  
in partial fulfillment of the requirements for the degree of

Master of Science  
in  
Chemistry

Eastern Mediterranean University  
August 2016  
Gazimağusa, North Cyprus

Approval of the Institute of Graduate Studies and Research

---

Prof. Dr. Cem Tanova  
Acting Director

I certify that this thesis satisfies the requirements as a thesis for the degree of Master of Science in Chemistry.

---

Prof. Dr. Mustafa Halilsoy  
Chair, Department of Chemistry

We certify that we have read this thesis and that in our opinion it is fully adequate in scope and quality as a thesis for the degree of Master of Science in Chemistry.

---

Assoc. Prof. Hamit Caner  
Co-Supervisor

---

Prof. Dr. Huriye İcil  
Supervisor

---

Examining Committee

1. Prof. Dr. Huriye İcil

2. Assoc. Prof. Dr. Hamit Caner

3. Asst. Prof. Dr. Süleyman Aşır

4. Asst. Prof. Dr. Nur Aydınlık

5. Asst. Prof. Dr. Hatice N. Hasipoğlu

## ABSTRACT

In recent years, amphiphilic polymers which consist of both hydrophilic and hydrophobic groups, have become more important in the biomedical, biochemical and pharmaceutical fields due to their ability to form supramolecular structure in the aqueous solutions.

In the present thesis, four novel amphiphilic chitosan polymer including different amounts of fluorescent polyimide chromophores with comb shaped structures was successfully synthesized by polycondensation reactions. The synthesized products were analyzed using FTIR, UV-vis and Fluorescence spectroscopy.

Unlike the Chitosan (CS) and Perylene-3,4,9,10- tetracarboxylic dianhydride (PDA), the new products of perylene diimide conjugated chitosan polymer are soluble in most of solvents such as DMSO, DMAc and DMF. The absorption bands were shifted bathochromically in these solvents as solvent polarity increases. The fluorescence quantum yield values of A1PCH, A2PCH, A3PCH and A4PCH were found 0.44, 0.76, 0.50 and 0.56, respectively, in DMF. Among these products, while A2PCH has the highest solubility and fluorescence properties, it has the lowest aggregation.

All of PCH polymers having fluorescent properties can be used in drug delivery systems.

**Keywords:** Amphiphilic polymers, Perylene polymers, Chitosan, Solubility

## ÖZ

Son yıllarda, hidrofobik ve hidrofilik gruplardan oluşan amfifilik polimerler, sulu çözeltilerde süpramoleküler yapı oluşturma yeteneğinden dolayı biyomedikal, biyokimyasal ve eczacılık alanlarında büyük öneme sahiptir.

Bu tezde, farklı miktarlarda floresans aromatik poliimit içeren 4 yeni amfifilik kitosan polimeri tarak şeklinde yapılar ile başarılı bir şekilde polikondensasyon reaksiyonu ile sentezlenmiştir. Sentezlenen ürünler FTIR, UV-vis ve floresans spektroskopisi kullanılarak analiz edilmiştir.

Kitosan (CS) ve perilen-3,4,9,10-tetrakarboksilik dianhidrit (PDA)' in aksine, yeni perilendiimit konjuge kitosan polimerleri DMSO, NMP, DMAc ve DMF gibi bir çok organik çözücü içerisinde çözülmüşlerdir. Bu çözücülerde absorpsiyon bantları çözücü polariteleri arttıkça kırmızıya doğru kaymışlardır. DMF'te A1PCH, A2PCH, A3PCH ve A4PCH'in floresans kuantum verimleri sırasıyla 0.44, 0.76, 0.50 and 0.56 bulunmuştur. Bu ürünler arasında, A2PCH en yüksek çözünürlük ve floresans özelliğine sahipken, en düşük aggregasyona sahiptir.

Floresans özelliğe sahip bütün PCH polimerleri ilaç taşıma sistemlerinde kullanılabilir.

**Anahtar kelimeler:** Amfifilik polimerler, Perilen polimerler, Kitosan ve Çözünürlük.

**‘Success is a journey, not a destination.’**

**Ben Sweetland**

## ACKNOWLEDGEMENT

First and primarily important, with my deepest respect and immense pleasure, I would like to thank my creditable supervisor Prof. Dr. Huriye İcil for her precious contributions, scientific encouragement and the belief that ‘I can do’ during every step my MSc. Programme. Certainly, one of the greatest opportunities that I met with her in my life.

Also I am extremely grateful to my admirable co-supervisor Assoc. Prof. Dr. Hamit Caner for his understanding, patience and tolerance by guiding my life with his knowledge and experiences during the time I spent with him. The second turning point in my life was meet him.

I would like to express my sincere feelings to Dr. Duygu Uzun for her scientific, morale support and spending precious time with me along my Master study. Her guidance helped me in all the time of research and writing of this thesis.

Besides, I would privately like to thank my friends, Sümeyye Kırkınıcı Yılmaz, Basma Basil, Melika Mostafanejad, Meltem Dinleyici, Adamu Abubakar, Courage Akpan and Hengameh Jowzaghi for being with me every moment that I need help.

Finally, I wish to say considerable thanks to my family for their endless support, love and confidence in every moment in my life.

# TABLE OF CONTENTS

ABSTRACT.....	iii
ÖZ.....	iv
ACKNOWLEDGEMENT.....	vi
LIST OF FIGURES.....	x
LIST OF TABLES.....	xiii
LIST OF SCHEMES.....	xv
LIST OF ABBREVIATIONS.....	xvi
1 INTRODUCTION.....	1
1.1 Perylene Diimides and Polymers.....	1
1.2 Chitosan Polymers.....	3
1.3 Amphiphilic Polymers.....	5
2 THEORETICAL.....	8
2.1 Synthesis and Applications of Perylene Diimides and Polymers.....	8
2.1.1 Synthesis.....	8
2.1.2 Applications.....	9
2.2 Synthesis and Applications of Chitosan Polymers.....	11
2.2.1 Synthesis.....	11
2.2.2 Applications.....	12
2.3 Comb Shaped Amphiphilic Polymers.....	13
2.4 Hydrophobic Drug Solubilization.....	14
2.5 Polymer Hydrophobicity and Aggregation.....	15
2.6 Polymeric Micelles for Drug Delivery.....	16
3 EXPERIMENTAL.....	19

3.1 Materials .....	19
3.2 Instruments .....	19
3.3 Methods of Synthesis .....	20
3.4 Synthesis of Perylene-3,4,9,10-tetracarboxylic dimide conjugated Chitosan (A1PCH).....	22
3.5 Synthesis of A2PCH.....	23
3.6 Synthesis of A3PCH.....	24
3.7 Synthesis of A4PCH.....	25
3.8 General Synthetic Mechanism.....	26
4 DATA AND CALCULATIONS .....	29
4.1 Optical and Photochemical Properties .....	29
4.1.1 Molar Absorbance Coefficient.....	29
4.1.2 Fluorescence Quantum Yield ( $\Phi_f$ ).....	32
4.1.3 Half-Width of Selected Absorption Band ( $\Delta\bar{\nu}_{1/2}$ ).....	34
4.1.4 Theoretical Radiative Lifetimes ( $\tau_0$ ).....	38
4.1.5 Theoretical Fluorescence Lifetimes ( $\tau_f$ ).....	41
4.1.6 Fluorescence Rate Constant ( $k_f$ ) .....	43
4.1.7 Rate Constant of Radiationless Deactivation ( $k_d$ ).....	45
4.1.8 Oscillator Strengths ( $f$ ).....	47
4.1.9 Singlet Energies ( $E_s$ ).....	49
5 RESULTS AND DISCUSSIONS .....	90
5.1 Synthesis and Characterization .....	90
5.2 Solubility of PCHs.....	90
5.3 Analysis of FTIR Spectra .....	93
5.4 Absorption and Fluorescence Properties .....	94



5.4.1 Absorption and Fluorescence Properties of A1PCH .....	95
5.4.2 Absorption and Fluorescence Properties of A2PCH .....	96
5.4.3 Absorption and Fluorescence Properties of A3PCH .....	97
5.4.4 Absorption and Fluorescence Properties of A4PCH .....	98
6 CONCLUSION .....	103
REFERENCES.....	105
APPENDIX.....	114
Appendix A: Curriculum Vitae .....	115

## LIST OF FIGURES

Figure 1.1: The Chemical Structure of PDI .....	2
Figure 1.2: Chemical Structures of (a) 100% Chitin and (b) Chitosan .....	4
Figure 1.3: Common Structures of Amphiphilic Polymers .....	5
Figure 1.4: The Structure of Perylene Diimide Conjugated Chitosan .....	7
Figure 2.1: The Basic Structure of Organic Photovoltaic Cell .....	10
Figure 2.2: The Chemical Structure with N-deacetylation of Chitosan .....	11
Figure 2.3: The Structure of Comb Shaped Amphiphilic Polymer .....	14
Figure 2.4: Schematic Illustration of Micelle Formation .....	17
Figure 2.5: A Block Copolymer Micelle .....	18
Figure 4.1: Representantative Plot to Calculate The Half-Width of The A2PCH in DMSO .....	34
Figure 4.2: FT-IR Spectrum of Perylene Dianhydride .....	52
Figure 4.3: FT-IR Spectrum of Chitosan .....	53
Figure 4.4: FT-IR Spectrum of A1PCH .....	54
Figure 4.5: FT-IR Spectrum of A2PCH .....	55
Figure 4.6: FT-IR Spectrum of A3PCH .....	56
Figure 4.7: FT-IR Spectrum of A4PCH .....	57
Figure 4.8: Absorption Spectrum of A1PCH in DMF .....	58
Figure 4.9: Absorption Spectrum of A1PCH in DMAc .....	59
Figure 4.10: Absorption Spectrum of A1PCH in DMSO .....	60
Figure 4.11: Emission Spectrum of A1PCH in DMF .....	61
Figure 4.12: Emission Spectrum of A1PCH in DMAc .....	62
Figure 4.13: Emission Spectrum of A1PCH in DMSO .....	63

Figure 4.14: Absorption Spectra of A1PCH in DMF, DMAc and DMSO .....	64
Figure 4.15: Emission Spectra of A1PCH in DMF, DMAc and DMSO .....	65
Figure 4.16: Absorption Spectrum of A2PCH in DMF .....	66
Figure 4.17: Absorption Spectrum of A2PCH in DMSO .....	67
Figure 4.18: Absorption Spectrum of A2PCH in DMAc .....	68
Figure 4.19: Emission Spectrum of A2PCH in DMF .....	69
Figure 4.20: Emission Spectrum of A2PCH in DMSO .....	70
Figure 4.21: Emission Spectrum of A2PCH in DMAc .....	71
Figure 4.22: Absorption Spectra of A2PCH in DMF, DMSO and DMAc .....	72
Figure 4.23: Emission Spectra of A2PCH in DMF, DMSO and DMAc .....	73
Figure 4.24: Absorption Spectrum of A3PCH in DMF .....	74
Figure 4.25: Absorption Spectrum of A3PCH in DMAc .....	75
Figure 4.26: Absorption Spectrum of A3PCH in DMSO .....	76
Figure 4.27: Emission Spectrum of A3PCH in DMF .....	77
Figure 4.28: Emission Spectrum of A3PCH in DMAc .....	78
Figure 4.29: Emission Spectrum of A3PCH in DMSO .....	79
Figure 4.30: Absorption Spectra of A3PCH in DMF, DMAc and DMSO .....	80
Figure 4.31: Emission Spectra of A3PCH in DMF, DMAc and DMSO .....	81
Figure 4.32: Absorption Spectrum of A4PCH in DMF .....	82
Figure 4.33: Absorption Spectrum of A4PCH in DMAc .....	83
Figure 4.34: Absorption Spectrum of A4PCH in DMSO .....	84
Figure 4.35: Emission Spectrum of A4PCH in DMF .....	85
Figure 4.36: Emission Spectrum of A4PCH in DMAc .....	86
Figure 4.37: Emission Spectrum of A4PCH in DMSO .....	87
Figure 4.38: Absorption Spectra of A4PCH in DMF, DMAc and DMSO .....	88

Figure 4.39: Emission Spectra of A4PCH in DMF, DMAc and DMSO ..... 89

## LIST OF TABLES

Table 4.1: The molar absorption coefficient values of A2PCH in various solvents..	30
Table 4.2: The molar absorption coefficient values of PCHs in various solvents .....	31
Table 4.3: Fluorescence quantum yield data of samples of PCH in DMF.....	34
Table 4.4: The half-width of A2PCH in different solvents.....	36
Table 4.5: The half-widths of other molecules of PCH in different solvents .....	37
Table 4.6: The theoretical radiative lifetimes of A2PCH in different solvents .....	39
Table 4.7: The theoretical radiative lifetimes for all of PCH in different solvents....	40
Table 4.8: The theoretical fluorescence lifetimes for all of PCH in DMF.....	42
Table 4.9: Fluorescence rate constant data of A2PCH .....	43
Table 4.10: Fluorescence rate constant data for all of PCH in different solvents.....	44
Table 4.11: The radiationless deactivation constant data for all of PCH in DMF .....	46
Table 4.12: Oscillator strengths of A2PCH in different solvents .....	47
Table 4.13: The oscillator strength values for all of PCH in different solvents .....	48
Table 4.14: A2PCH's singlet energies in different solvents .....	50
Table 4.15: The singlet energy values for all of PCH in different solvents.....	51
Table 5.1: Solubility properties of PDA and CS.....	91
Table 5.2: Solubility test of A1PCH, A2PCH, A3PCH and A4PCH .....	92
Table 5.3: The UV-vis absorption and fluorescence maximum wavelengths of A1PCH .....	95
Table 5.4: The UV-vis absorption and fluorescence maximum wavelengths of A1PCH .....	96
Table 5.5: The UV-vis absorption and fluorescence maximum wavelengths of A1PCH .....	97

Table 5.6: The UV-vis absorption and fluorescence maximum wavelengths of A4PCH .....	98
Table 5.7: Optical and photochemical properties of A1PCH .....	100
Table 5.8: Optical and photochemical properties of A2PCH .....	100
Table 5.9: Optical and photochemical properties of A3PCH .....	101
Table 5.10: Optical and photochemical properties of A4PCH .....	101
Table 5.11: The comparison of aggregation and fluorescence quantum yield in DMF .....	102

## LIST OF SCHEMES

Scheme 3.1: General mechanism for synthesis of PCH.....	20
Scheme 3.2: General structure of Perylene-3,4,9,10-tetracarboxylicdimide conjugated Chitosan.....	21

## LIST OF ABBREVIATIONS

Å	Armstrong
A	Absorption
A	Electron acceptor
AP	Amphiphilic polymer
AU	Arbitrary unit
Avg.	Average
C	Concentration
CAC	Critical aggregation concentration
CHL	Chloroform
CMC	Critical micelle concentration
CP	Comb polymer
CS	Chitosan
CT	Charge transfer
$\delta$	Chemical shift
D	Electron donor
DA	Deacetylation
DMF	Dimethylformamide
DMSO	Dimethyl sulfoxide
DSSC	Dye sensitized solar cells
Eqn.	Equation
$E_s$	Singlet energy
$\epsilon$	Molar absorption coefficient
$\epsilon_{\max}$	Maximum extinction coefficient/molar absorptivity



$f$	Oscillator strength
FT-IR	Fourier Transform Infrared Spectroscopy
H	Hour
HOMO	Highest Occupied Molecular Orbital
IR	Infrared Spectrum/Spectroscopy
$k_d$	Rate constant of radiationless deactivation
$k_f$	Fluorescence rate constant
$l$	Path length
LUMO	Lowest Unoccupied Molecular Orbital
M	Molar concentration
max	Maximum
min	Minimum
mmol	Millimole
mol	Mol
$\Phi_f$	Fluorescence quantum yield
OFED	Organic Field Effect Transistor
OLED	Organic Light Emitting Diode
PCH	Perylene dimide conjugated chitosan
PDA	Perylene-3,4,9,10-tetracarboxylic dianhydride
PDI	Perylene Diimide
Std.	Standard
$\tau_0$	Theoretical radiative lifetime
$t$	Time
TFAc	Trifluoroacetic acid
UV	Ultraviolet

UV-Vis	Ultraviolet visible light absorption
$\Delta\bar{\nu}_{1/2}$	Half-width (of the selected absorption)
$\nu_{\max}$	Maximum wavenumber
$\lambda_{\text{exc}}$	Excitation wavelength
$\lambda_{\text{em}}$	Emission wavelength

# Chapter 1

## INTRODUCTION

### 1.1. Perylene Diimides and Polymers

Perylene-3,4,9,10-tetracarboxylic dianhydride (PDA) is a very important commercial molecule which has a very wide use especially in the production of photovoltaic cells, solar cells and dye pigments. One of its derivatives is perylene imides. Perylene-3,4,9,10-tetracarboxylic acid diimides, also known as Perylene diimides (PDIs) were first synthesized and characterized by Kardos in 1913. PDIs were first widely used as red colored dyes in textile industry. Recently, it is used as a high performance pigment primarily in the red, violet and black shades. PDI's imide nitrogen atom and its bay core positions provide sites for easy chemical modifications which enhance its versatility. The structure of PDI is shown in Figure 1.1 [1,2].

Aromatic polyimides were first manufactured by Marston Bogert in 1908. High molecular weight aromatic polyimides were synthesized in 1955 through a two stage polycondensation reaction. The importance of polycondensation reaction in the biosynthesis of the most important biopolymers in the field of polymer chemistry has been studied by many researchers [3,4].

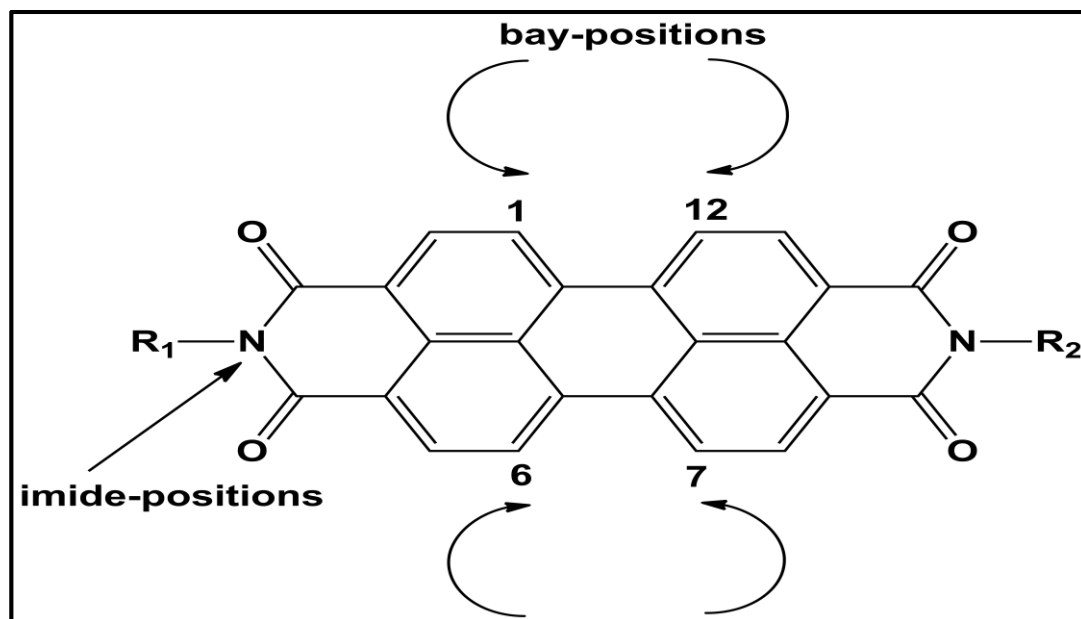


Figure 1.1: The Chemical Structure of PDI [1]

PDI as a significant versatile organic chromophore and its polymer derivatives like perylene-3,4,9,10-tetracarboxylic acid-bis-(N,N'-bis[2-(2-{2-[2-(2-hydroxyethoxy)-ethoxy]-ethoxy]-ethoxy)-ethyl]polyimide (EOPPI) are promising compounds due to their powerful absorption and fluorescence, electroactive and photoactive properties. PDI and its polymer derivatives have unique remarkable thermal, chemical and photochemical stabilities with very high fluorescence efficiencies. As well as positive properties of PDI and its polymer derivatives, they have disadvantages such as weak solubility and aggregation features in most of the well known organic solvents owing to their intermolecular and powerful  $\pi$ - $\pi$  stacking interactions. In addition, they have a low solid-state fluorescence quantum efficiency which is a result of their self-quenching. One of the reasons for reduction in fluorescence intensity is self quenching which is the quenching of excited atom by interaction with atom in ground state. [5,6].

As well known, solubility is a cardinal issue for many biological applications. Hence, syntheses of many perylene polymer derivatives have been synthesized in order to get a better solubility. Icil and her co-workers (2001) reported that perylene derivatives are characterized by excellent water solubility [7].

Perylene dimide molecule and its derivative polymers are utilized as fluorescent probes in a wide range of applications in organic chemistry because perylene polymers form a characteristic excimer in excited states [8]. Kyung and Zimmermann (2012) determined their water solubility and fluorescent properties of perylene dimide derivatives and they showed that perylene derivatives are biocompatible fluorophores which may be useful in biological applications [9].

## **1.2 Chitosan Polymers**

Chitin, next to cellulose, is the second most abundant biopolymer in nature. It was found in the shell of crustaceans, the cuticles of insects and the cell of fungi. Structurally, chitin is a linear chain polymer consisting of  $\beta$ -(1-4)-2-acetamido-2-deoxy-D-glucose units. Chitosan (CS), a natural biopolymer, is the N-deacetylated form of chitin. Unlike the chitin, CS is a random copolymer which consists of amino and acetamido groups. The structures of these two polymers are illustrated below (Figure 1.2). Recent studies show that CS and its derivatives have become beneficial polysaccharides in pharmaceutical and biotechnology areas. They are used as a carrier for drug delivery systems and biomedical material having biocompatible, biodegradable, woundhealing and non-toxic properties [10].

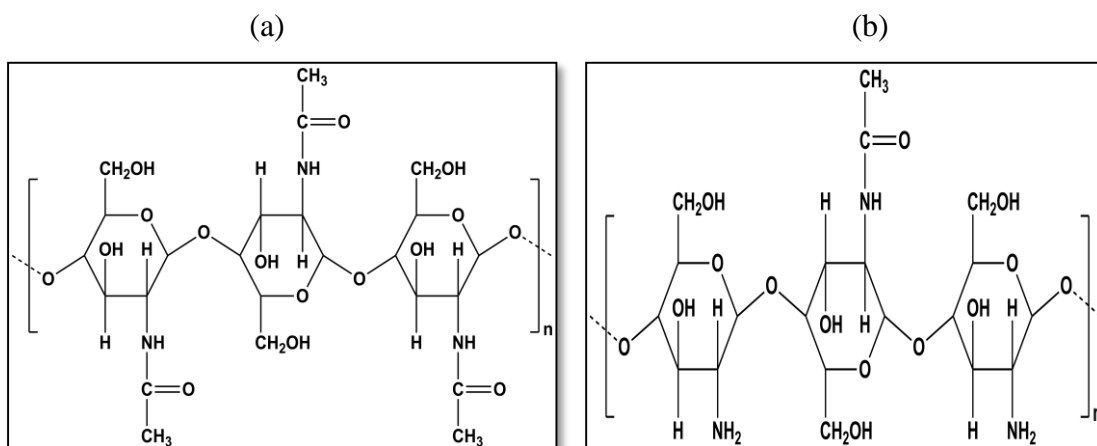


Figure 1.2: Chemical Structures of (a) 100% Chitin and (b) Chitosan [11]

CS has unique solution features when compared to that of chitin. While chitin is not soluble in most of the organic solvents, CS is easily soluble in dilute acetic acid at a pH range of less than or equal to 6 owing to the existence of free amine groups ( $-NH_2$ ) on its backbone. Amine groups can be protonated and become positively charged amino groups ( $-NH_3^+$ ). If the pH increases to values higher than 6, amine groups become deprotonated. Therefore, CS loses its charge and it will be insoluble [11,12].

As a consequence, the application of CS is limited because of its insolubility. It has no amphiphilicity and can not form micelles in water [13]. To overcome its solubility issue, different chemical agents have been used such as cholesterol, stearic acid, deoxychloric acid and methoxy poly(ethylene glycol). Thus, nanoparticles of CS derivatives like cholesterol hydrophobically modified chitosan can be formed. Furthermore, they can be used for delivery of bioactive agents such as anti cancer drug [14].

In recent years, the number of a wide variety of CS related studies in different areas have been increased due to its positive features. Liu et. al (2013) synthesized self assembled nanoparticles for gene delivery based on amphiphilic chitosan derivative and hyaluronic acid [15]. However, CS was used in antimicrobial films to ensure edible protecting layer for food applications by Dutta Works [16].

### 1.3 Amphiphilic Polymers

An amphiphilic polymer is composed of two parts: hydrophilic and hydrophobic groups. Hydrophilic functional groups such as amine and hydroxy sites are usually arranged on a hydrophobic polymer chain, a long hydrocarbon chain most probably forming an amphiphilic structure. The polar hydrophilic part displays a powerful affinity to polar solvent. On the other hand, the nonpolar part is called hydrophobic or lipophilic part. Amphiphilic groups may be bonded in three ways as shown below in Figure 1.3; the polar group (a), the end of the nonpolar chain (b), in the middle of the nonpolar chain (c) [17].

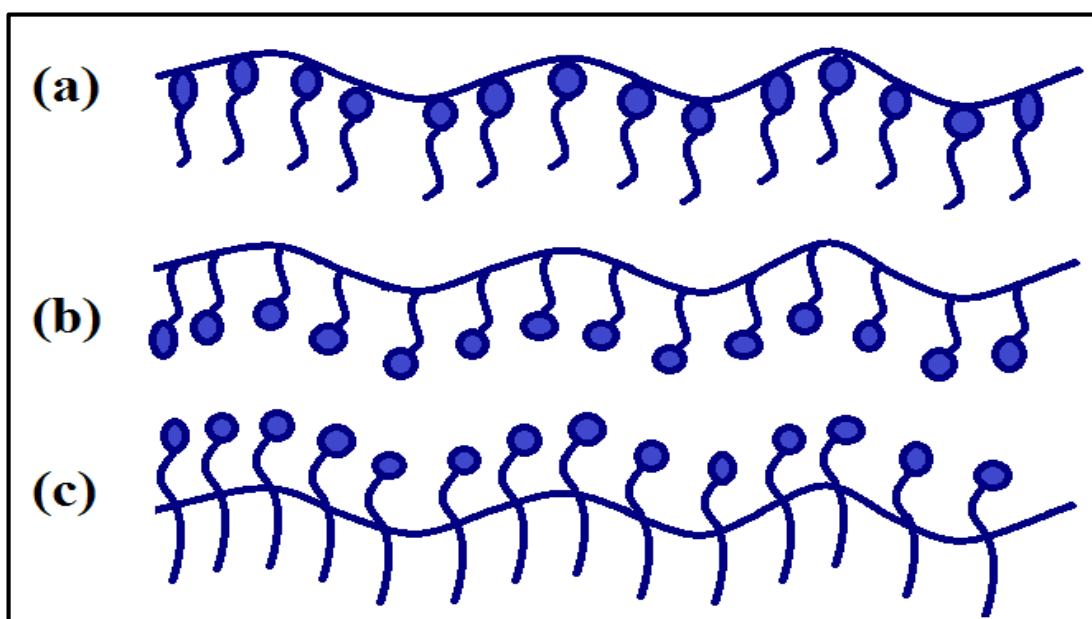


Figure 1.3: Common Structures of Amphiphilic Polymers [17]

During the past decades, biocompatible polymers have fascinated more interest in biomedical and biotechnological applications. Nowadays, amphiphilic polymers have been employed both for hydrophilic and hydrophobic drugs as a potential drug carrier [18].

Amphiphilic polymers (APs) have two types of characteristic core shell structure. The hydrophobic section that behaves as an inner core and hydrophilic section that behaves as an outer core. Furthermore, an AP can form micelle structures through these two segments in the aqueous medium by self assembly. Polymeric micelles can be utilized as drug delivery appliances especially for lowly water soluble drug [19]. Ji et. al (2015) reported that an AP could form an aggregate in water because of its hydrophobic groups [20].

APs has a critical aggregation concentration (CAC) in an aqueous solution [21]. Nowadays, the number of studies on APs have increased due to their positive unique properties. APs have various applications in literature. APs have been used as a biocatalyst [22]. Their aggregation behaviour and emulsification characteristics have been investigated and characterized [23]. They have other uses in lipase immobilization [24] and phase transfer reaction [25].



The cardinal aim of this study is to synthesize an amphiphilic chitosan polymer having a comb shaped fluorescent peryleneimide chromophores for biomedical applications. The synthesized products were characterized by FTIR, UV-Vis, Emission spectrum techniques. The photophysical and optical properties were also explored.

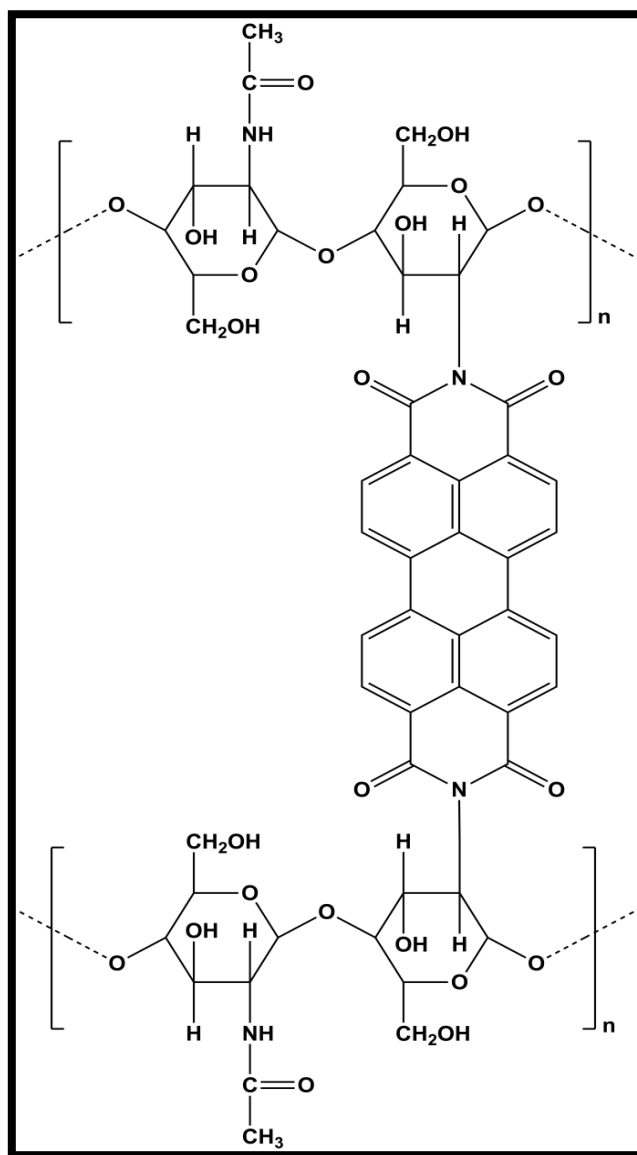


Figure 1.4: The Structure of Perylene Diimide Conjugated Chitosan

## Chapter 2

### THEORETICAL

#### 2.1 Synthesis and Applications of Perylene Diimides and Polymers

##### 2.1.1 Synthesis

Aromatic polyimides first invented by Marston Bogert in 1908. High molecular weight aromatic polyimides were synthesized in 1955 via a two stage polycondensation reaction of pyromellitic dianhydride with diamines [3].

In synthesis of polymers, polycondensation reactions have a great importance. At present, many polymers are produced industrially by polycondensation reactions are produced in amount of millions of tonnes such as polyurethanes, polyamides and polyesters. Many polymers obtained by polycondensation reactions are produced in amount of thousands of tonnes such as polycarbonates, unsaturated polyesters and polyoxides. Eventually, the manufacturing of the last group of polymers such as polyimides, polybenzimidazoles and also a lot of semiconducting and light sensitive polymers is on a little scale but this group of polymers are irreplaceable [26].

Condensation processes occur when two or more molecules react with each other with simultaneous loss of small molecules such as water or ammonia. Polyimides have been synthesized from aromatic anhydrides and aliphatic/aromatic diamides. The condensation reactions occur by two stages. In the first stage, a noncyclized, soluble, linear high polymer is formed by a fast reaction in a suitable polar solvent at

low temperatures. Secondly, polymer can be generated into an appropriate shape and after that cyclized by heating at high temperatures [27].

Also, The examples about the synthesis of perylene containing polyimides by polycondensation reactions are given in the literature. Damaceanu et. al (2012) reported that poly(ether-peryleneimide)s and also Rusu and his co-workers (2010) synthesized perylene containing copolyimides by polycondensation reaction at high temperature [28,29].

### **2.1.2 Applications**

Since perylene and its derivatives were discovered by Kardos, Perylene dimide (PDI) utilized in industry such as red dyes and pigments. PDIs are inexpensive, nontoxic and powerful compounds. As well as these properties, they have individual features such as strong absorption and emission and high fluorescence quantum yield near unit.

In the last decades, PDI derivatives became more important due to their thermally, chemically and photostable fluorescent dyes properties. All these particular features made it useful in the areas of photovoltaic cells, chemical sensors, electroluminescent devices, organic field effect transistors (OFETs), organic light emitting diodes (OLED), fluorescent solar collectors, laser dyes, light emitting diodes and fluorescent labelling in medicine and biochemistry [30].

P-type (electron donating) semiconductors are the most of organic conducting materials. Unlike these, PDIs as an electron acceptor because of easily reduction at low potential, are defined as n-type semiconductors in which the major charge

carriers are their conduction band. So, their high electron affinity is associated with using in PV cells [31].

Beside these wonderful features, PDIs have the disadvantage on its solubility properties due to planarity and extended  $\pi$ -conjugation. They are causing strong intermolecular  $\pi$ - $\pi$  interactions in the aggregated state and the loss of exciton energy is unavoidable. Therefore, by the aggregated PDIs, the photovoltaic conversion is limited. For reducing molecular aggregation in PDI, there are two different methods. First one is introducing bulky substituents at the imide nitrogen and second method uses the present core position [32]. Singh and his co-workers (2014) researched the role of aggregation effects in the performance of PDI and strived to prevent the aggregation of PDI for use in Organic Photovoltaic devices through these methods [33].

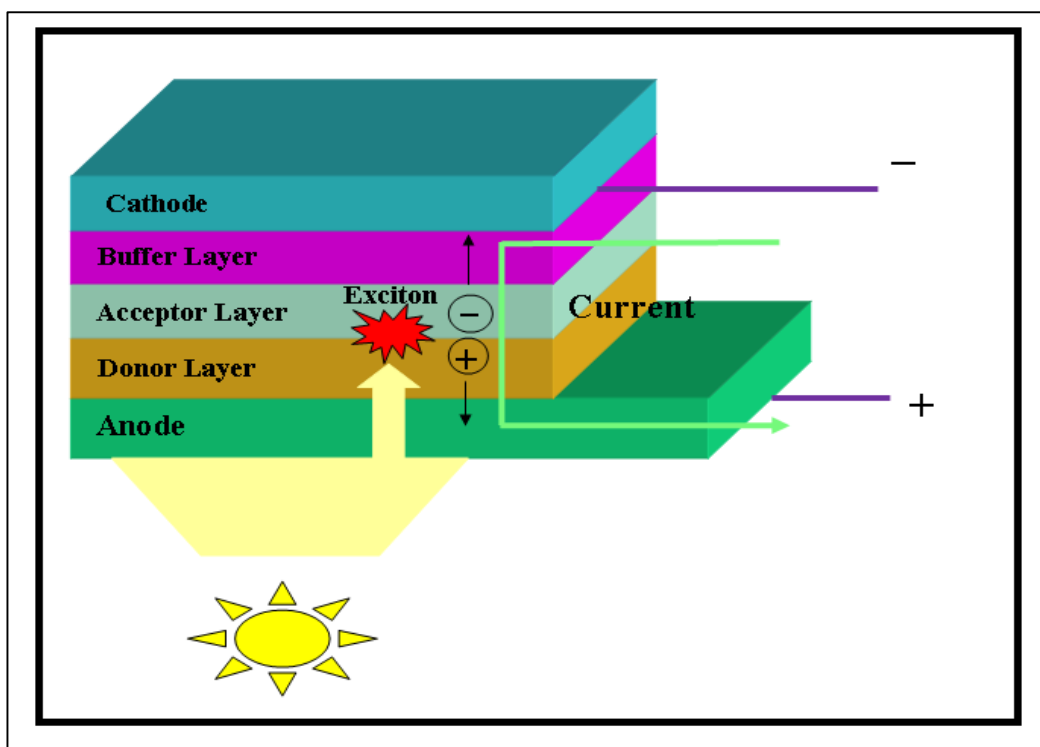


Figure 2.1: The Basic Structure of Organic Photovoltaic Cell [34]

## 2.2 Synthesis and Applications of Chitosan Polymers

### 2.2.1 Synthesis

Chitosan, the second most abundant polysaccharide after cellulose in the nature is a N-deacetylated derivative of chitin. Henry Braconnot, the French scientist, discovered chitin in a mushroom in 1811. Later, Chitin was isolated from insect shells in 1820. Reuget discovered a product. When chitin was boiled in potassium hydroxide. This new product was then named as ‘Chitosan’ in 1894 by Hoppe-Seyler [35].

Chitosan is ocured from the alkaline deacetylation (DA) of chitin. The chemical structure with N-deacetylation of chitosan was given as below (Figure 2.2). The acetyl groups belonging to chitin are hydrolyzed. These hydrolyzed acetyl groups are converted to free amino groups. This stage causes the degree of deacetylation (DD) or the ratio of deacetylated to acetylated part. The DA reaction can be implemented chemically with concentrated NaOH solution and is effected by temperature and time. DD is frequently used to describe chitosan besides other features such as molecular weight, crystallinity and distribution of amine groups [36].

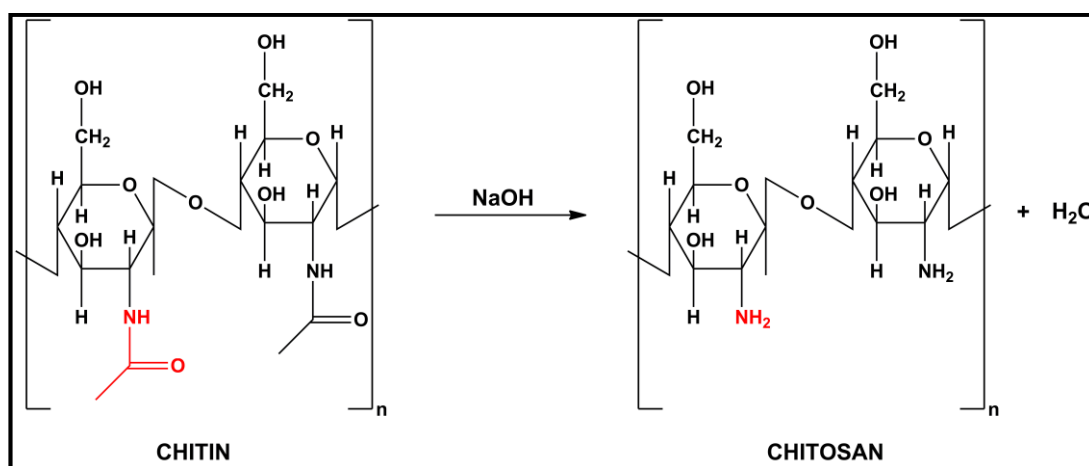


Figure 2.2: The Chemical Structure with N-Deacetylation of Chitosan [37]

The DA process nearly never achieves 100%. It is generally accepted that the molecules are called chitin or chitosan according to degree of deacetylation, e.g. if degree of deacetylation is higher than 50, this molecule is called chitosan or vice versa [38,39]. The studies on this topic are given in the literature. Caner (2002) indicated that the molecule of CS has different conformations due to degree of deacetylation. When the degree of deacetylation is high, CS will be highly charged and it will have a more flexible conformation. If the degree of deacetylation is low, the CS molecule will be lower charged and adopts a more coiled shape [11].

### **2.2.2 Applications**

Unlike chitin, it is easier to work with Chitosan because of the protonation of amine groups in dilute acid solution. Chitosan has many beneficial properties related to the degree of deacetylation such as bioactivity, biodegradability, biocompatibility, hydrophilicity, anti-bacterial property, ion-chelating ability [40]. All these characteristic properties make it more convenient for a broad range of fields such as biomedical engineering, pharmacy, dentistry, biotechnology, chemistry, cosmetics, textile and agriculture. Also chitosan is used like an adsorbent to clean different wastewaters [41].

Recently, Chitosan began to use for photovoltaic applications. Because, Chitosan which has a range of functional ionizable groups such as free amine groups on acetylated units, carboxyl groups on the acetylated units and the hydroxyl groups on the carbons, is an electron donating bio-polyelectrolyte. In this way, Chitosan can be used as electrically sensitive cationic polymer for solar cell [42].

Additionally, for biomedical and pharmaceutical applications chitosan is accepted as one of the most significant polymer. In recent years, the number of studies in these areas increased with Chitosan. Otherwise, in the future, Fluorescent Chitosan polymer is applied as multifunctional photonic equipment such as biochips, biolabels, drug delivery system and bioelectronics. Ozdal (2009) synthesized a novel perylene substituted fluorescent Chitosan polymer [43].

### **2.3 Comb Shaped Amphiphilic Polymers**

In recent years, amphiphilic polymers, which consist of both hydrophobic and hydrophilic parts, have become more valuable in the biomedical and biochemical field. Because in the aqueous surroundings APs have the ability to create supramolecular structures. While the hydrophilic parts maintain the polymer solubility in water, hydrophobic groups responsible from the formation of self assembly in the aqueous surroundings because of hydrophobic interaction. The majority of APs are block copolymers which are form with hydrophilic and hydrophobic monomers through copolymerisation. Polyamines such as polyethylenimine, poly-lysine and carbohydrate polymers such as chitosan have been used to create comb shaped amphiphilic polymers for drug and gene delivery [44].

A comb polymer (CP) consist of a backbone (polymer A) with attached side chains (polymer B). Generally, backbone and side chains have different chemical features because of depending on with their molecular weight distribution (MWD). It is accepted that every monomeric unit on the backbone polymer A has a reactive side and this reactive side can interact with the coreactive chain end on the side chains polymer B. In this way, CPs are formed with several numbers of added side chains

on the backbone. Schematic representation of the comb polymer is shown in figure (Figure 2.3) [45].

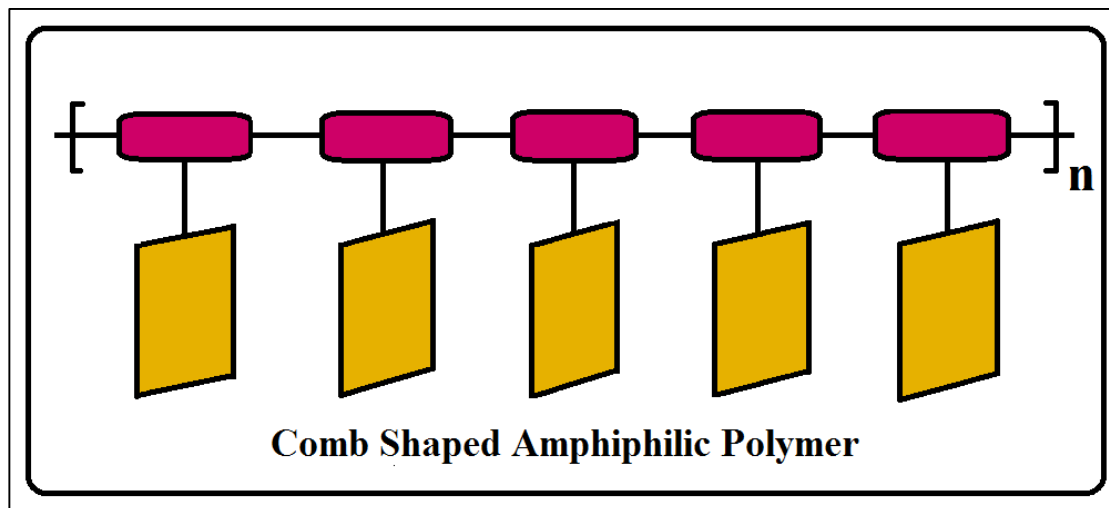


Figure 2.3: The Structure of Comb Shaped Amphiphilic Polymer

## 2.4 Hydrophobic Drug Solubilization

In pharmaceutical industry, most of drugs have a significant problem regarding to poor water solubility. In order to overcome this problem, a new method, Drug delivery system is developed by scientist [46]. Various techniques were improved such as using suitable solvents, hydrophobically modified polysaccharides, dendrimers and surfactant micelles [47].

At the end of the last years, The interest was increased to both amphiphilic block copolymers as drug delivery agent and polymeric micelles for increasing the solubility. There have been a few researches about solubilization of hydrophobic drugs using block copolymeric micelles. Block copolymers which have amphiphilic property, show a wide solubility difference amongst their hydrophilic and



hydrophobic groups. The solubilization of doxorubicin-conjugated block copolymer micelles was investigated in 1990 by Professor Kataoka's group [48].

The importance of Chitosan is increasing daily in drug delivery system due to its properties, but there is a substantial limit on its application for instance high molecular weight and viscosity. The other point which limits applications of CS is its low water solubility at neutral pH. Fortunately, it is possible to overcome these drawbacks by employing low molecular weight of chitosan (LMWC). LMWC is soluble in a broad pH range in water and it can be more easy way to conduct a chemical modification [49]. In shortly, when amphiphilic polymers as chitosan present at low concentrations in an aqueous system, they act to decrease the interfacial free energy and then at concentrations above the critical micelle concentration (CMC), amphiphilic molecules are dissolved in water. Thus they can form aggregates in solution [50].

## **2.5 Polymer Hydrophobicity and Aggregation**

Biopolymers have been used as hydrophilic backbone for a long time in order to create amphiphilic polymers by hydrophobic substitution. Aggregation of APs has a growing importance day by day in biological and pharmaceutical applications. Nowadays, solution features of block copolymer, self-aggregates or hydrophobized water-soluble polymers have been broadly reported [51]. Polymer behavior is extremely complicated in solution because polymers can take different forms due to the large size and low molecular weight. Besides, there is a relationship between aggregation, hydrophobicity and solubility in solution [52].

Hydrophobic effect is the driving force for amphiphilic self-assembling systems. In 1970s, it was emerged by Charles Tanford. Hydrophobic molecule tend to aggregate in water, so minimizing their surface contact [53]. Therefore, aggregation processes are occurred largely by hydrophobic effect. At this point, there is a very important issue that interactions between aromatic groups have a significant role in aggregation [54].

For the formation of aggregation, there is a critical value called as Critical Aggregation Concentration (CAC), an important parameter in investigation the aggregation behaviors of biological macromolecules. If the concentration is below the CAC, aggregation is not observed and it is usually lower than Critical Micelle Concentration [55].

## **2.6 Polymeric Micelles for Drug Delivery**

In the past years, polymeric micelles self-assembled from amphiphilic block copolymers have been thoroughly explored in aqueous solution. Their unique features as drug delivery carriers have been identified such as the high stability, good biocompatibility, high drug loading, etc. Additionally, these micelles can also be used as anticancer drug vehicles [56].

Micelle is an aggregation of surfactant molecules in a colloidal suspension and they are dynamic structures, which means that they are constantly balanced with free monomers. At average number of monomers to form micelle may also called as aggregation number. Micelles generally consist of 50-200 monomers [57]. Schematic drawing of micelle formation is shown below (Figure 2.4 ).

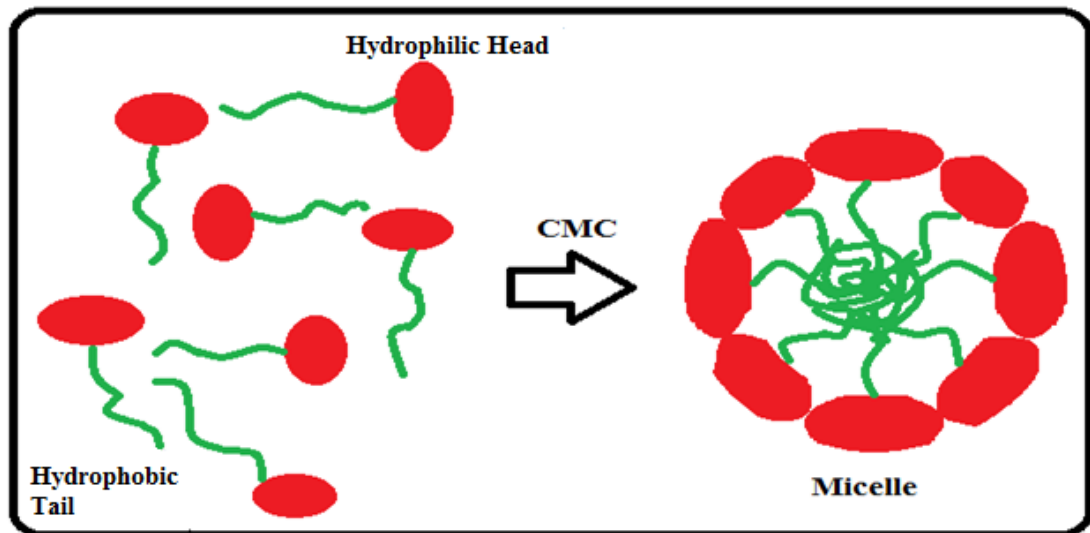


Figure 2.4: Schematic Illustration of Micelle Formation [50]

In early 1980, Polymeric micelles were first found as drug delivery carriers by Helmut Ringsdorf. Amphiphilic copolymers formed hydrophobic and hydrophilic segments create micelles and normally they are spherically shaped core-shell structure with the hydrophilic outer shell and the hydrophobic inner core in aqueous solutions. A simple illustration of a block copolymer micelle is given in Figure 2.5. As well as, other micelle types are known e.g. like worm micelle. Polymeric micelle sizes are commonly in the range of 10-100 nm. There are tasks of these core and shell segments of micelles. While hydrophilic shells compose steric barriers to micelle aggregation and provide micelle solubility in aqueous media, Hydrophobic cores act as drug reservoirs [58].

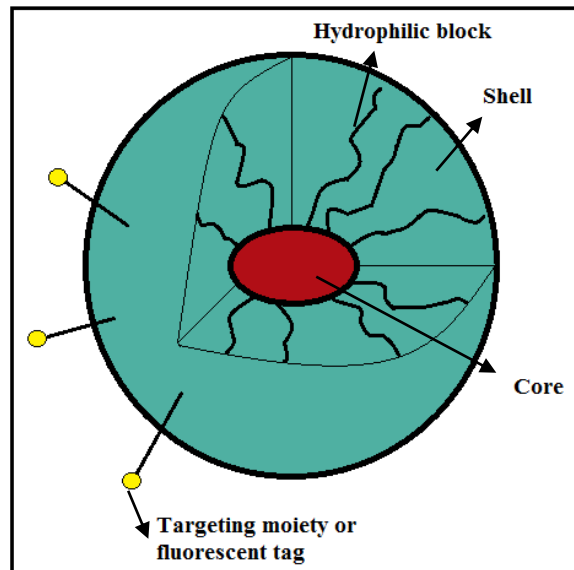


Figure 2.5: A Block Copolymer Micelle [58]

Polymeric micelles can usually dissolve depending on Critical Micelle Concentration (CMC). For the formation and the static stability of polymeric micelle, CMC is an important parameter. When the concentration is higher than CMC, amphiphilic polymers can form micelle in aqueous environment and when diluted below this CMC, micelles may collapse. CMC is principally controllable by the length of hydrophobic part. If the length is longer, CMC value will be lower [57].

## Chapter 3

### EXPERIMENTAL

#### 3.1 Materials

Low molecular weight chitosan (LMWC), Perylene-3,4,9,10-tetracarboxylic dianhydride (PDA), zinc acetate and isoquinoline were supplied from Aldrich. For spectroscopic measurements, all the chemicals were purified before processing. Additionally, before application, according to the standard literature procedure, all used solvents were distilled [59].

#### 3.2 Instruments

##### Fourier Transform Infrared Spectra

The samples were analyzed using a JASCO FT-IR spectrophotometer through KBr disks.

##### Ultraviolet Absorption Spectra (UV-vis)

The samples in different solvents were investigated utilizing a Varian Cary-100 Spectrophotometer.

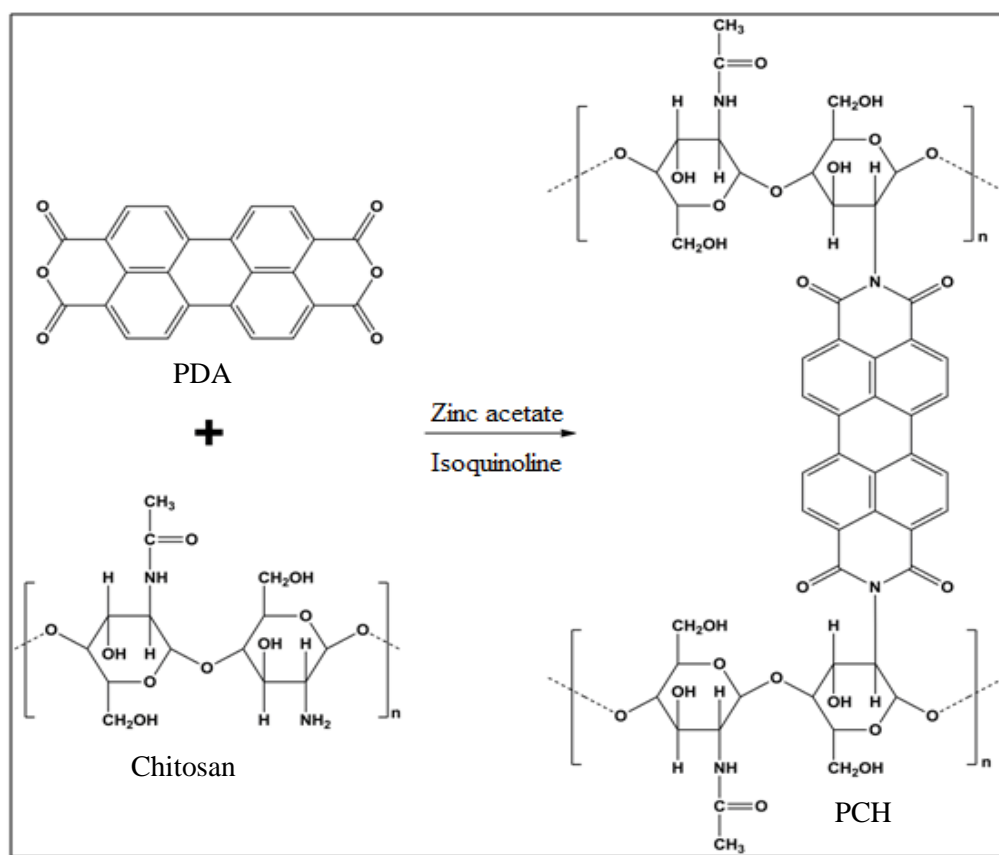
##### Emission Spectra

The samples in various solvents were investigated with a Varian Cary Eclipse Spectrophotometer.

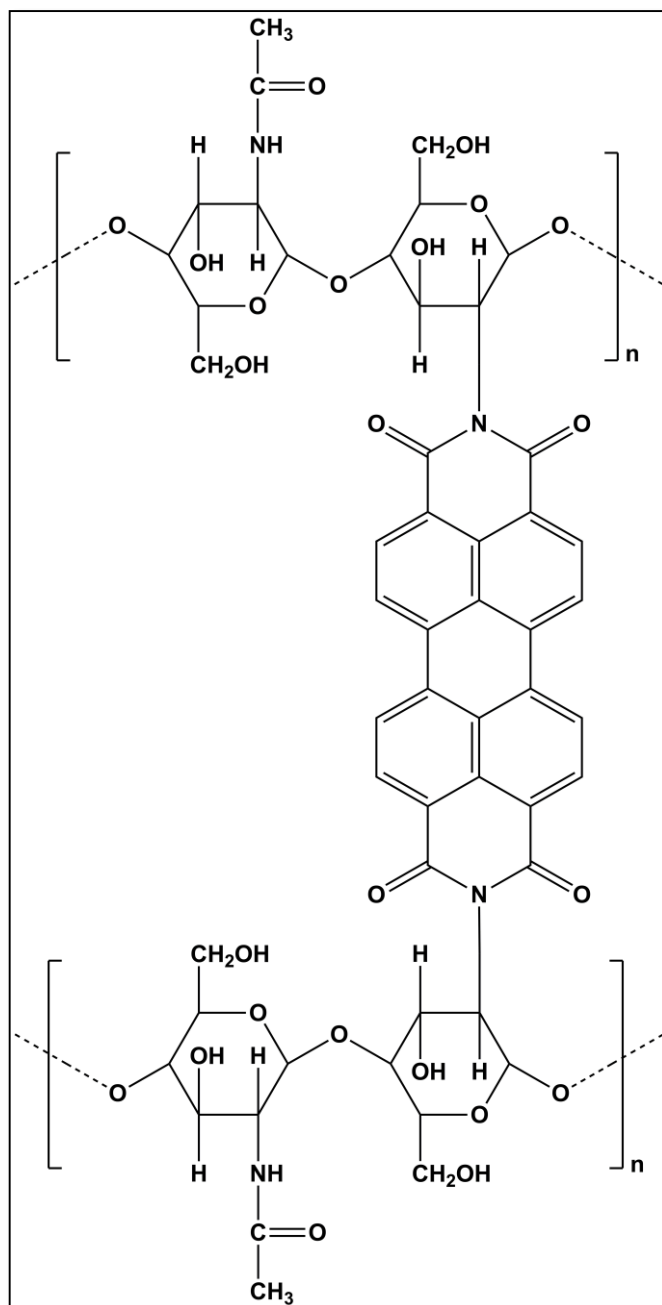
### 3.3 Methods of Synthesis

This chapter describes the synthesis of Perylene-3,4,9,10-tetracarboxylic dimide conjugated Chitosan (PCH).

PCH was successfully synthesized via polycondensation reactions of PDA and LMWC using isoquinoline and zinc acetate. General reaction is illustrated below in Scheme 3.1.



Scheme 3.1: General mechanism for synthesis of PCH



Scheme 3.2: General structure of of Perylene-3,4,9,10-tetracarboxylic dimide conjugated Chitosan

### **3.4 Synthesis of Perylene-3,4,9,10-tetracarboxylic dimide conjugated**

#### **Chitosan (A1PCH)**

PDA (0.064 mmol, 25 mg), 75-85% deacetylated LMWC (4,9640 mmol, 0.8 g), zinc acetate (0.05 mmol, 12 mg) were heated and stirred in carefully dried solvent isoquinoline (40 ml) under argon atmosphere at 80°C for 4 h, at 120 °C for 6 h, at 140 °C for 3 h, at 160 °C for 26 h, at 180 °C for 15 h, at 190 °C for 10 h and 200 °C for 14 h, respectively. The warm solution at 70°C was transferred into 400 ml of cold methanol. The obtained precipitate which filtered with distilled methanol was washed thoroughly 8 times for 1 h with acetic acid (1%) in order to remove excess chitosan homopolymer and the resulting precipitate filtered by suction filtration. The synthesized crude product purified by Soxhlet extraction with pure water for 40 h and chloroform for 140 h. The pure product was dried by vacuum oven. The compound termed as A1PCH was obtained as a dark powder.

**Color:** Black

**IR (KBr, cm<sup>-1</sup>):**  $\nu$  = 3424, 3050, 2919, 2651, 1700, 1682, 1655, 1639, 1591, 1359, 1273, 1019, 810, 753.

**UV-vis (DMF) ( $\lambda_{\max}/\text{nm}$ ):** 456, 487, 523

**Fluorescence (DMF)( $\lambda_{\max}/\text{nm}$ ):** 536, 576, 626

**$\Phi_f$  (Fluorescence Quantum Yield):** 0.44



### 3.5 Synthesis of A2PCH

PDA (0.129 mmol, 51 mg), 75-85% deacetylated LMWC (5.012mmol, 0.802), zinc acetate (0.05 mmol, 12 mg) were heated and stirred in carefully dried solvent isoquinoline (40 ml) under argon atmosphere at 80°C for 4 h, at 120 °C for 6 h, at 140 °C for 3 h, at 160 °C for 26 h, at 180 °C for 15 h, at 190°C for 5 h and 200 °C for 10 h, respectively. The warm solution at 70°C was transferred into 400 ml of cold methanol. The obtained precipitate which filtered with distilled methanol was washed thoroughly 8 times for 1 h with acetic acid (1%) in order to remove excess chitosan homopolymer and the resulting precipitate was filtered by suction filtration. The synthesized crude product purified by Soxhlet extraction with pure water for 36 h and chloroform for 85 h. The pure product was dried by vacuum oven. The compound term as A2PCH was obtained as a dark powder.

**Color:** Black

**IR (KBr, cm<sup>-1</sup>):**  $\nu$  = 3427, 3061, 2922, 2855, 1701, 1659, 1592, 1360, 1228, 1201, 1021, 810, 746.

**UV-vis (DMF) ( $\lambda_{\text{max}}$ /nm):** 458, 488, 524

**Fluorescence (DMF)( $\lambda_{\text{max}}$ /nm):** 535, 575, 627

**$\Phi_f$  (Fluorescence Quantum Yield):** 0.76

### 3.6 Synthesis of A3PCH

PDA (0.255 mmol, 100 mg), 75-85% deacetylated LMWC (4.9640 mmol, 0.8 g), zinc acetate (0.05 mmol, 12 mg) were heated and stirred in carefully dried solvent isoquinoline (40 ml) under argon atmosphere at 80°C for 4 h, at 120 °C for 6 hours, at 140 °C for 3 h, at 160 °C for 26 h, at 180 °C for 15 h, at 190 °C for 10 h and 200 °C for 35 h, respectively. The warm solution at 70°C was transferred into 400 ml of cold methanol. The obtained precipitate that filtered with distilled methanol was washed thoroughly 8 times for 1 h with acetic acid (1%) in order to remove excess chitosan homopolymer. Again the resulting precipitate was filtered by suction filtration. The synthesized crude product purified by Soxhlet extraction with pure water for 25 h and chloroform for 140 h. The pure product was dried by vacuum oven. The compound term as A3PCH was obtained as a dark powder.

**Color:** Black

**IR (KBr, cm<sup>-1</sup>):**  $\nu$  =3449, 3160, 3051, 2921, 2854, 1688, 1592, 1577, 1361, 1275, 810, 748.

**UV-vis (DMF) ( $\lambda_{\text{max}}$ /nm):** 460, 488, 523

**Fluorescence (DMF)( $\lambda_{\text{max}}$ /nm):** 534, 575, 624

**$\Phi_f$  (Fluorescence Quantum Yield):** 0.50

### 3.7 Synthesis of A4PCH

PDA (0.382 mmol, 150 mg), 75-85% deacetylated LMWC (4.9640 mmol, 0.8 g), zinc acetate (0.05 mmol, 13 mg) were heated and stirred in carefully dried solvent isoquinoline (40 ml) under argon atmosphere at 80°C for 4 h, at 120 °C for 6 h, at 140 °C for 3 h, at 160 °C for 26 h, at 180 °C for 15 h, at 190 °C for 5 h and 200 °C for 64 h, respectively. The warm solution at 70°C was transferred into 400 ml of cold methanol. The obtained precipitate which filtered with distilled methanol was washed thoroughly 8 times for 1 h with acetic acid (1%) in order to remove excess chitosan homopolymer and again the resulting precipitate was filtered by suction filtration. In order to eliminate the existing PDA, the product stirred with 5 % NaOH solution for 1 hour at room temperature and after, it refluxed for 1 h at 110 °C. Then, it purified by Soxhlet extraction with pure water for 96 h and chloroform for 16 h. The pure product was dried by vacuum oven. The compound term as A4PCH was obtained as a dark powder.

**Color:** Black

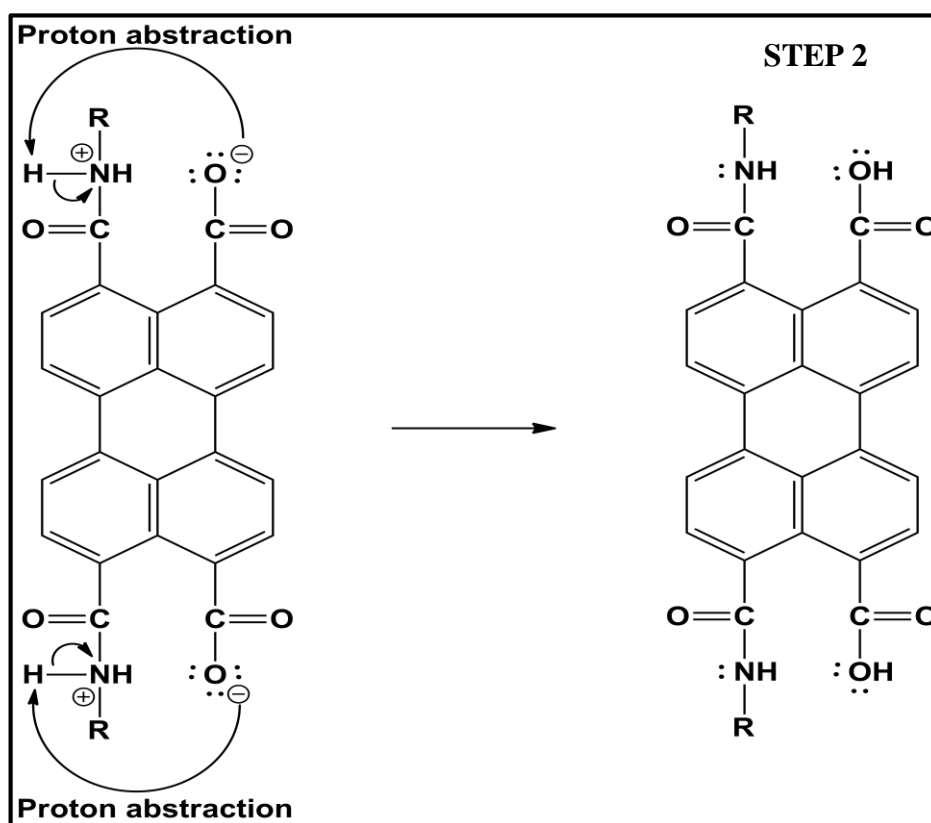
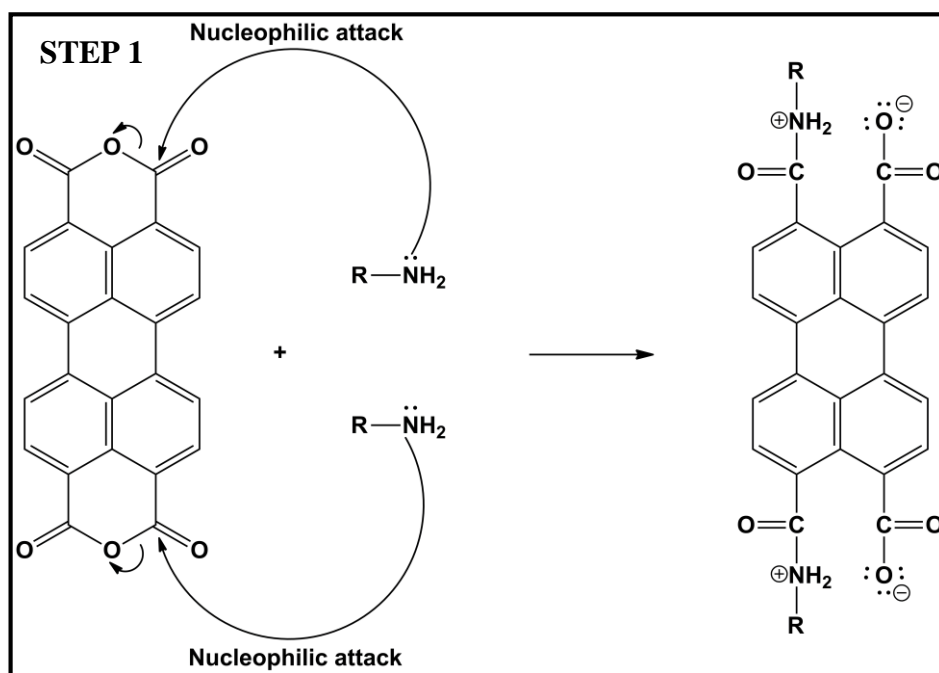
**IR (KBr, cm<sup>-1</sup>):**  $\nu$  =3425, 3053, 2963, 2922, 2850, 1692, 1591, 1576, 1360, 1275, 1224, 1023, 810, 747

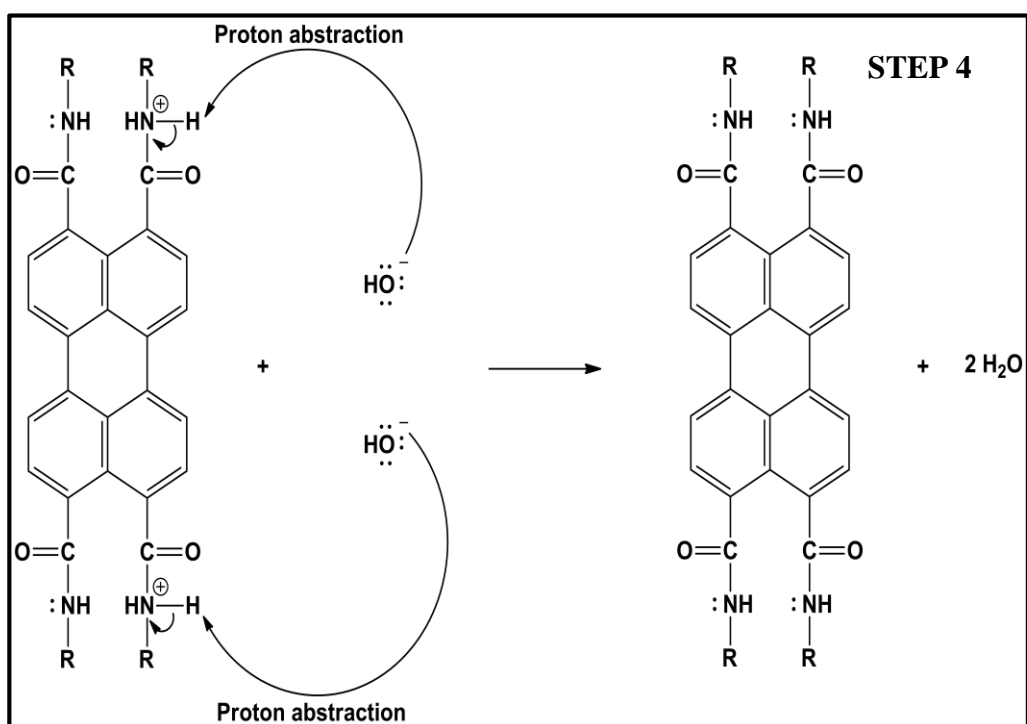
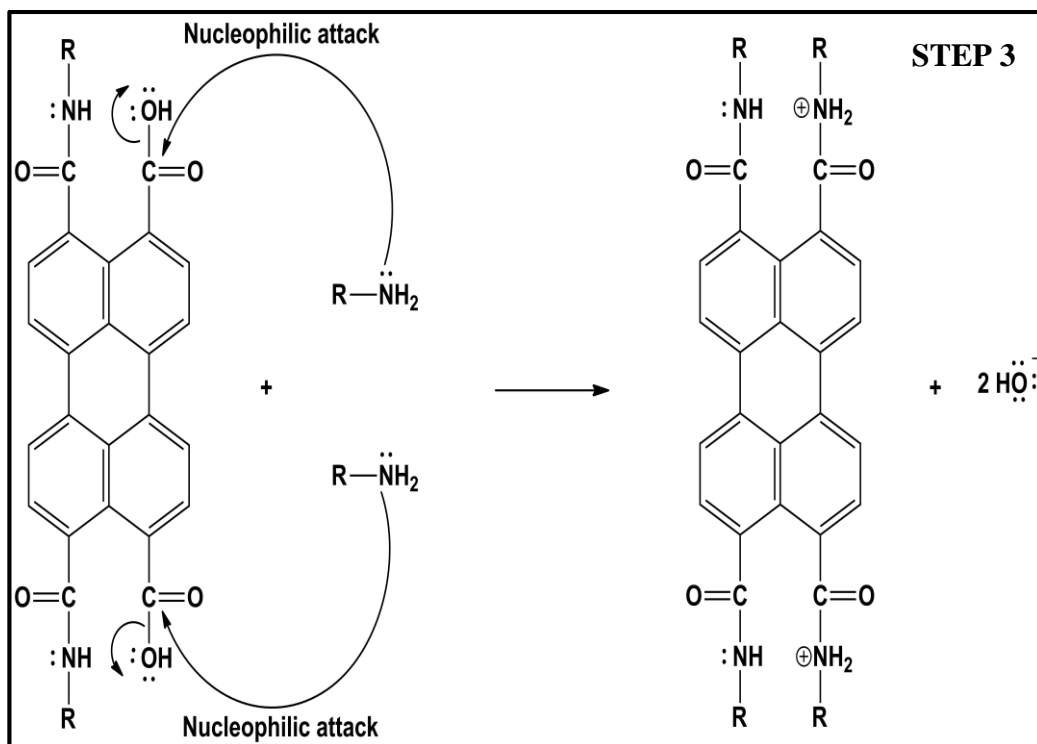
**UV-vis (DMF) ( $\lambda_{\text{max}}$ /nm):** 460, 488, 523

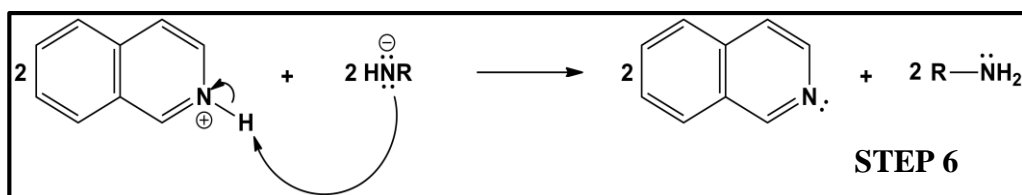
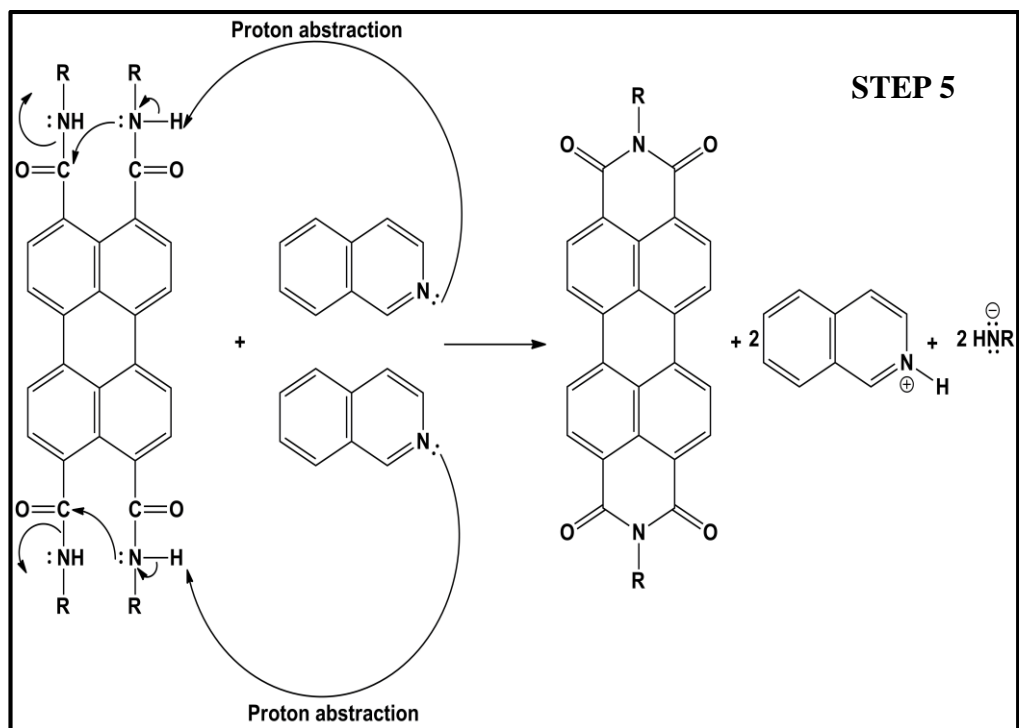
**Fluorescence (DMF)( $\lambda_{\text{max}}$ /nm):** 535, 575, 625

**$\Phi_f$  (Fluorescence Quantum Yield):** 0.56

### 3.8 General Synthetic Mechanism







## Chapter 4

### DATA AND CALCULATIONS

#### 4.1 Optical and Photochemical Properties

##### 4.1.1 Molar Absorption Coefficient

An absorption spectrum is associated with two parameters; maximum absorption wavelength ( $\lambda_{\max}$ ) and the molar extinction coefficient ( $\epsilon_{\max}$ ). The Molar Absorption Coefficient which is also known as the Molar Extinction Coefficient, is a constant for a particular substance dissolved in a given solvent and measured at a selected wavelength. The relation between  $\epsilon$ , sample concentration ( $c$ ) and thickness ( $l$ ) was expressed in the equation of absorbance by the Lambert Beer Law. Solutions of different concentrations of the synthesized compound were prepared and the maximum absorption wavelength was found for each concentration. Finally,  $\epsilon$  was calculated from the plot of absorbance and concentration. The equation 4.1 was given below [60].

$$\epsilon_{\max} = \frac{A}{C.l} \quad \text{Eqn. 4.1}$$

Where;

**$\epsilon_{\max}$** : Molar extinction coefficient

**A**: Absorbance

**c**: Concentration

**l**: Cell length

From the plot;

$$\text{Slope} = 49000$$

So;

$$\epsilon_{\text{max}} = 49000 \text{ L. mol}^{-1} \cdot \text{cm}^{-1}$$

Table 4.1: The molar absorption coefficient values of A2PCH in various solvents

<b>Solvent</b>	<b><math>\lambda_{\text{max}}</math> (nm)</b>	<b>Absorbance</b>	<b><math>\epsilon_{\text{max}}</math> (<math>\text{M}^{-1} \cdot \text{cm}^{-1}</math>)</b>
<b>DMSO</b>	526	0.49	49000
<b>DMF</b>	524	0.139	13900
<b>DMAc</b>	523	0.29	29000

The values of  $\epsilon_{\text{max}}$  were calculated in the same way for the others three compounds of PCH in varied solvents.



Table 4.2: The molar absorption coefficient values of PCHs in various solvents

Solvent	A1PCH			A3PCH			A4PCH		
	$\lambda_{\max}$ (nm)	Absorbance	$\epsilon_{\max}$ ( $M^{-1} \cdot cm^{-1}$ )	$\lambda_{\max}$ (nm)	Absorbance	$\epsilon_{\max}$ ( $M^{-1} \cdot cm^{-1}$ )	$\lambda_{\max}$ (nm)	Absorbance	$\epsilon_{\max}$ ( $M^{-1} \cdot cm^{-1}$ )
DMSO	526	0.309	30900	525	0.427	42700	526	0.3	30000
DMF	523	0.55	55000	523	0.47	47000	523	0.3	30000
DMAc	522	0.157	15700	522	0.22	22000	524	0.3	30000

#### 4.1.2 Fluorescence Quantum Yield ( $\Phi_f$ )

Fluorescence which is the emission of light after absorption by a matter, occurs when one atom or molecule relaxes from electronic excited state ( $S_1$ ) to ground state ( $S_0$ ). The fluorescence quantum yield gives us information about efficiency of the fluorescence process. Also,  $\Phi_f$  is described as the ratio of the number of photons emitted to the number of photons absorbed. For relative quantum yield measurements, there are two approaches: a single point and a comparative method. Comparative method was developed by Williams and et. al. [61]. Comparative method is more time consuming than a single point method but it provides much higher accuracy by comparing the integrated fluorescence intensity and the absorption for sample and reference.

$\Phi_f$  is often calculated by comparing a sample with a reference substance of known quantum yield ( $\Phi_r$ ) such that

$$\Phi_f(U) = \Phi_r \times \frac{A_r}{A_u} \times \frac{S_u}{S_r} \times \left[ \frac{n_u}{n_r} \right]^2 \quad \text{Eqn. 4.2}$$

Where,

$\Phi_f(U)$ : Fluorescence quantum yield of unknown

$\Phi_r$ : Fluorescence quantum yield of reference

$A_r$ : Absorbance of the reference at the excitation wavelength

$A_u$ : Absorbance of the unknown excitation wavelength

$S_r$ : The integrated emission area across the band of unknown

$n_r$ : Refractive index of reference solvent

$n_u$ : Refractive index of unknown solvent

$\Phi_f$  of samples was calculated in different solvents using N,N'-bis(dodecyl)-3, 4, 9, 10- perylenebis(discaroximide) in chloroform as reference at  $\lambda_{\max}= 485$  nm. Therefore, the unknown sample were excited at 485 nm according to reference sample [62].

**$\Phi_f$  calculation of A2PCH in DMF :**

$$\Phi_r = 1$$

$$A_r = 0.1003$$

$$A_u = 0.1002$$

$$S_u = 661.386$$

$$S_r = 851.81$$

$$n_r = 1.4458$$

$$n_u = 1.4305$$

$$\Phi_f(U) = 1 \times \frac{0.1003}{0.1002} \times \frac{661.386}{851.81} \times \left[ \frac{1.4305}{1.4458} \right]^2$$

$$\Phi_f(U) = 1 \times 1.001 \times 0.7764 \times 0.9789$$

$$\Phi_f(U) = 0.76$$

In DMF, the fluorescence quantum yield of the samples of PCH were calculated based on the similar process and the obtained  $\Phi_f$  values were given in the Table 4.3.

Table 4.3: Fluorescence quantum yield data of samples of PCH in DMF

	A1PCH	A2PCH	A3PCH	A4PCH
Solvent	$\Phi_f$	$\Phi_f$	$\Phi_f$	$\Phi_f$
DMF	0.44	0.76	0.50	0.56

#### 4.1.3 Half-Width of Selected Absorption Band ( $\Delta\bar{\nu}_{1/2}$ )

The half-widths of the molecules are important to define the theoretical lifetime. It was determined by using equation 4.3.

$$\Delta\bar{\nu}_{1/2} = \bar{\nu}_1 - \bar{\nu}_2 \quad \text{Eqn.4.3}$$

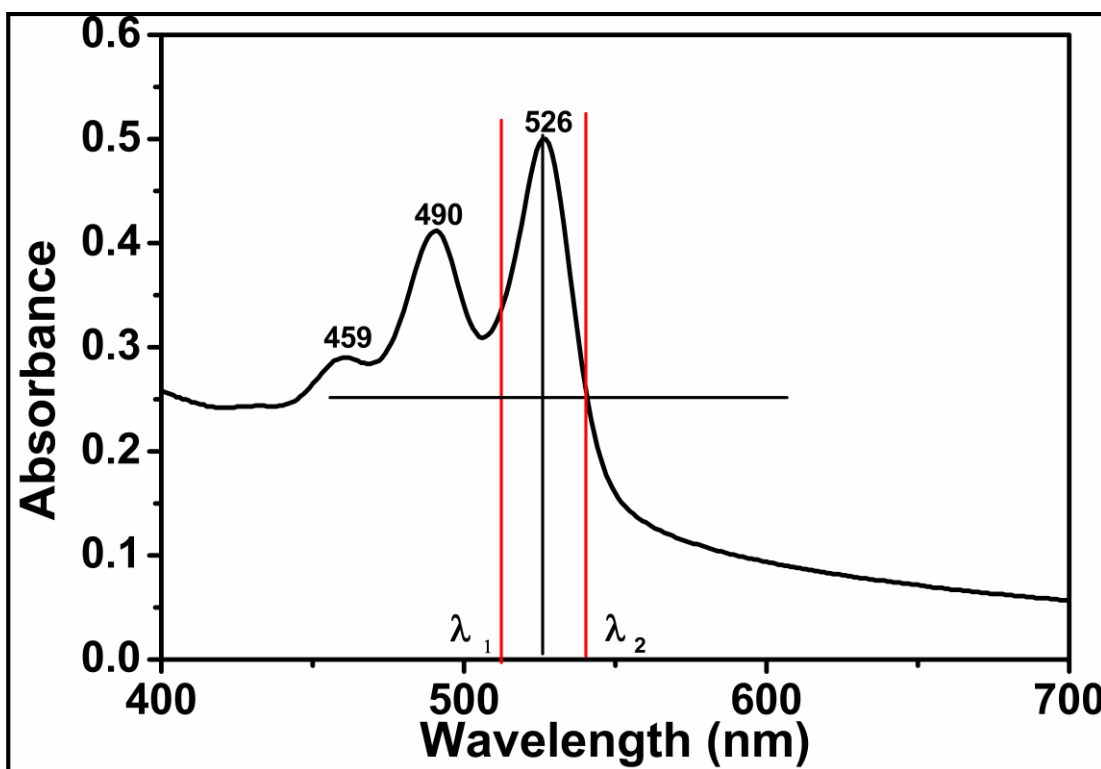


Figure 4.1: Representantative plot to calculate the Half-width of the A2PCH in DMSO

As shown in Figure 4.1;

$$\lambda_{\max} = 526 \text{ nm}$$

Absorption of half-width = 0.29

$$\lambda_1 = 520 \text{ nm}$$

$$\lambda_2 = 534 \text{ nm}$$

$$\lambda_1 = 520 \text{ nm} \times \frac{10^{-9} \text{ m}}{1 \text{ nm}} \times \frac{1 \text{ cm}}{10^{-2} \text{ m}} = 5.2 \times 10^{-5} \text{ cm}$$

$$\bar{\nu}_1 = \frac{1}{\lambda_1} = \frac{1}{5.2 \times 10^{-5}} = 19230.77 \text{ cm}^{-1}$$

$$\lambda_2 = 534 \text{ nm} \times \frac{10^{-9} \text{ m}}{1 \text{ nm}} \times \frac{1 \text{ cm}}{10^{-2} \text{ m}} = 5.34 \times 10^{-5} \text{ cm}$$

$$\bar{\nu}_2 = \frac{1}{\lambda_2} = \frac{1}{5.34 \times 10^{-5}} = 18726.59 \text{ cm}^{-1}$$

$$\Delta\bar{\nu}_{1/2} = \bar{\nu}_1 - \bar{\nu}_2 = 19230.77 - 18726.59$$

$$= 504.18 \text{ cm}^{-1}$$

Similarly, The Half-widths of A2PCH have been calculated in different solvents. The obtained datas are summarized in Table 4.4.

Table 4.4: The half-width of A2PCH in different solvents

<b>Solvent</b>	$\lambda_{\max}$ <b>(nm)</b>	$\lambda_1$ <b>(nm)</b>	$\lambda_2$ <b>(nm)</b>	$\Delta\bar{\nu}_{1/2}$ <b>(cm<sup>-1</sup>)</b>
<b>DMSO</b>	526	520	534	504.18
<b>DMF</b>	524	516	528	440.45
<b>DMAc</b>	523	517	530	474.43

Also, the Half-width values calculated with same solvents for other PCH molecules and are summarized in Table 4.5.

Table 4.5: The half-widths of other molecules of PCH in different solvents

Solvents	A1PCH				A3PCH				A4PCH			
	$\lambda_{\max}$ (nm)	$\lambda_1$ (nm)	$\lambda_2$ (nm)	$\Delta\bar{\nu}_{1/2}$ ( $\text{cm}^{-1}$ )	$\lambda_{\max}$ (nm)	$\lambda_1$ (nm)	$\lambda_2$ (nm)	$\Delta\bar{\nu}_{1/2}$ ( $\text{cm}^{-1}$ )	$\lambda_{\max}$ (nm)	$\lambda_1$ (nm)	$\lambda_2$ (nm)	$\Delta\bar{\nu}_{1/2}$ ( $\text{cm}^{-1}$ )
<b>DMSO</b>	526	513	540	974.6	525	516	544	997.5	526	514	539	902.4
<b>DMAc</b>	522	507	538	1136.5	522	512	538	943.9	524	510	538	1020.5
<b>DMF</b>	523	508	542	1234.8	523	509	535	954.8	523	523	538	533.1

#### 4.1.4 Theoretical Radiative Lifetimes ( $\tau_0$ )

The Theoretical Radiative Lifetimes of all compounds were figured out based on the following equation 4.4.

$$\tau_0 = \frac{3.5 \times 10^8}{\bar{\nu}_{\max}^2 \times \varepsilon_{\max} \times \Delta\bar{\nu}_{1/2}} \quad \text{Eqn: 4.4}$$

#### $\tau_0$ calculation of A2PCH in DMSO:

$$\lambda_{\max} = 526 \text{ nm} \times \frac{10^{-9} \text{ m}}{1 \text{ nm}} \times \frac{100 \text{ cm}}{1 \text{ m}} = 5.26 \times 10^{-5} \text{ cm}$$

$$\bar{\nu}_{\max} = \frac{1}{5.26 \times 10^{-5}} = 19011.41 \text{ cm}^{-1}$$

$$\bar{\nu}_{\max}^2 = 3.61 \times 10^8 \text{ cm}^{-2}$$

#### The Theoretical Radiative Lifetime;

$$\tau_0 = \frac{3.5 \times 10^8}{\bar{\nu}_{\max}^2 \times \varepsilon_{\max} \times \Delta\bar{\nu}_{1/2}} = \frac{3.5 \times 10^8}{3.61 \times 10^8 \times 49000 \times 504.18}$$

$$\tau_0 = 3.92 \times 10^{-8} \text{ s} = 39.2 \text{ ns}$$

Similarly,  $\tau_0$  of A2PCH were calculated in different solvents and the data obtained are presented below in Table 4.6.



Table 4.6: The theoretical radiative lifetimes of A2PCH in different solvents

<b>Solvent</b>	$\lambda_{\max}$ (nm)	$\epsilon_{\max}$ (M <sup>-1</sup> . cm <sup>-1</sup> )	$\bar{\nu}_{\max}^2$ (cm <sup>-2</sup> )	$\Delta\bar{\nu}_{1/2}$ (cm <sup>-1</sup> )	$\tau_0$ (ns)
<b>DMSO</b>	526	49000	3.61 x 10 <sup>8</sup>	504.18	39.2
<b>DMF</b>	524	13900	3.64 x 10 <sup>8</sup>	440.45	157
<b>DMAc</b>	523	29000	3.65 x 10 <sup>8</sup>	474.43	69.7

Also, the theoretical radiative lifetimes calculated with same solvents for other PCH molecules and are summarized below in Table 4.7.

Table 4.7: The theoretical radiative lifetimes for all of PCH in different solvents

Solvents	A1PCH				A3PCH				A4PCH			
	$\epsilon_{\max}$ (M <sup>-1</sup> . cm <sup>-1</sup> )	$\bar{\nu}^2_{\max}$ (cm <sup>-2</sup> )	$\Delta\bar{\nu}_{1/2}$ (cm <sup>-1</sup> )	$\tau_0$ (ns)	$\epsilon_{\max}$ (M <sup>-1</sup> . cm <sup>-1</sup> )	$\bar{\nu}^2_{\max}$ (cm <sup>-2</sup> )	$\Delta\bar{\nu}_{1/2}$ (cm <sup>-1</sup> )	$\tau_0$ (ns)	$\epsilon_{\max}$ (M <sup>-1</sup> . cm <sup>-1</sup> )	$\bar{\nu}^2_{\max}$ (cm <sup>-2</sup> )	$\Delta\bar{\nu}_{1/2}$ (cm <sup>-1</sup> )	$\tau_0$ (ns)
<b>DMSO</b>	30900	3.65x 10 <sup>8</sup>	974.7	32.2	42700	3.63x 10 <sup>8</sup>	997.5	22.6	30000	3.61x 10 <sup>8</sup>	902.4	35.8
<b>DMAc</b>	15700	3.67x 10 <sup>8</sup>	1136.5	53.4	22000	3.67x 10 <sup>8</sup>	943.9	45.9	30000	3.64x 10 <sup>8</sup>	1020.5	31.4
<b>DMF</b>	55000	3.65x 10 <sup>8</sup>	1234.8	14.1	47000	3.65x 10 <sup>8</sup>	954.8	21.4	30000	3.65x 10 <sup>8</sup>	533.1	59.9

#### 4.1.5 Theoretical Fluorescence Lifetimes ( $\tau_f$ )

Fluorescence Lifetime was calculated by using Turro's formula shown below [63].

$$\tau_f = \tau_0 \cdot \Phi_f \quad \text{Eqn: 4.5}$$

**The theoretical fluorescence lifetime of A2PCH in DMF:**

$$\tau_f = \tau_0 \cdot \Phi_f$$

$$\tau_0 = 157 \text{ ns}$$

$$\tau_f = \tau_0 \cdot \Phi_f = 157 \times 0.76 = 119.32 \text{ ns}$$

However, the theoretical fluorescence lifetimes calculated with same solvent for other PCH molecules and are summarized in Table 4.8.

Table 4.8: The theoretical fluorescence lifetimes for all of PCH in DMF

Solvent	A1PCH			A3PCH			A4PCH		
	$\Phi_f$	$\tau_0$ (ns)	$\tau_f$ (ns)	$\Phi_f$	$\tau_0$ (ns)	$\tau_f$ (ns)	$\Phi_f$	$\tau_0$ (ns)	$\tau_f$ (ns)
DMF	0.44	14.1	6.204	0.50	21.4	10.7	0.56	59.9	33.54

#### 4.1.6 Fluorescence Rate Constant ( $k_f$ )

The fluorescence rate constant was calculated according to following Turro's equation.

$$k_f = \frac{1}{\tau_0} \quad \text{Eqn: 4.6}$$

#### The fluorescence rate constant of A2PCH calculation in DMSO

$$k_f = \frac{1}{\tau_0}$$

$$k_f = \frac{1}{39.2 \text{ ns}} = \frac{1}{3.9 \times 10^{-8} \text{ s}}$$

$$k_f = 2.56 \times 10^7 \text{ s}^{-1}$$

Similarly, Fluorescence rate constants of A2PCH were detected in different solvents and the obtained data were represented in Table 4.9.

Table 4.9: Fluorescence rate constant data of A2PCH

Solvent	$\lambda_{\text{max}}$ (nm)	$\tau_0$ (ns)	$k_f$ ( $\text{s}^{-1}$ )
DMSO	526	39.2	$2.56 \times 10^7$
DMF	524	157	$6.37 \times 10^6$
DMAc	523	69.7	$1.43 \times 10^7$

Also, the fluorescence rate constant calculated with same solvents for other PCH molecules and are summarized in Table 4.10.

Table 4.10: Fluorescence rate constant data for all of PCH in different solvents

Solvent	A1PCH		A3PCH		A4PCH	
	$\tau_0$ (ns)	$k_f$ (s <sup>-1</sup> )	$\tau_0$ (ns)	$k_f$ (s <sup>-1</sup> )	$\tau_0$ (ns)	$k_f$ (s <sup>-1</sup> )
DMSO	32.2	3.10 x 10 <sup>7</sup>	22.6	4.42 x 10 <sup>7</sup>	35.8	2.79 x 10 <sup>7</sup>
DMF	14.1	7.08 x 10 <sup>7</sup>	21.4	4.67 x 10 <sup>7</sup>	59.9	1.67 x 10 <sup>7</sup>
DMAc	53.4	1.87 x 10 <sup>7</sup>	45.9	2.18 x 10 <sup>7</sup>	31.4	3.18 x 10 <sup>7</sup>

#### 4.1.7 Rate Constant of Radiationless Deactivation ( $k_d$ )

The radiationless deactivation's rate constants of A2PCH were calculated by using the following equation.

$$k_d = \frac{k_f}{\Phi_f} - k_f \quad \text{Eqn: 4.7}$$

**The radiationless deactivation's rate constant calculations for A2PCH in DMF:**

$$k_d = \frac{k_f}{\Phi_f} - k_f$$

$$k_d = \frac{6.37 \times 10^6}{0.76} - 6.37 \times 10^6$$

$$k_d = 2.01 \times 10^6 \text{s}^{-1}$$

At the same time, the radiationless deactivation rate constant calculated with same solvents for other PCH molecules and are summarized in Table 4.11.

Table 4.11: The radiationless deactivation constant data for all of PCH in DMF

Solvent	A1PCH			A3PCH			A4PCH		
	$\Phi_f$	$k_f$ (s <sup>-1</sup> )	$k_d$ (s <sup>-1</sup> )	$\Phi_f$	$k_f$ (s <sup>-1</sup> )	$k_d$ (s <sup>-1</sup> )	$\Phi_f$	$k_f$ (s <sup>-1</sup> )	$k_d$ (s <sup>-1</sup> )
DMF	0.44	7.08 x 10 <sup>7</sup>	9.01x 10 <sup>7</sup>	0.50	4.67x 10 <sup>7</sup>	4.67 x 10 <sup>7</sup>	0.56	1.67 x 10 <sup>7</sup>	1.31 x 10 <sup>7</sup>



#### 4.1.8 Oscillator Strengths ( $f$ )

Oscillator strength which indicates the electronic transition capacity within atomic and molecular systems, is a dimensionless quantity. The oscillator strengths of CPDIs were determined by using the equation given below.

$$f = 4.32 \times 10^{-9} \times \Delta\bar{\nu}_{1/2} \times \epsilon_{\max} \quad \text{Eqn: 4.8}$$

##### Oscillator Strength of A2PCH in DMSO:

$$f = 4.32 \times 10^{-9} \times \Delta\bar{\nu}_{1/2} \times \epsilon_{\max}$$

$$f = 4.32 \times 10^{-9} \times 504.18 \times 49000 \quad f = 0.11$$

In the same way, A2PCH's Strengths of Oscillator were calculated in different solvents and the obtained datas were described in the Table 4.12.

Table 4.12: Oscillator strengths of A2PCH in different solvents

Solvent	$\Delta\bar{\nu}_{1/2}$ ( $\text{cm}^{-1}$ )	$\epsilon_{\max}$ ( $\text{L.mol}^{-1} \cdot \text{cm}^{-1}$ )	$f$
DMSO	504.18	49000	0.11
DMF	440.45	13900	0.03
DMAc	474.43	29000	0.06

Besides, The oscillator strengths calculated according to same method in the identical solvents for other PCH molecules and the obtained results were summarized in Table 4.13.

Table 4.13: The oscillator strength values for all of PCH in different solvents

Solvent	A1PCH			A3PCH			A4PCH		
	$\Delta\bar{\nu}_{1/2}$ ( $\text{cm}^{-1}$ )	$\epsilon_{\text{max}}$ ( $\text{L.mol}^{-1} \cdot \text{cm}^{-1}$ )	$f$	$\Delta\bar{\nu}_{1/2}$ ( $\text{cm}^{-1}$ )	$\epsilon_{\text{max}}$ ( $\text{L.mol}^{-1} \cdot \text{cm}^{-1}$ )	$f$	$\Delta\bar{\nu}_{1/2}$ ( $\text{cm}^{-1}$ )	$\epsilon_{\text{max}}$ ( $\text{L.mol}^{-1} \cdot \text{cm}^{-1}$ )	$f$
<b>DMSO</b>	974.66	30900	0.13	997.49	42700	0.18	902.38	30000	0.12
<b>DMF</b>	1234.85	55000	0.29	954.77	47000	0.19	533.09	30000	0.07
<b>DMAc</b>	1136.5	15700	0.08	943.89	22000	0.09	1020.48	30000	0.13

#### 4.1.9 Singlet Energies ( $E_s$ )

For a chromophore, Singlet energy is a required the minimum quantity of energy. Chromophore gets induced from ground state to excited state through this singlet energy. The formula below is used to calculate singlet energies according to Turro's equation.

$$E_s = \frac{2.86 \times 10^5}{\lambda_{max}} \quad \text{Eqn: 4.9}$$

#### $E_s$ calculation of A2PCH in DMSO:

At  $\lambda_{max}$  : 526 nm

$$\lambda_{max} \quad 526 \text{ nm} \times \frac{10^{-9} \text{ m}}{1 \text{ nm}} \times \frac{1 \text{ \AA}}{10^{-10} \text{ m}} = 5260 \text{ \AA}$$

$$E_s = \frac{2.86 \times 10^5}{\lambda_{max}}$$

$$E_s = 54.37 \text{ kcal. mol}^{-1}$$

A2PCH's singlet energies were calculated using the same method as above in most of different solvents and all the results are summarized in the following Table 4.14.

Table 4.14: A2PCH's singlet energies in different solvents

<b>Solvent</b>	$\lambda_{\max}$ (Å)	<b>E<sub>s</sub></b> (kcal. mol <sup>-1</sup> )
<b>DMSO</b>	5260	54.37
<b>DMF</b>	5240	54.58
<b>DMAc</b>	5230	54.68

Additionally, The singlet energies calculated using identical solvents for other A2PCH molecules with same method and the obtained results were summarized in Table 4.15.

Table 4.15: The singlet energy values for all of PCH in different solvents

Solvent	A1PCH		A3PCH		A4PCH	
	$\lambda_{\max}$ (Å)	$E_s$ (kcal. mol <sup>-1</sup> )	$\lambda_{\max}$ (Å)	$E_s$ (kcal. mol <sup>-1</sup> )	$\lambda_{\max}$ (Å)	$E_s$ (kcal. mol <sup>-1</sup> )
DMF	5230	54.68	5230	54.68	5230	54.68
DMSO	5260	43.37	5250	54.78	5260	43.37
DMAc	5220	54.79	5220	54.79	5240	54.58

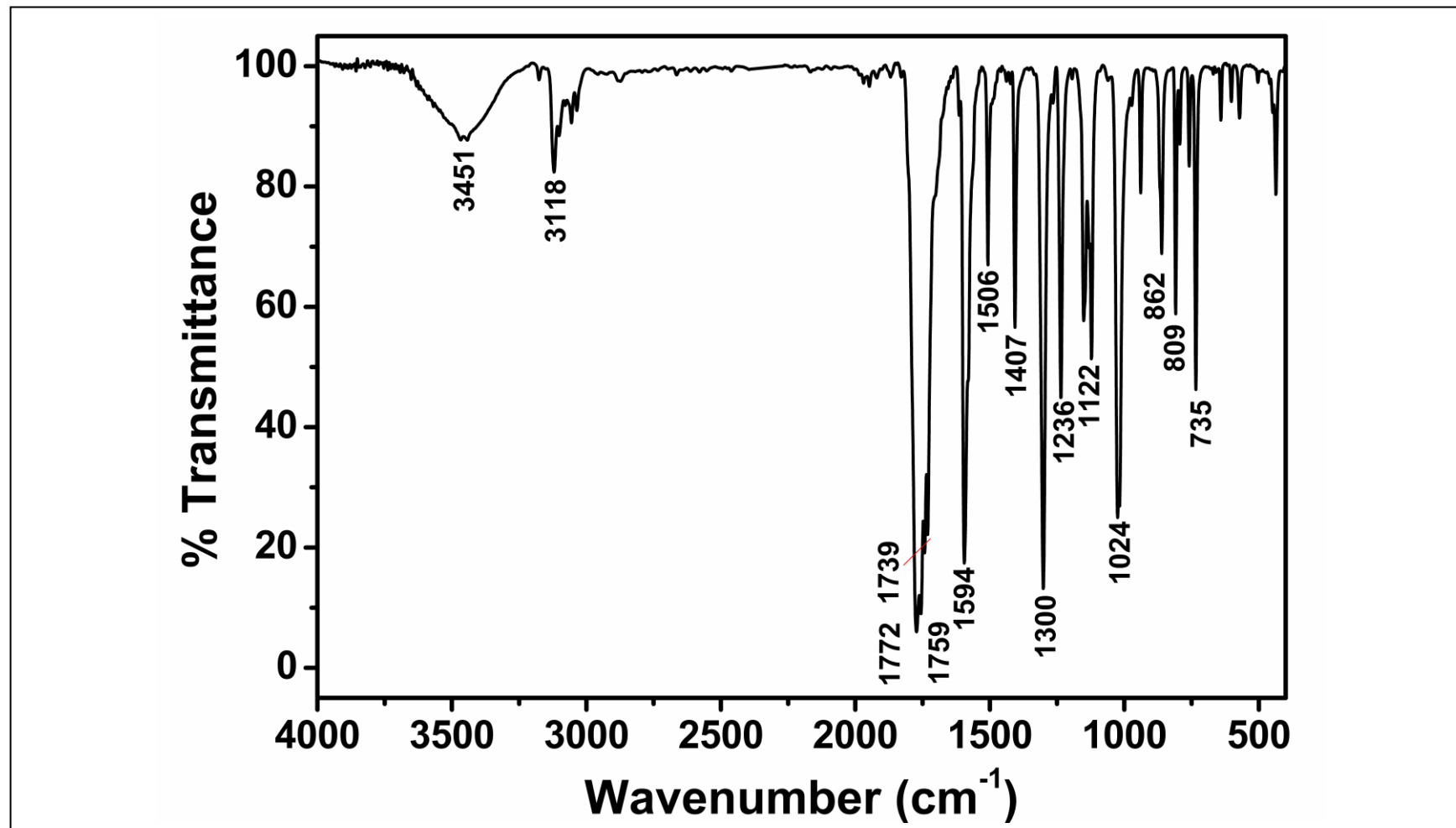


Figure 4.2: FT-IR Spectrum of Perylene dianhydride

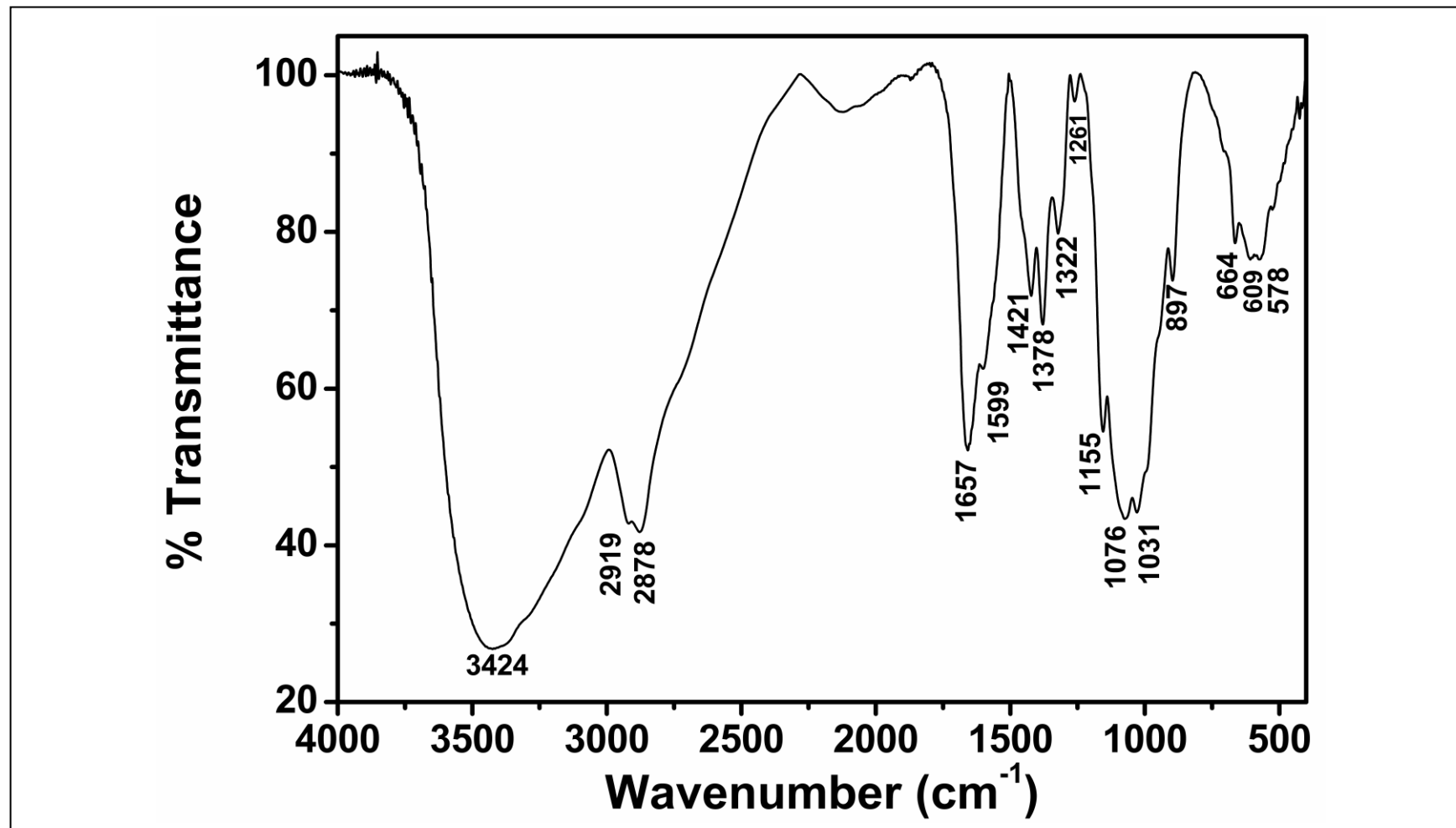


Figure 4.3: FT-IR Spectrum of Chitosan

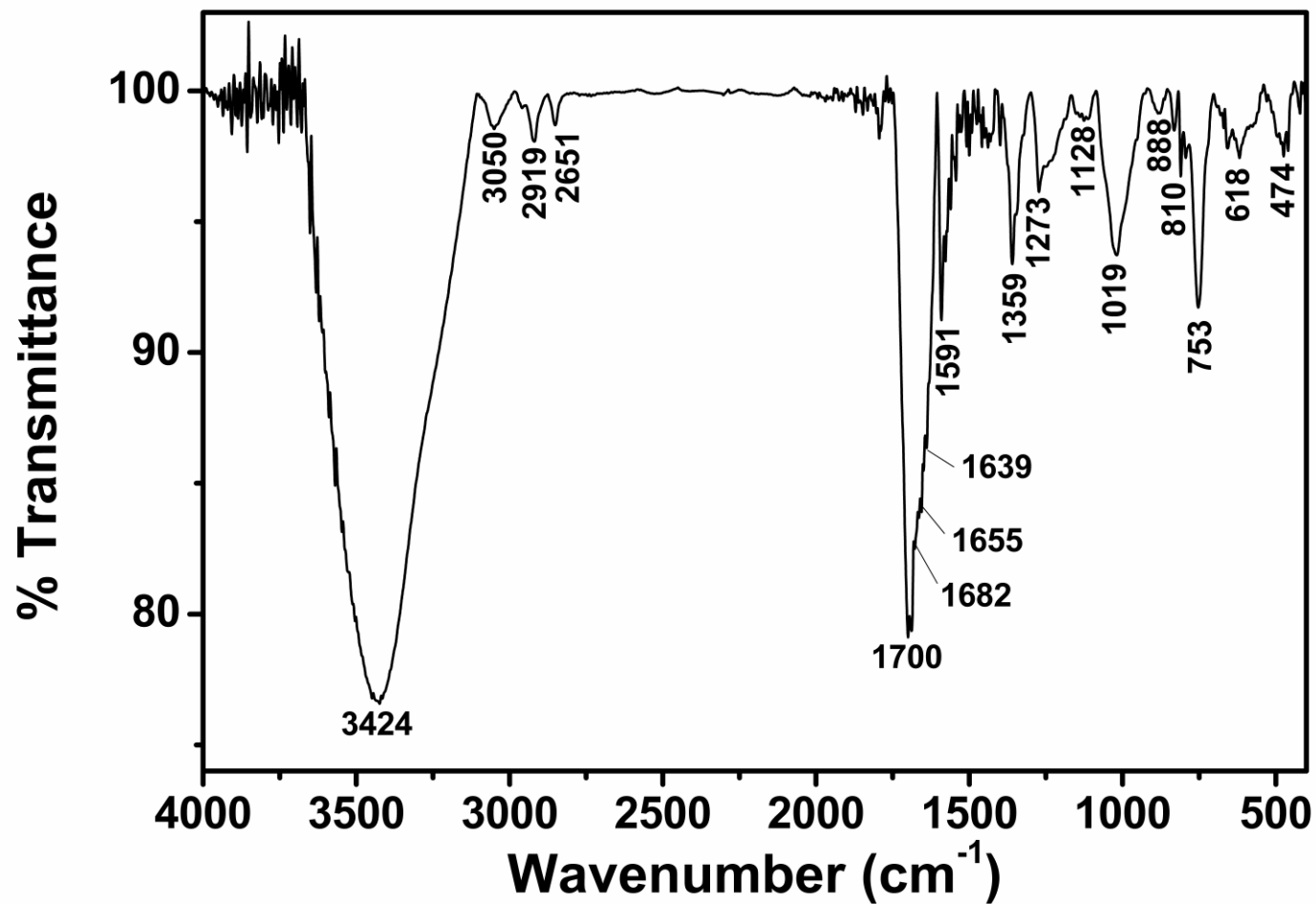


Figure 4.4: FT-IR Spectrum of A1PCH



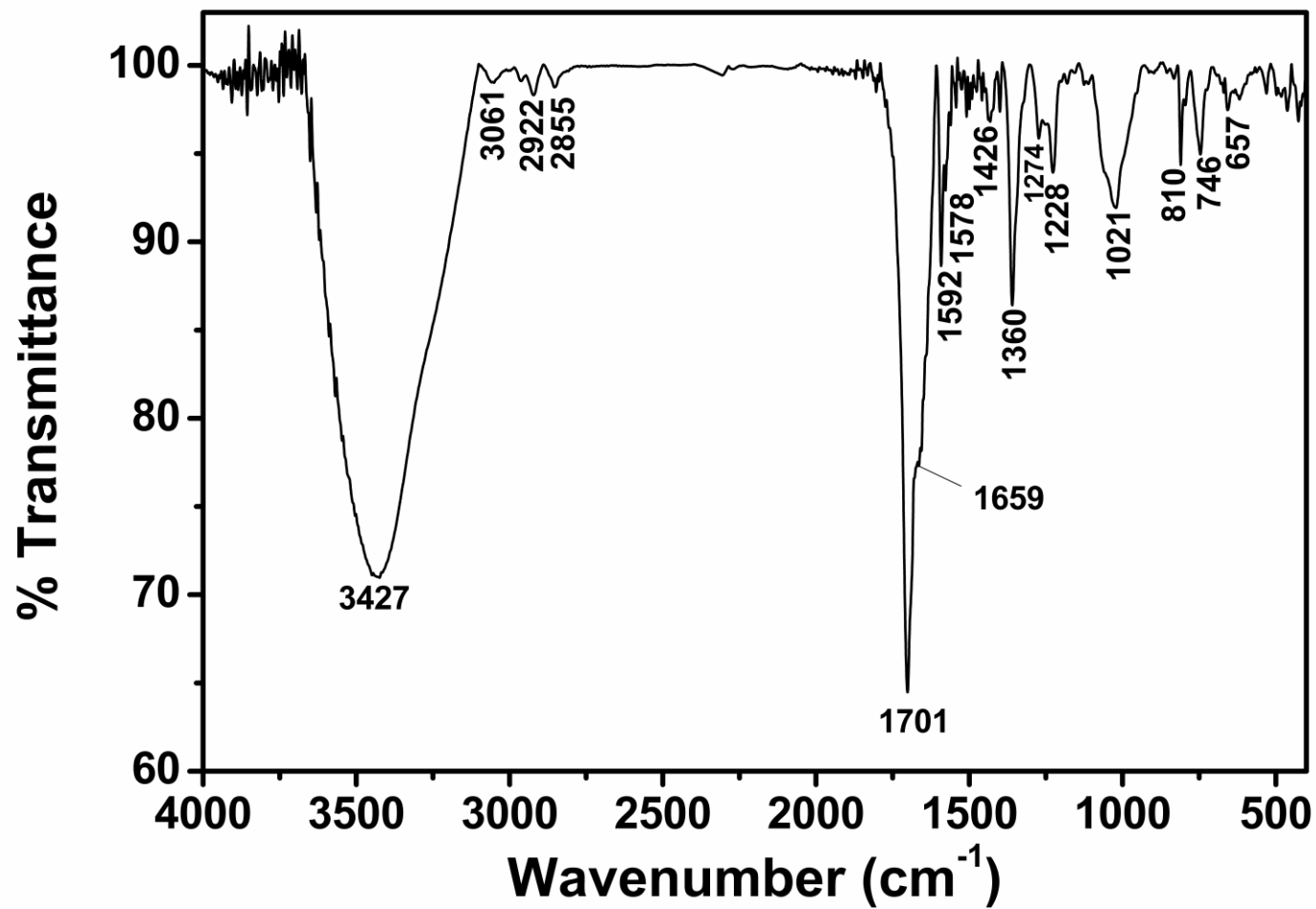


Figure 4.5: FT-IR Spectrum of A2PCH

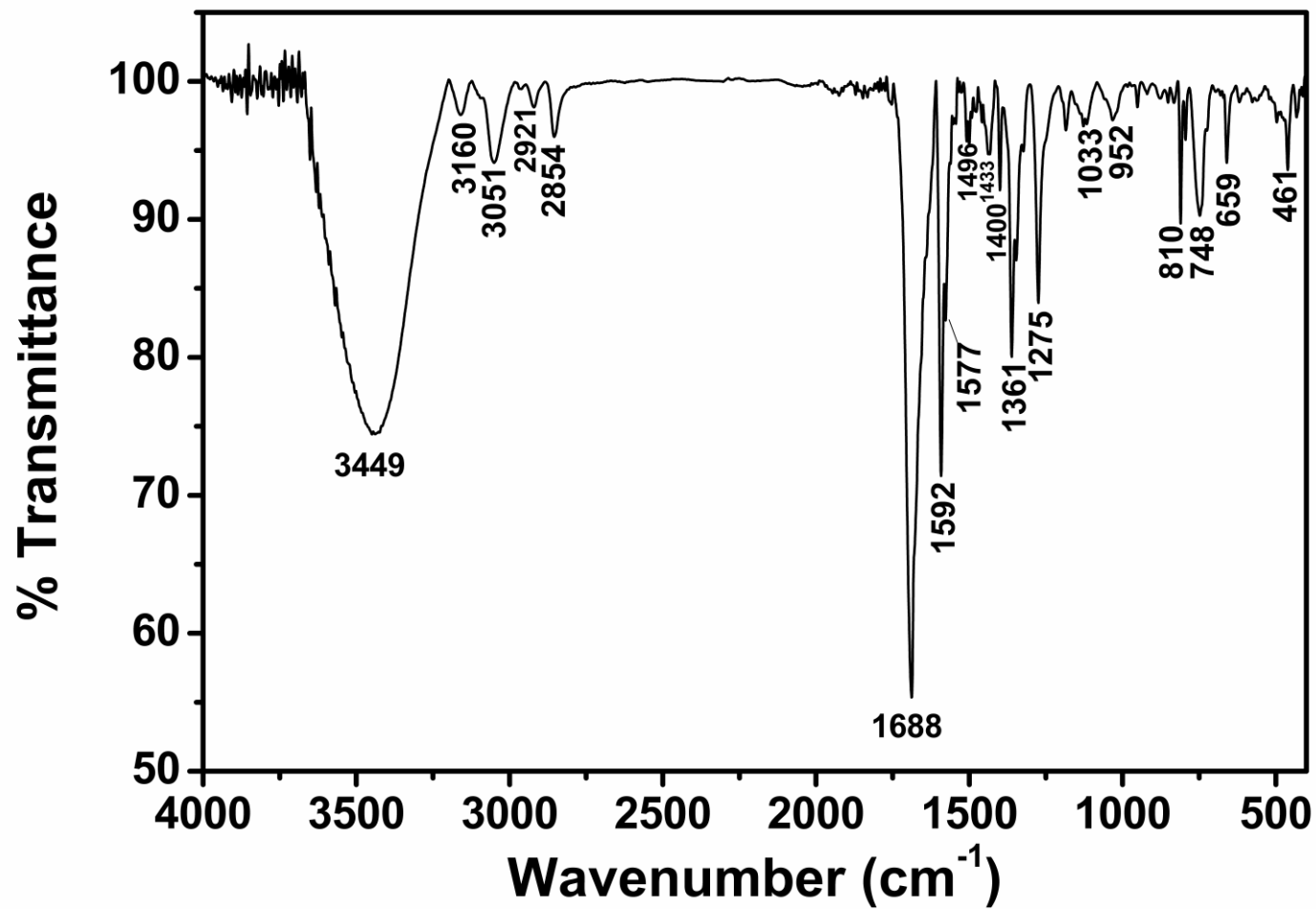


Figure 4.6: FT-IR Spectrum of A3PCH

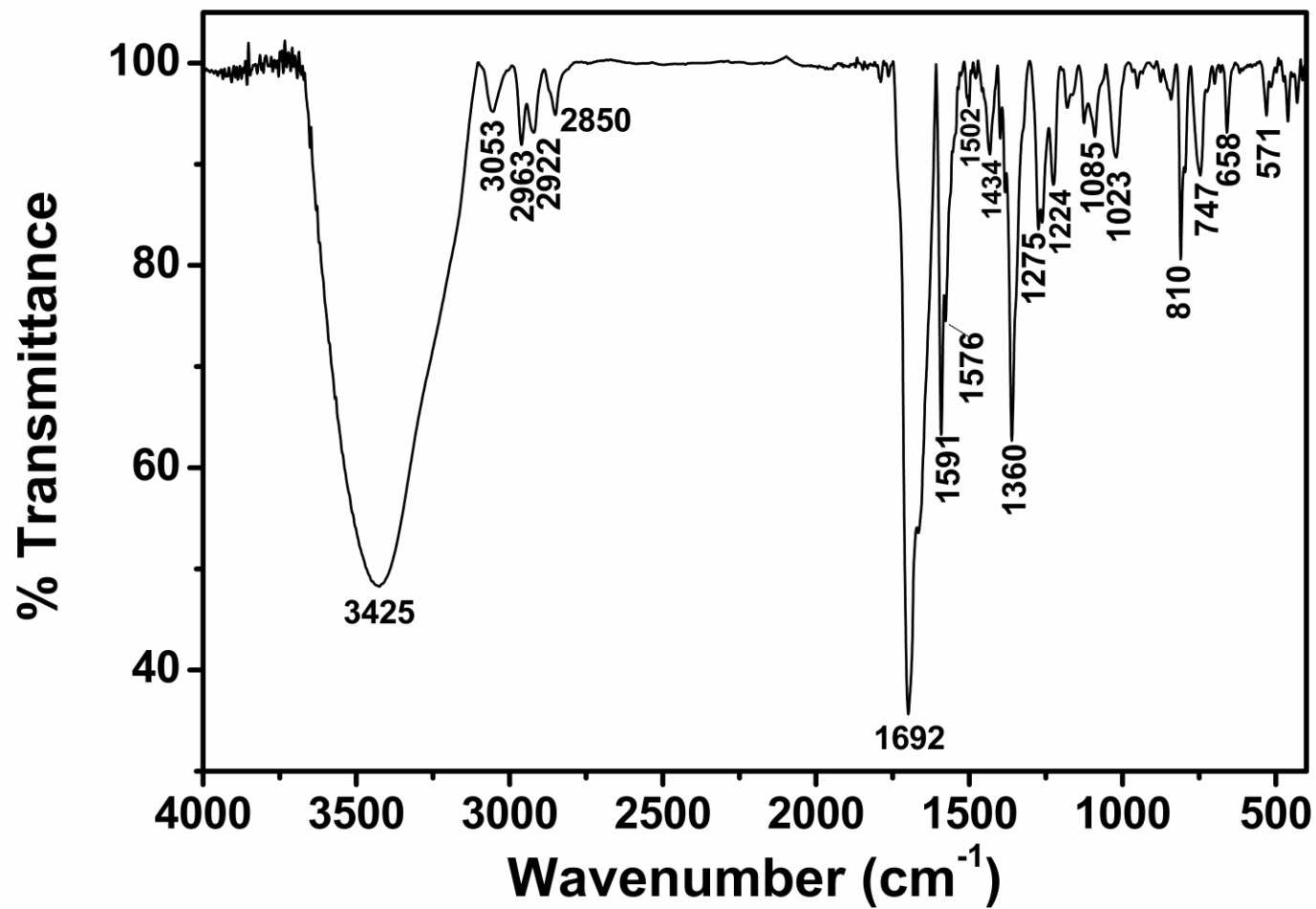


Figure 4.7: FT-IR Spectrum of A4PCH

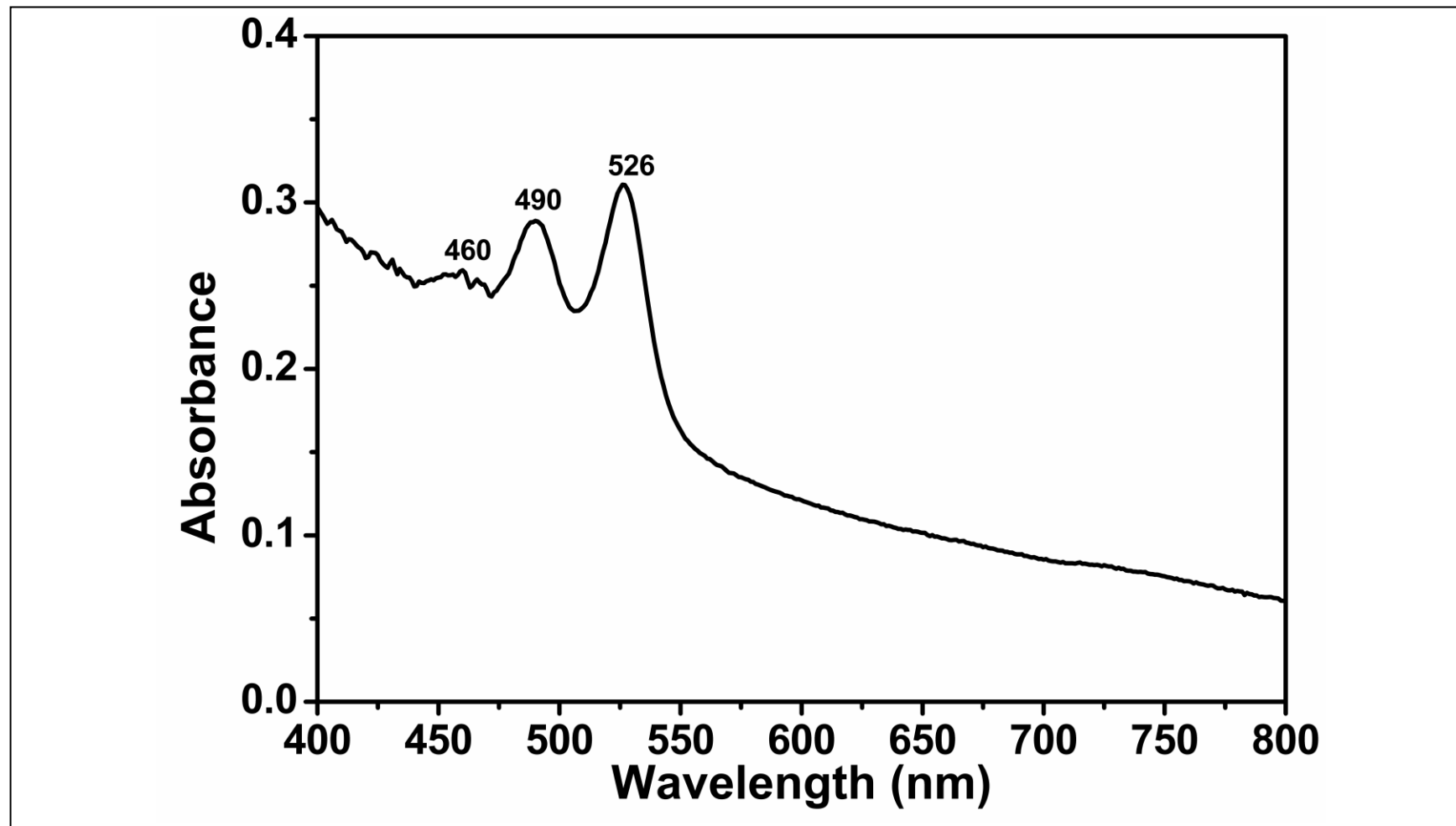


Figure 4.8: Absorption Spectrum of A1PCH in DMF

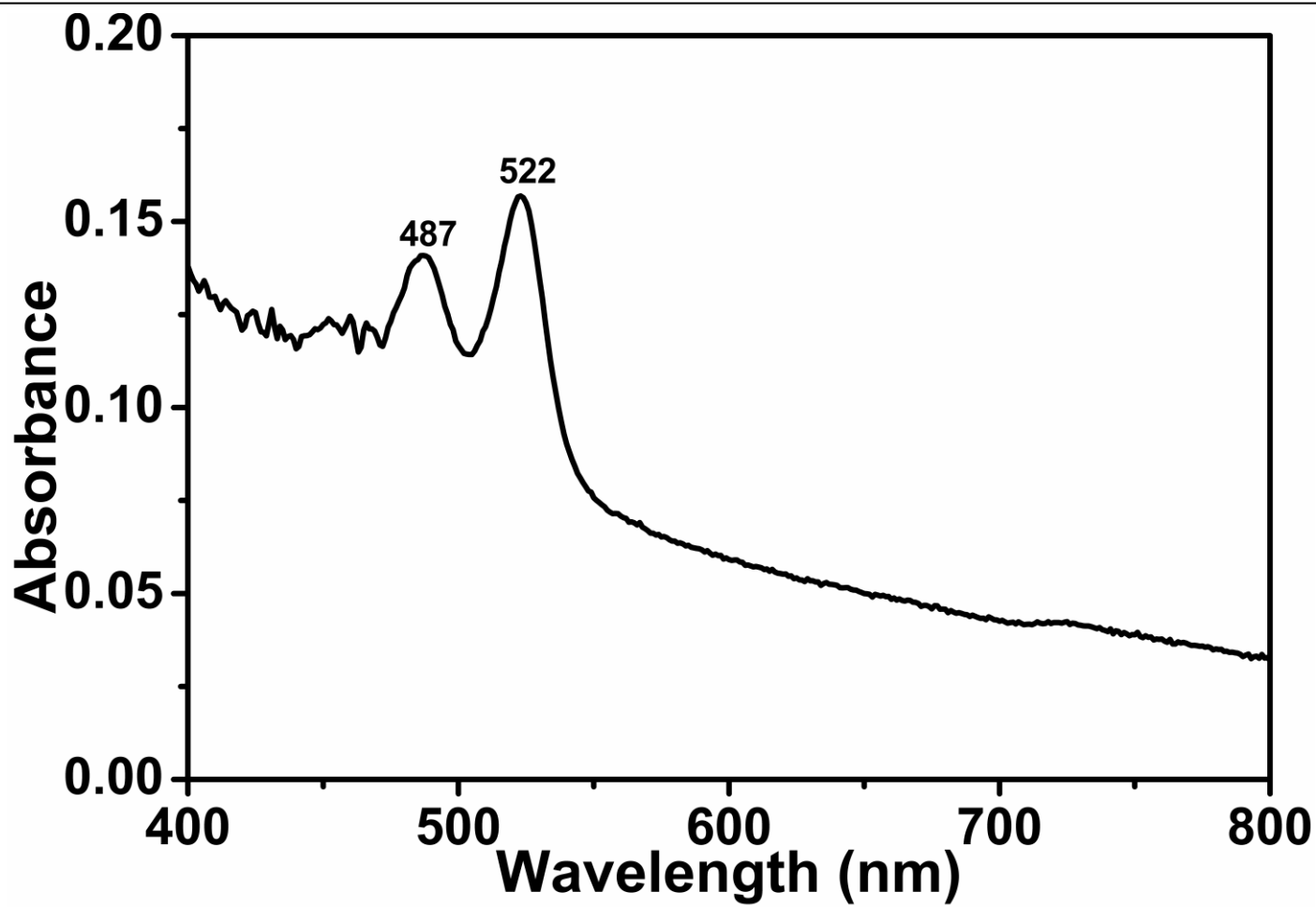


Figure 4.9: Absorption Spectrum of A1PCH in DMAc

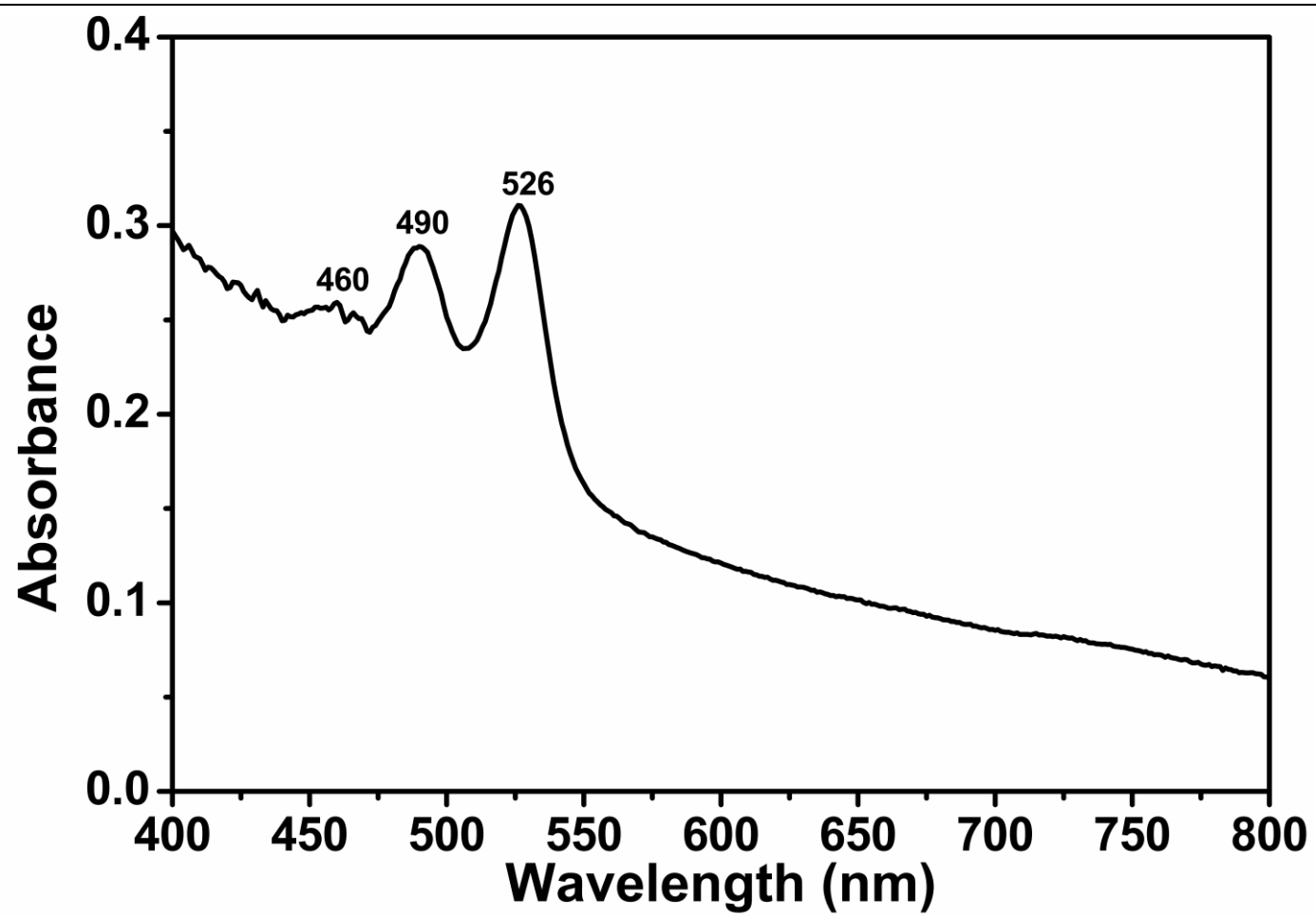


Figure 4.10: Absorption Spectrum of A1PCH in DMSO

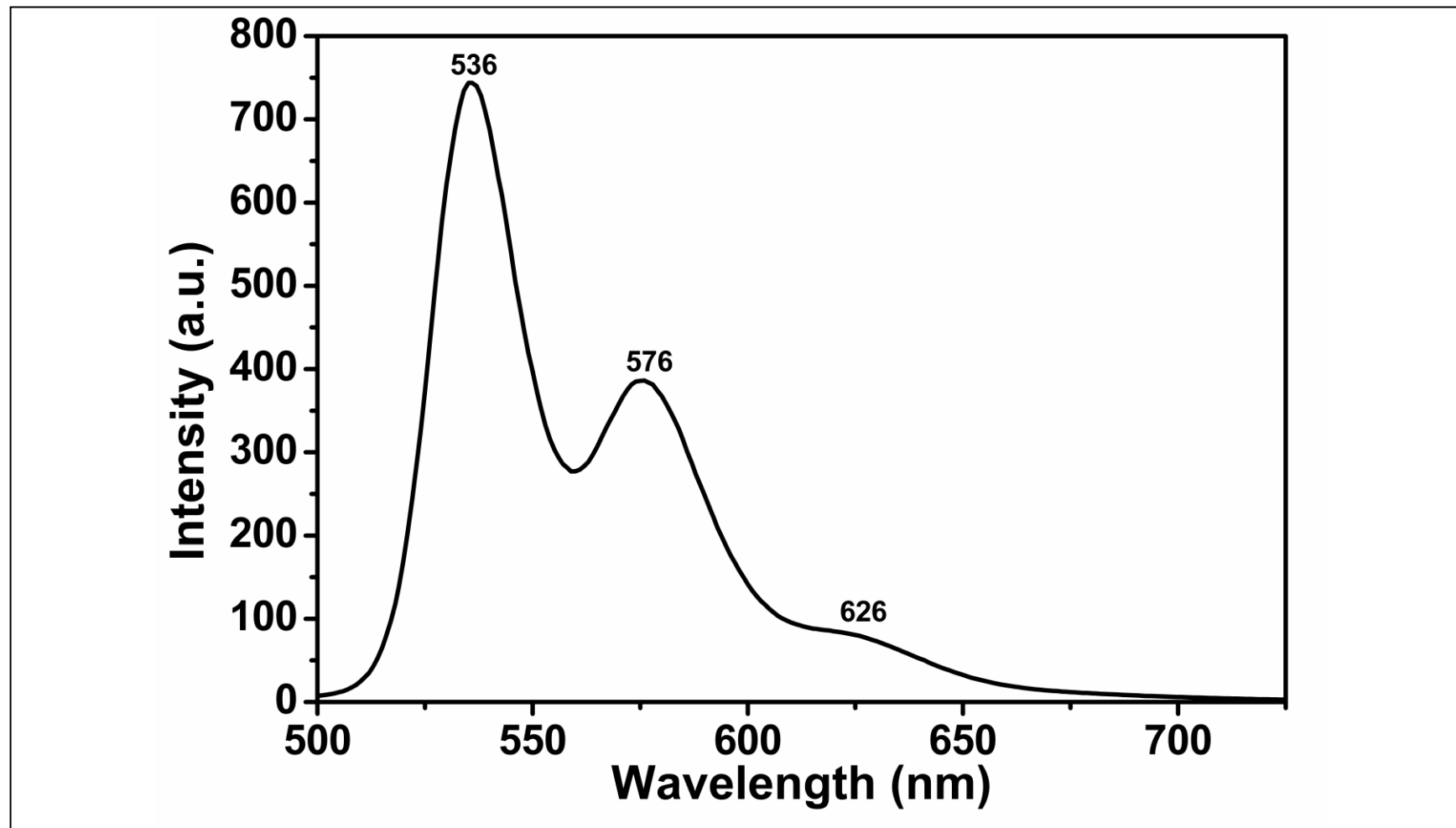


Figure 4.11: Emission Spectrum of A1PCH in DMF

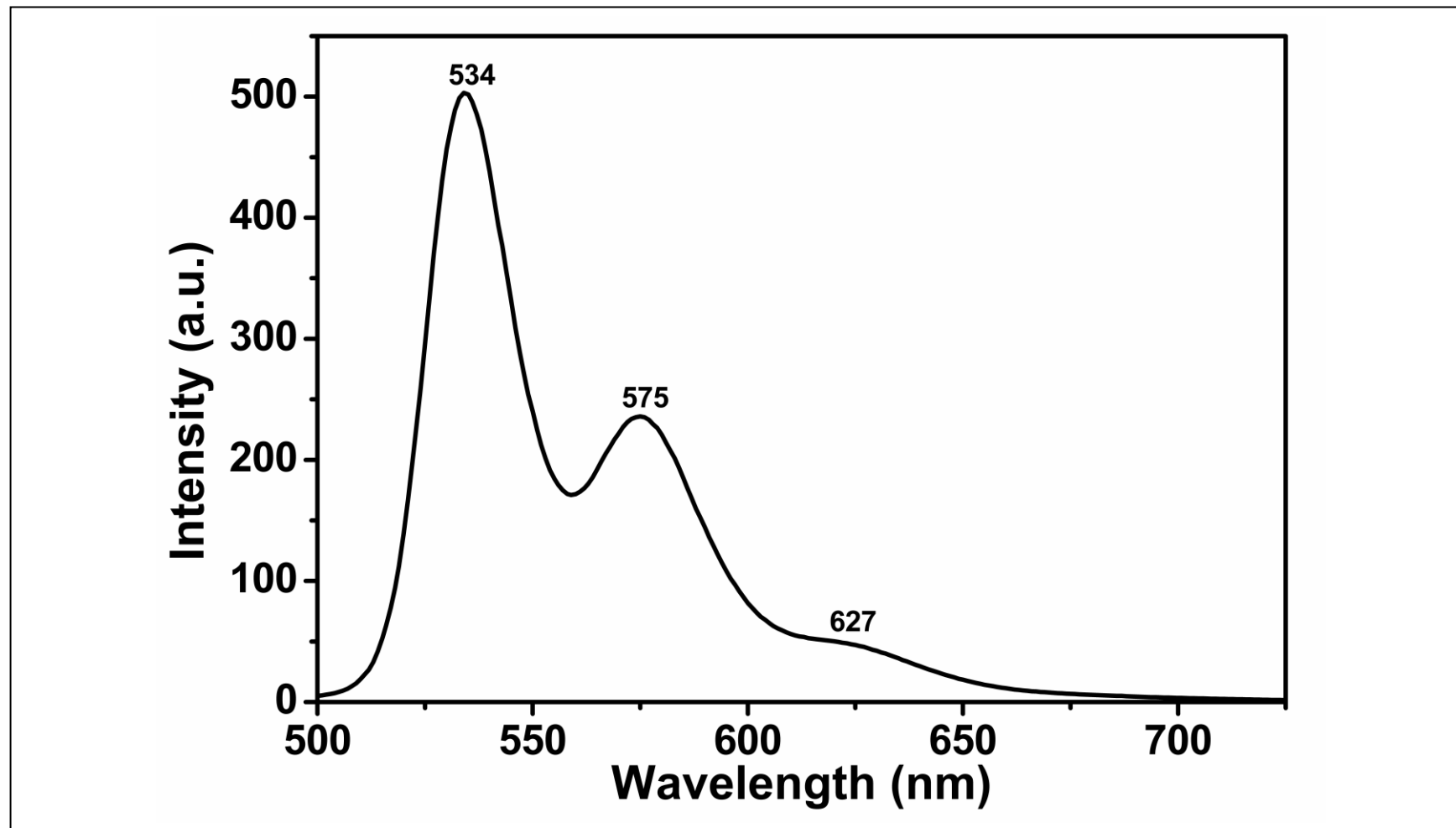


Figure 4.12: Emission Spectrum of A1PCH in DMAc



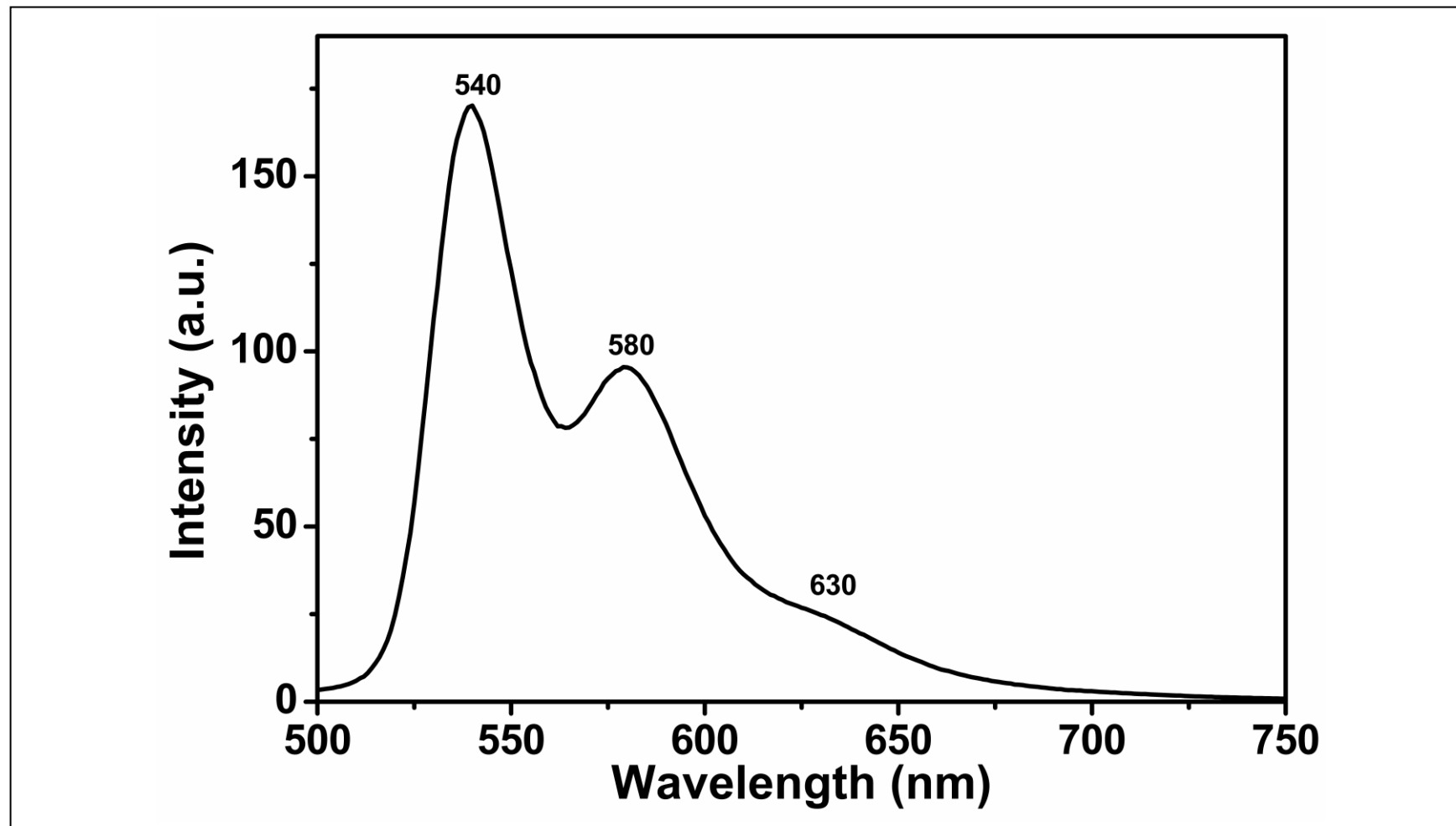


Figure 4.13: Emission Spectrum of A1PCH in DMSO

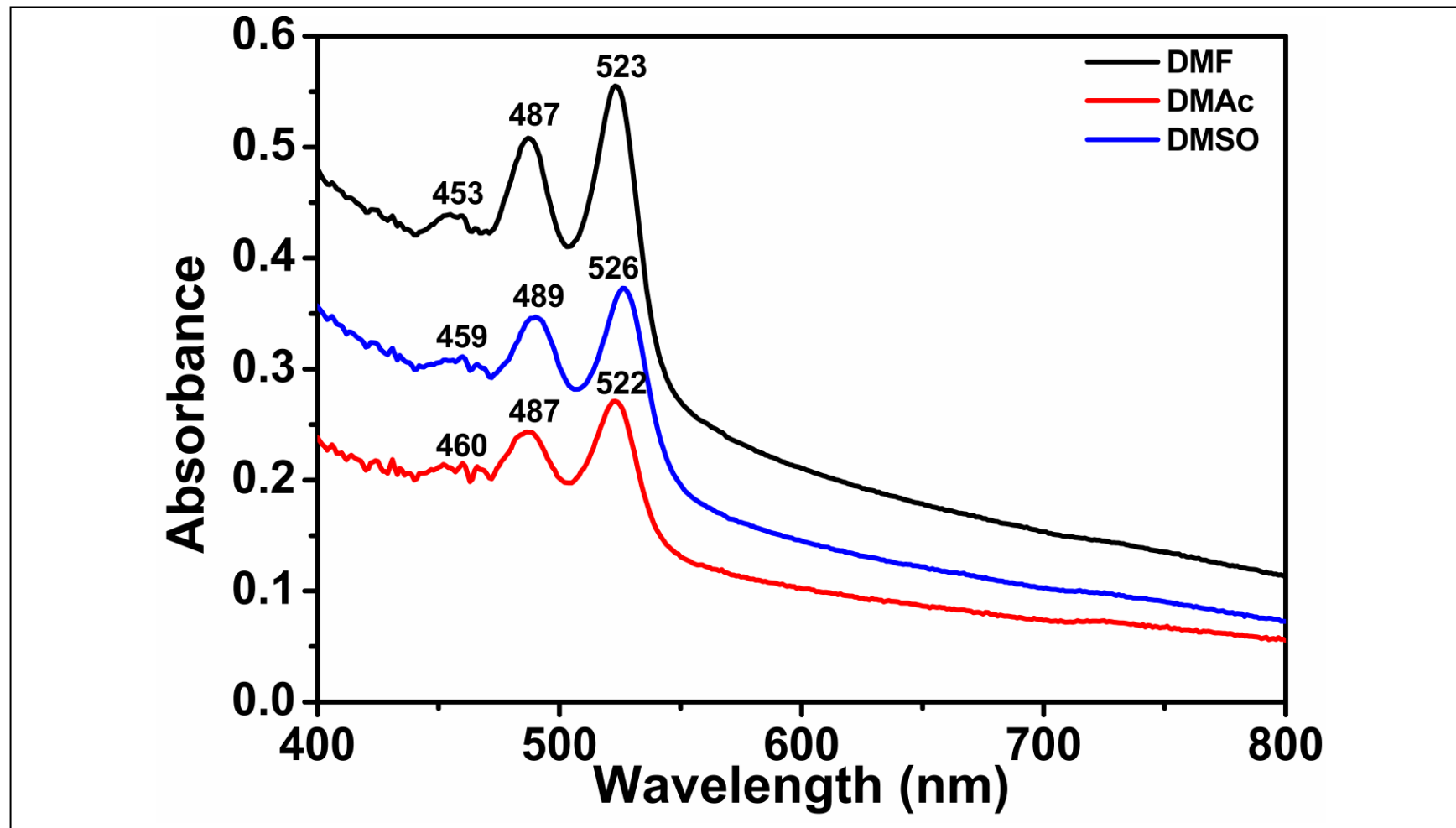


Figure 4.14: Absorption Spectra of A1PCH in DMF,DMAc and DMSO

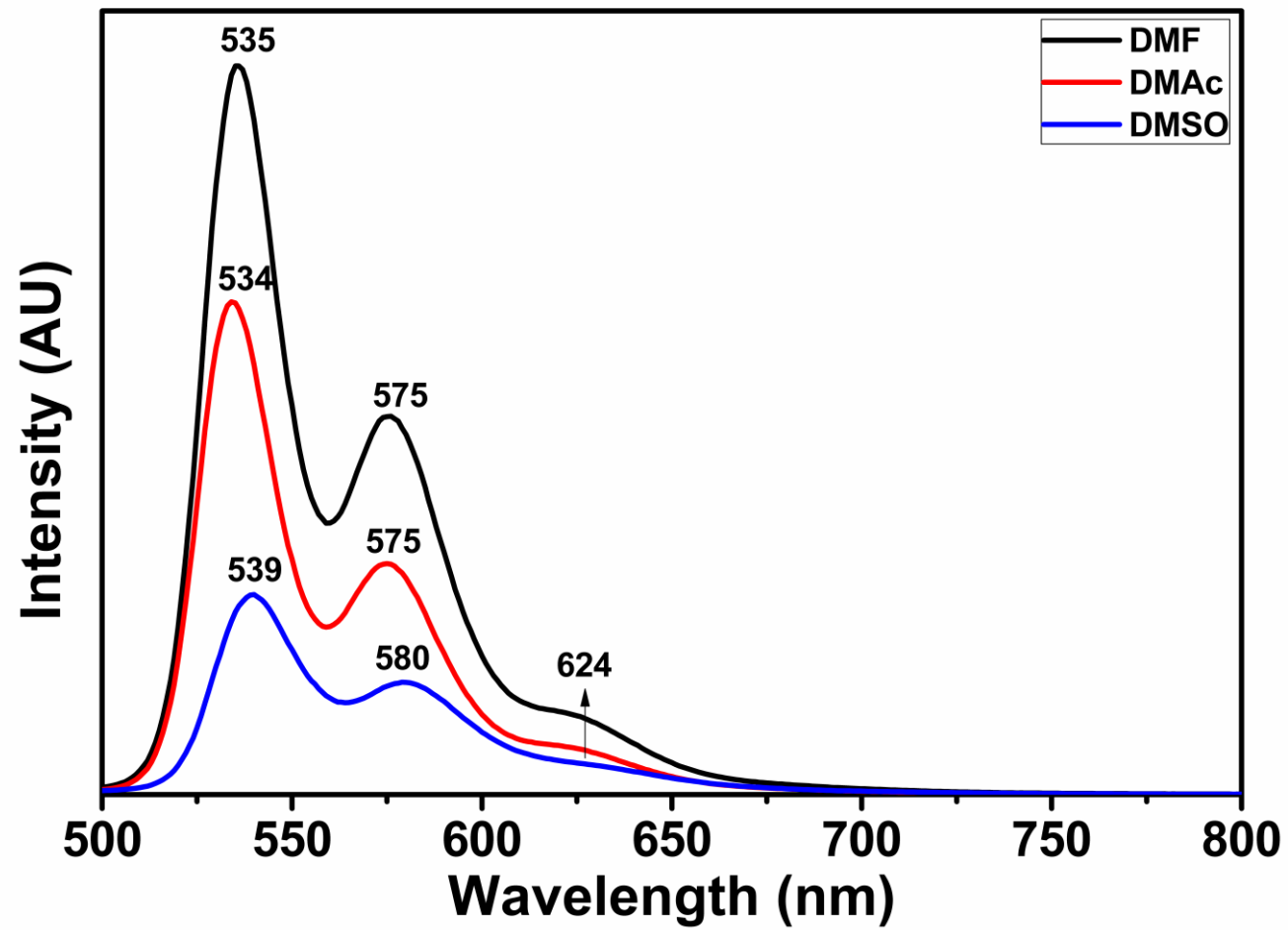


Figure 4.15: Emission Spectra of A1PCH in DMF, DMAc and DMSO

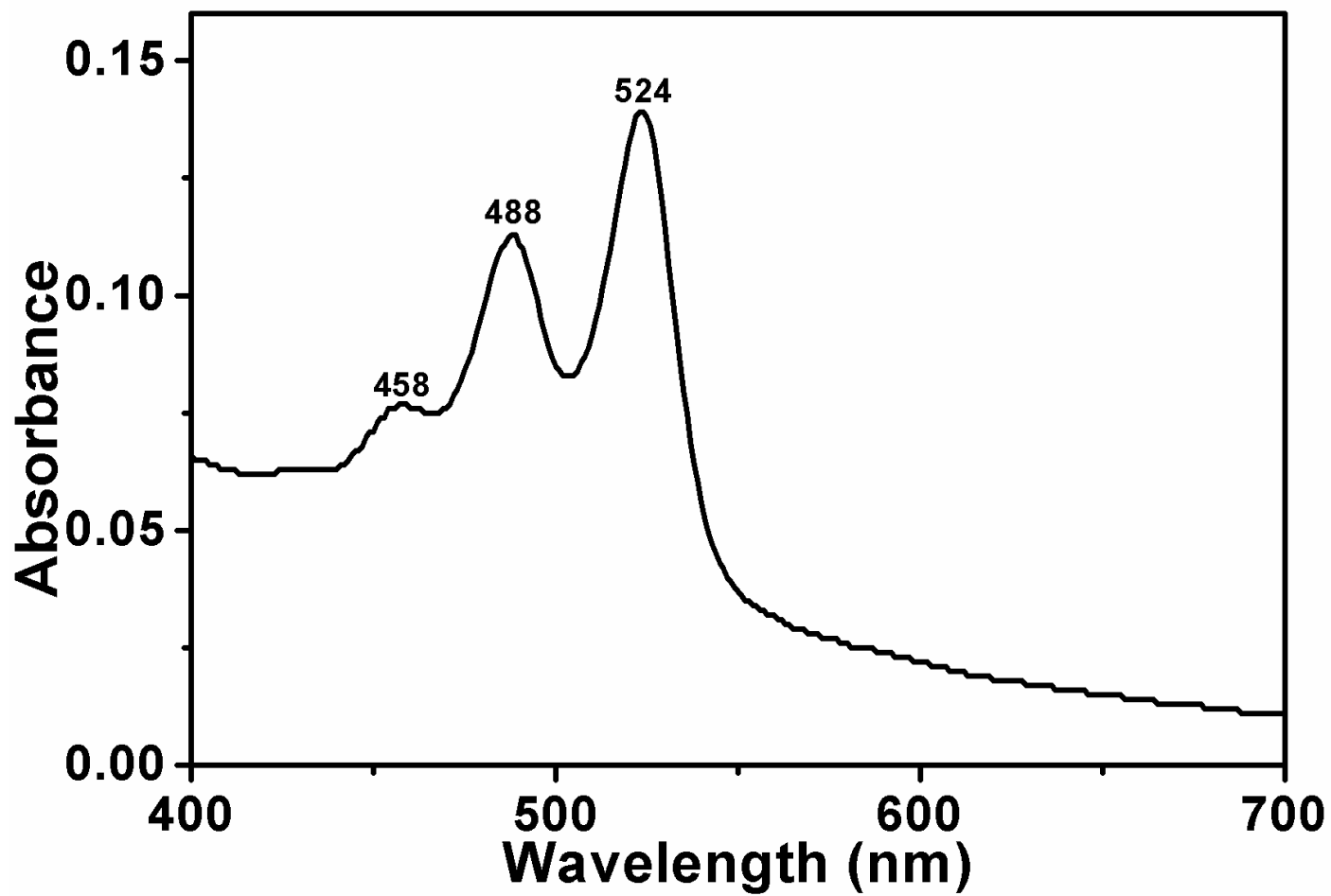


Figure 4.16: Absorption Spectrum of A2PCH in DMF

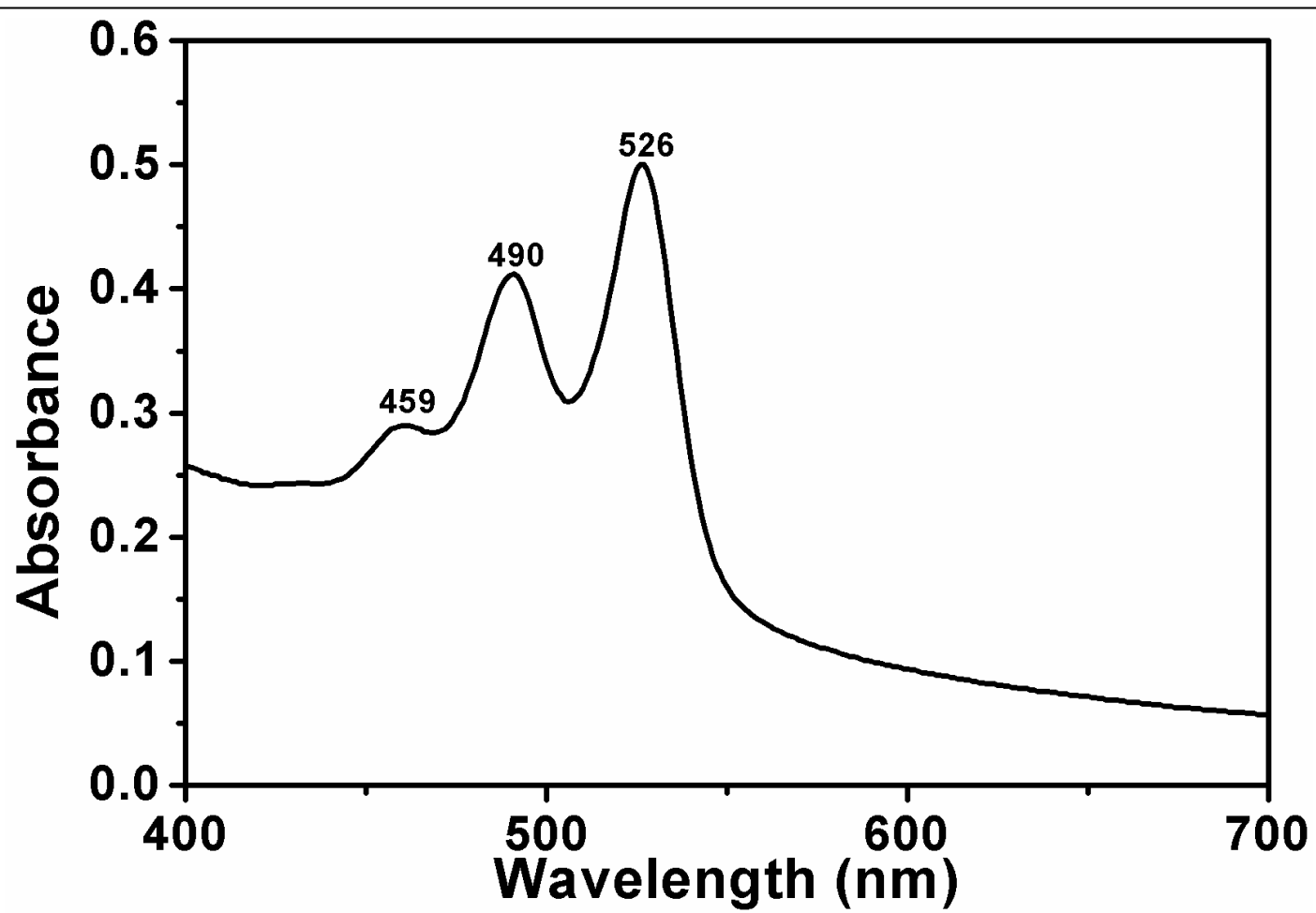


Figure 4.17: Absorption Spectrum of A2PCH in DMSO

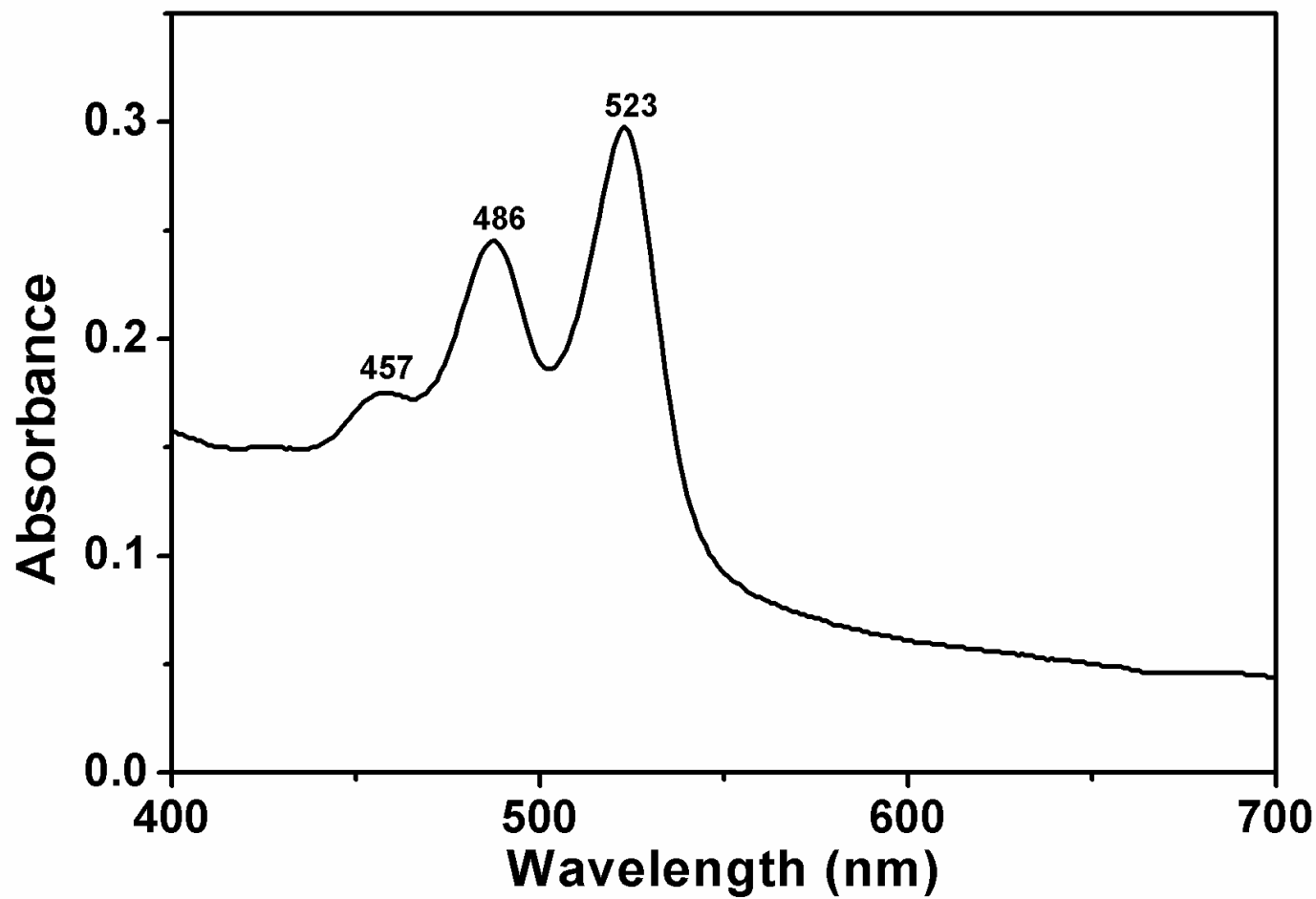


Figure 4.18: Absorption Spectrum of A2PCH inDMAc

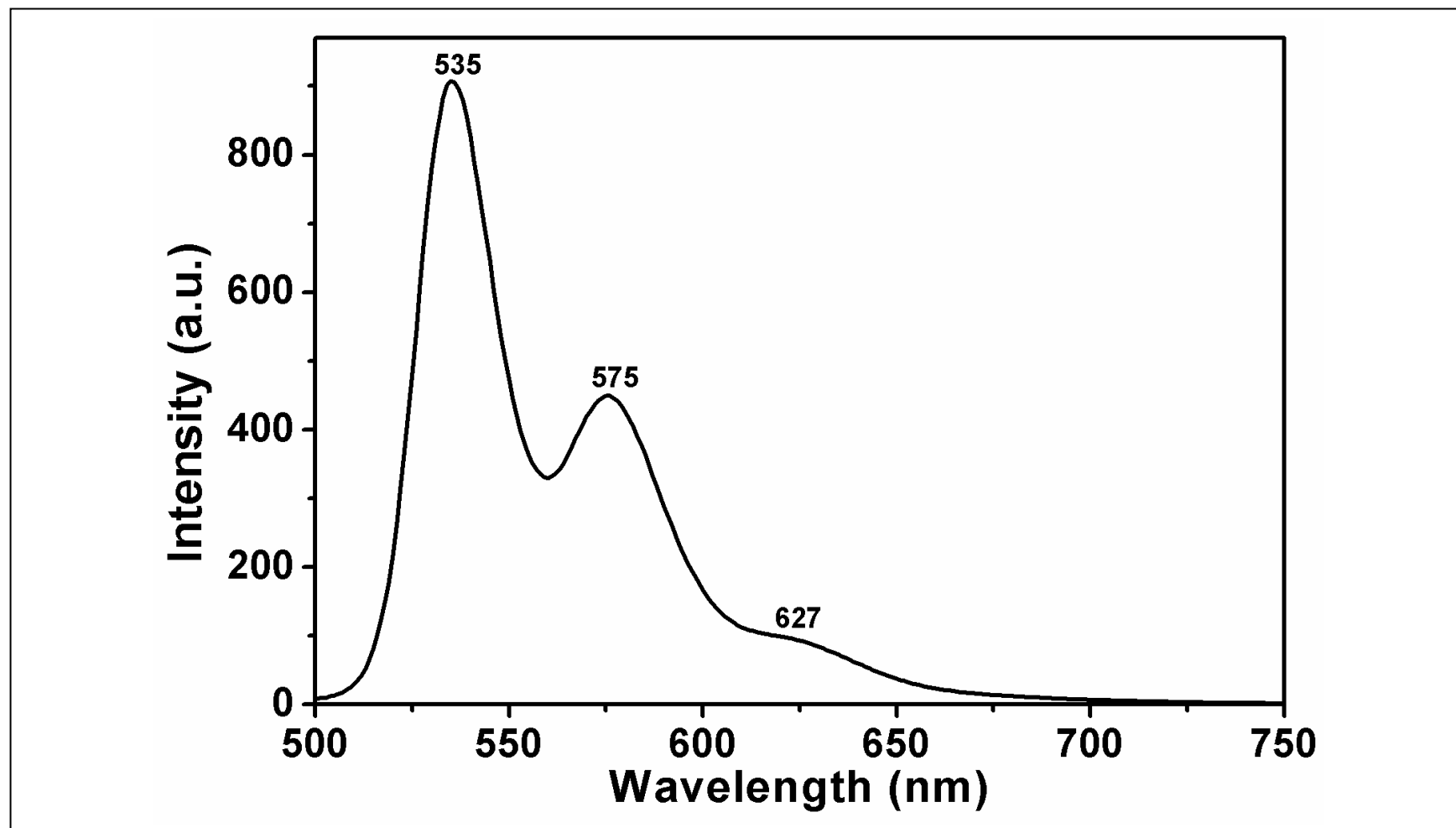


Figure 4.19: Emission Spectrum of A2PCH inDMF

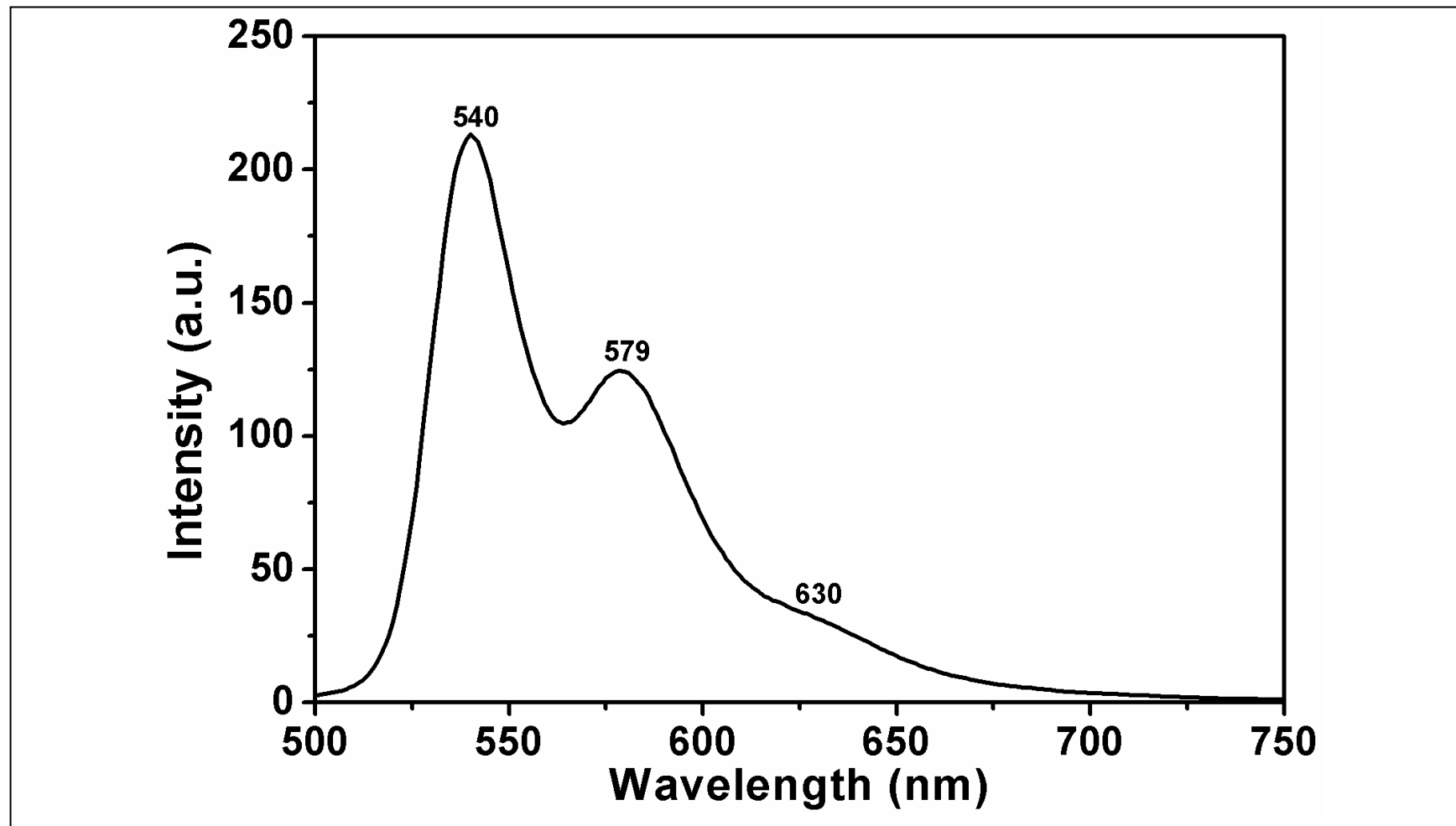


Figure 4.20: Emission Spectrum of A2PCH inDMSO



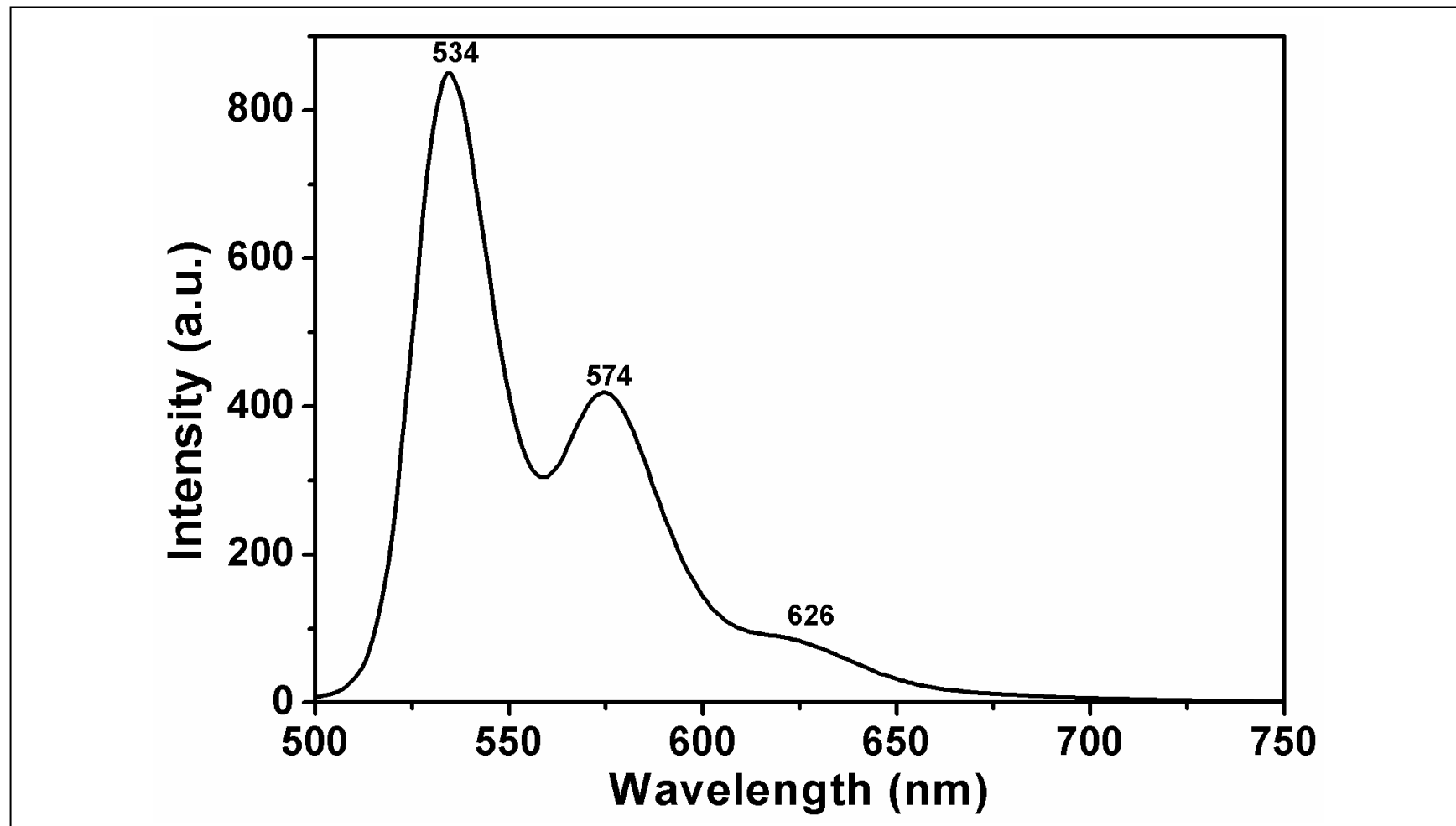


Figure 4.21: Emission Spectrum of A2PCH inDMAc

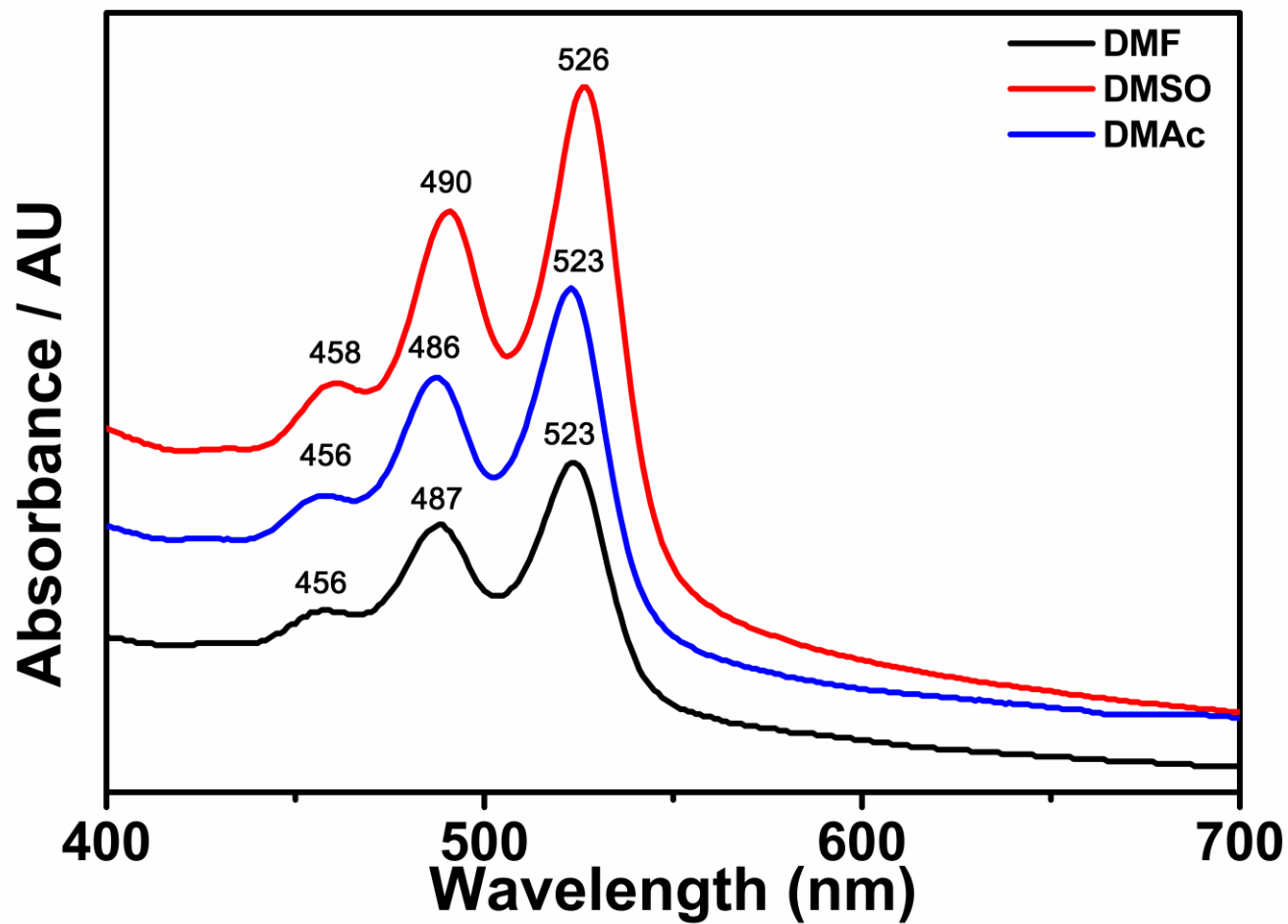


Figure 4.22: Absorption Spectra of A2PCH in DMF, DMSO and DMAc

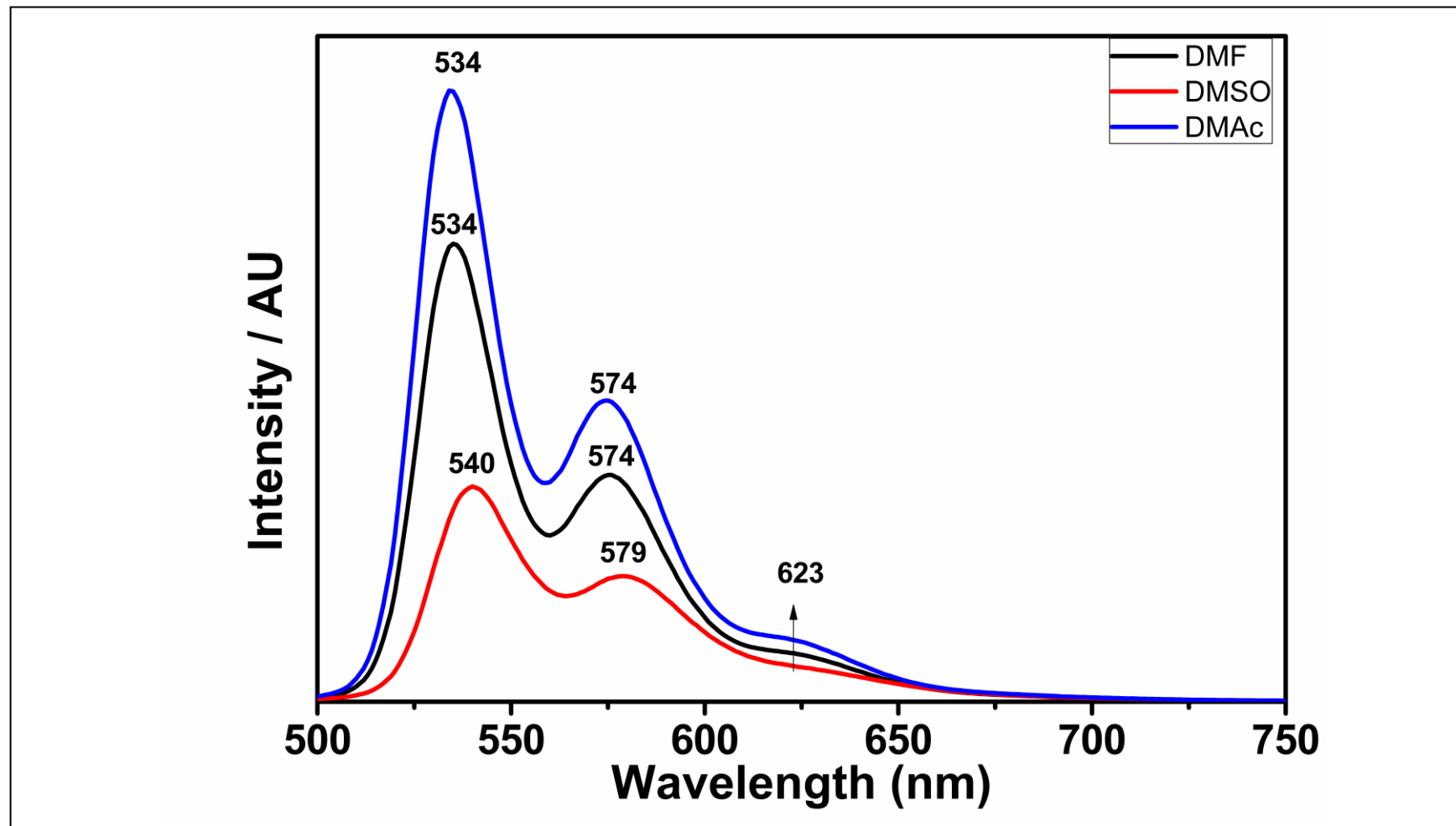


Figure 4.23: Emission Spectra of A2PCH in DMF, DMSO and DMAc

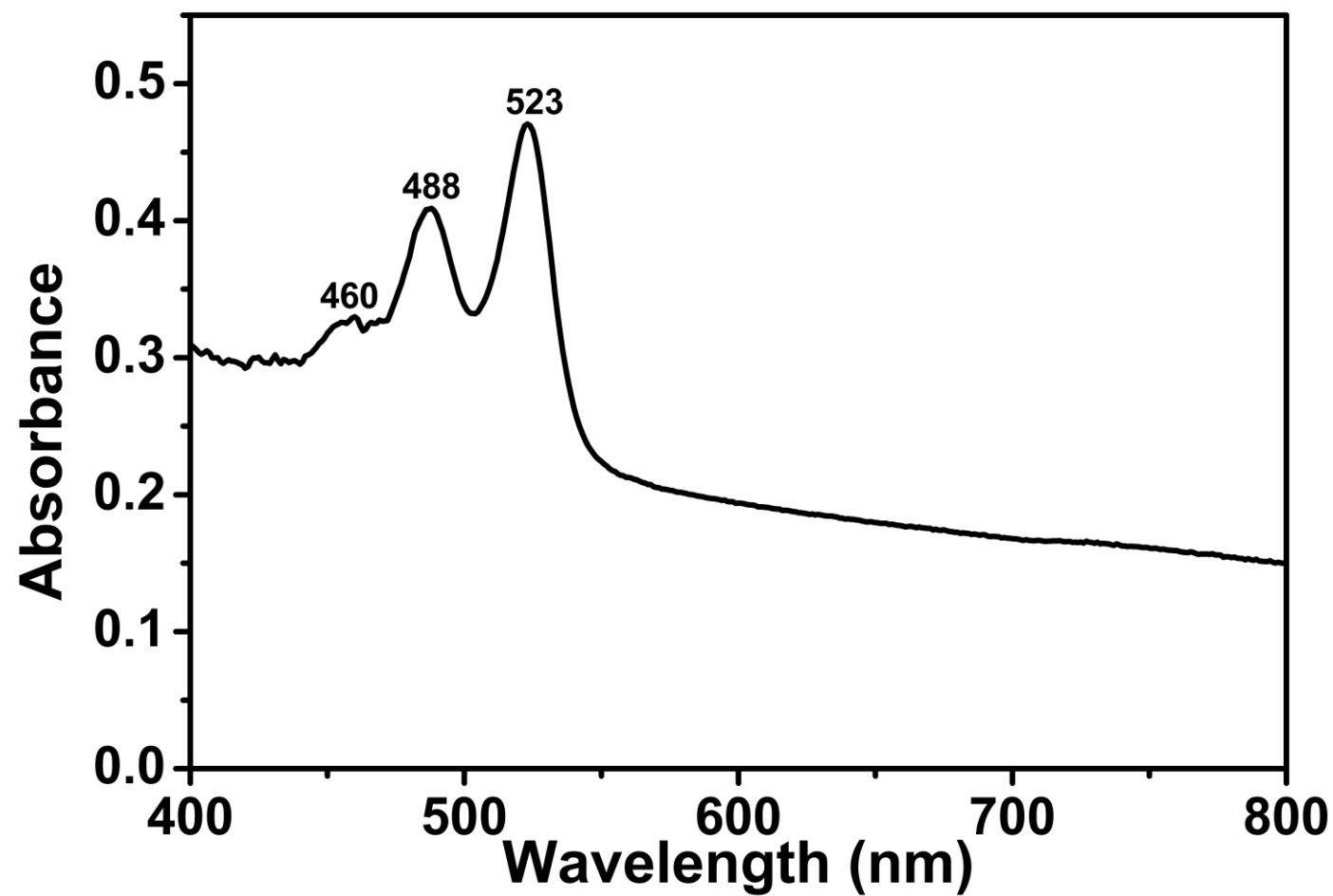


Figure 4.24: Absorption Spectrum of A3PCH in DMF

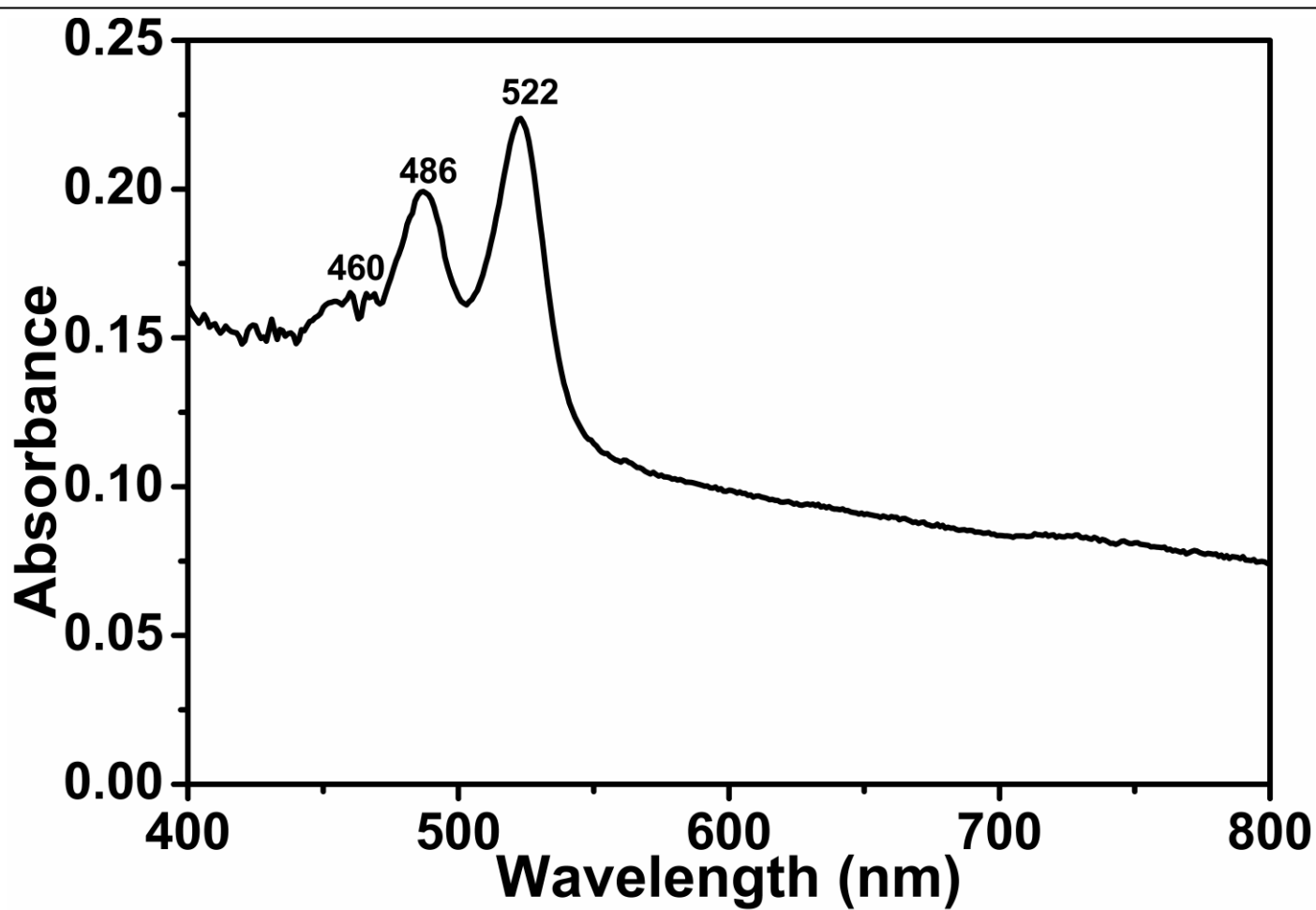


Figure 4.25: Absorption Spectrum of A3PCH in DMAc

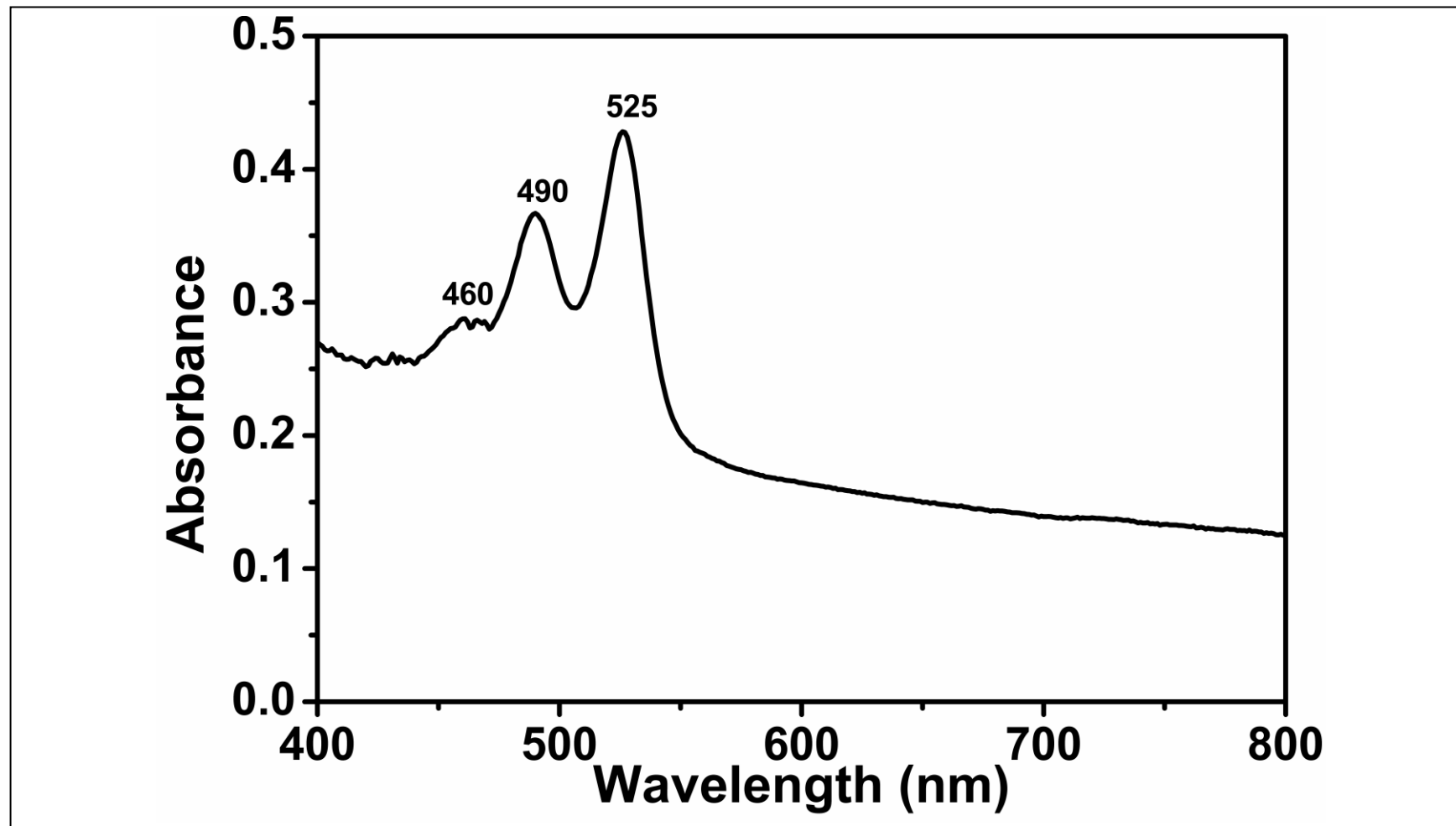


Figure 4.26: Absorption Spectrum of A3PCH in DMSO

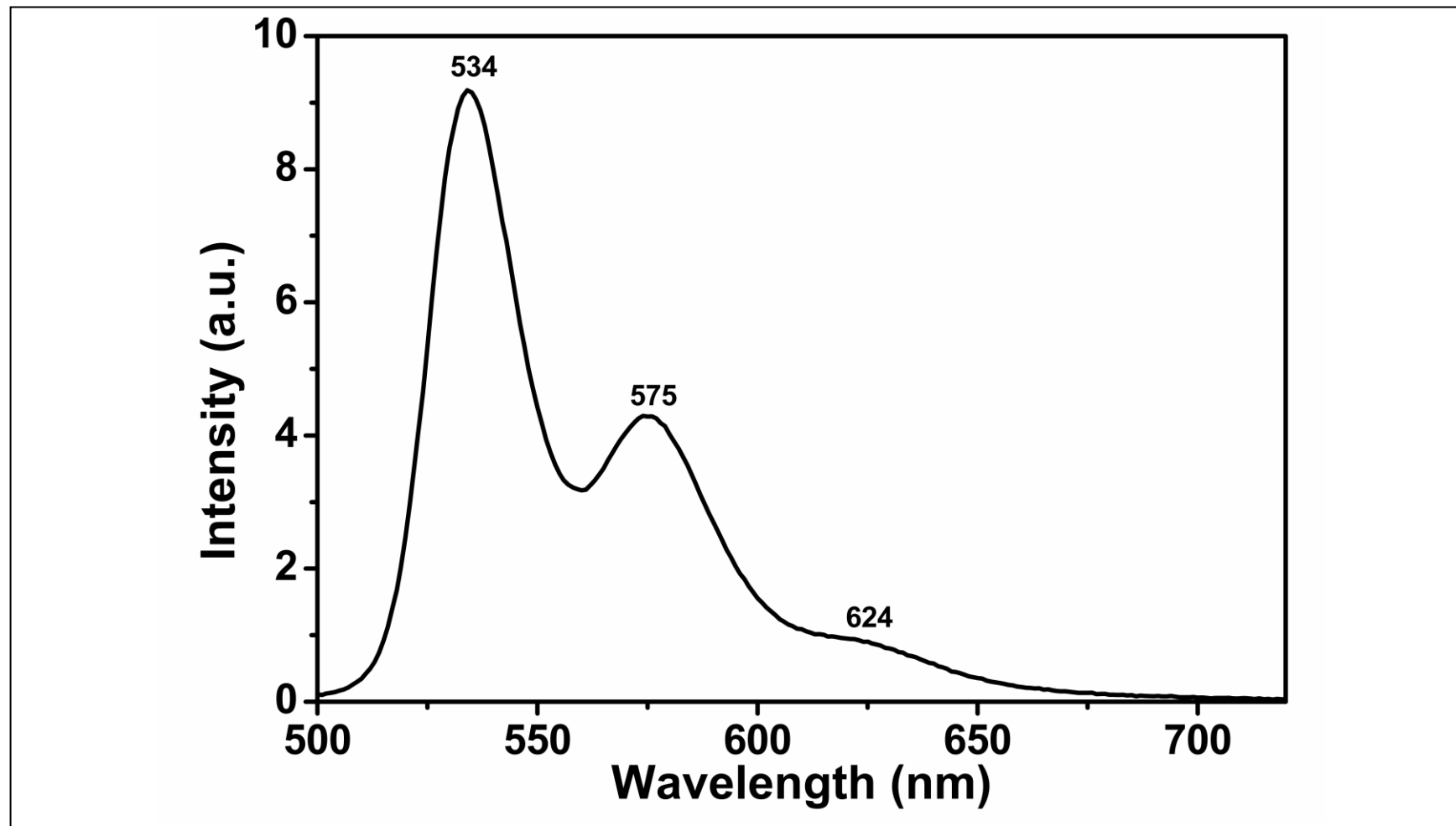


Figure 4.27: Emission Spectrum of A3PCH in DMF

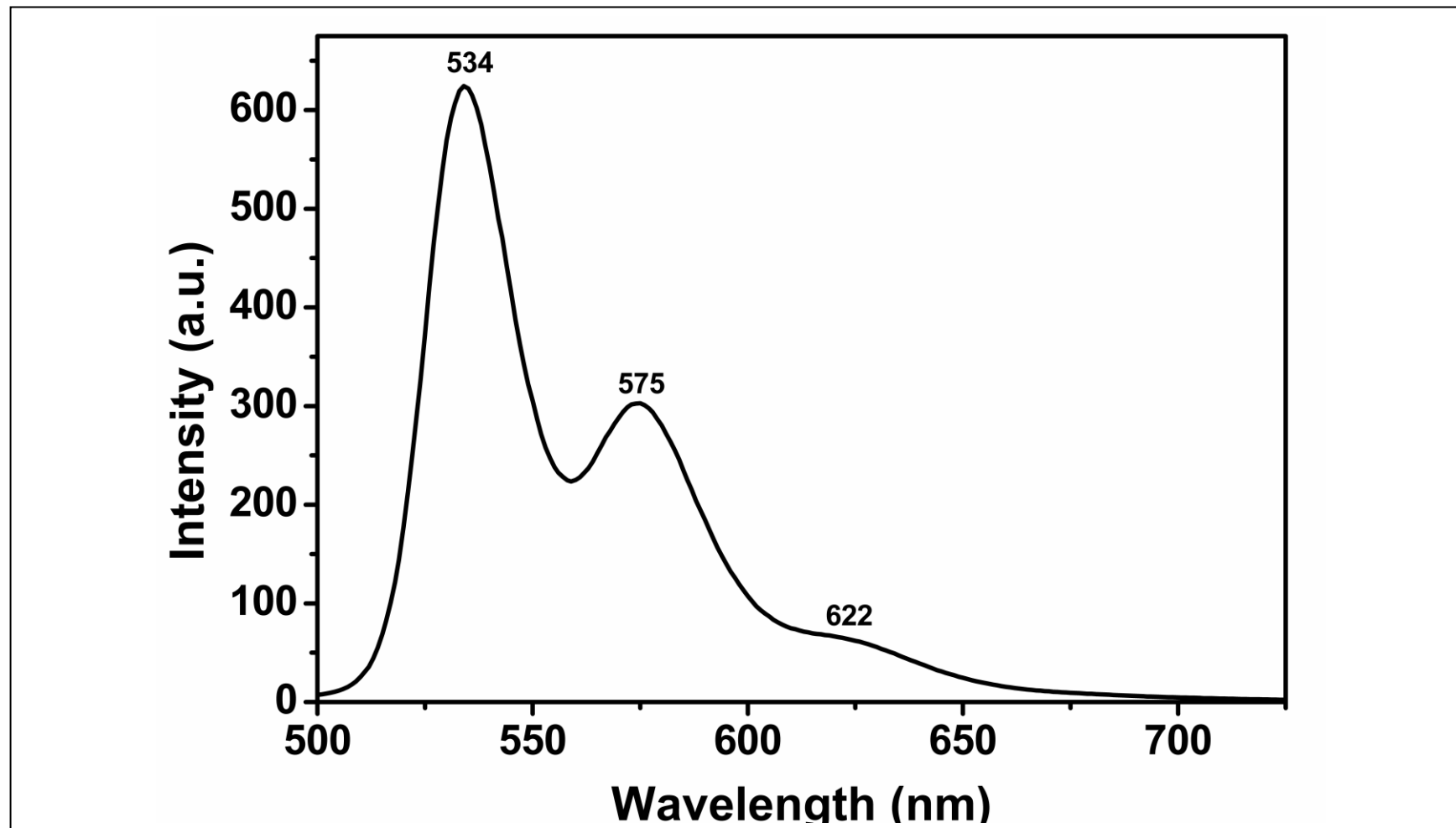


Figure 4.28: Emission Spectrum of A3PCH in DMAc



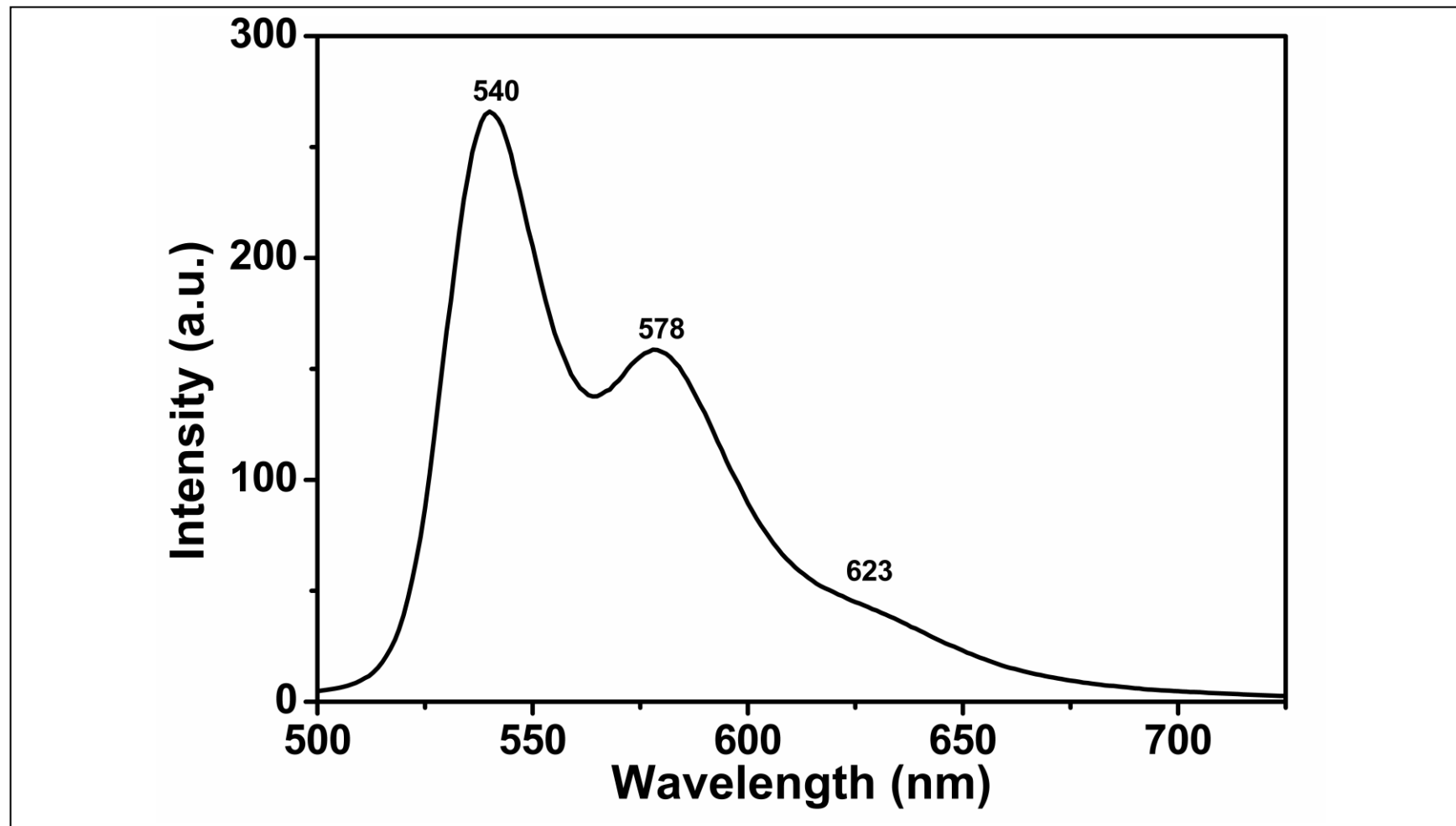


Figure 4.29: Emission Spectrum of A3PCH in DMSO

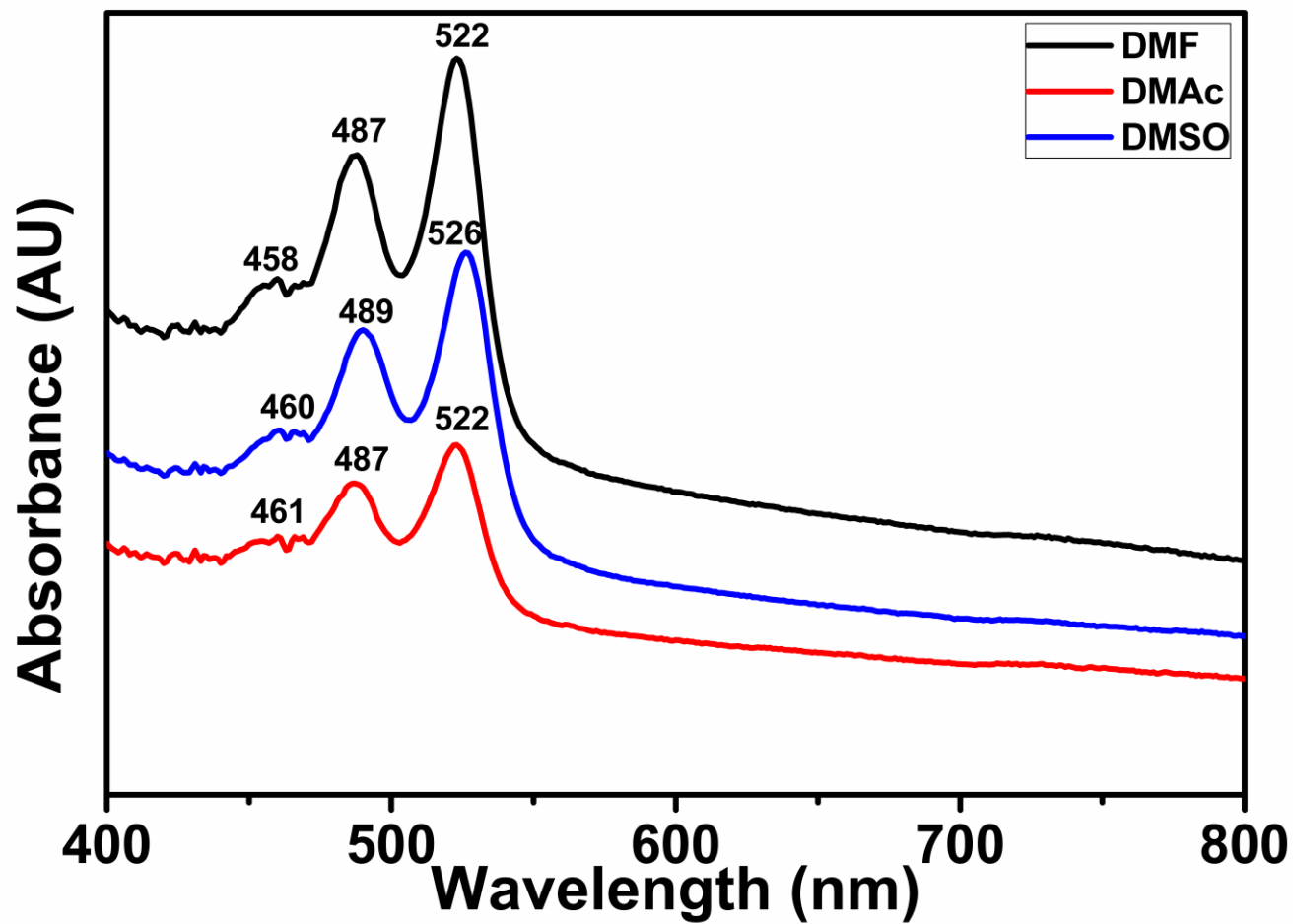


Figure 4.30: Absorption Spectra of A3PCH in DMF, DMAc and DMSO

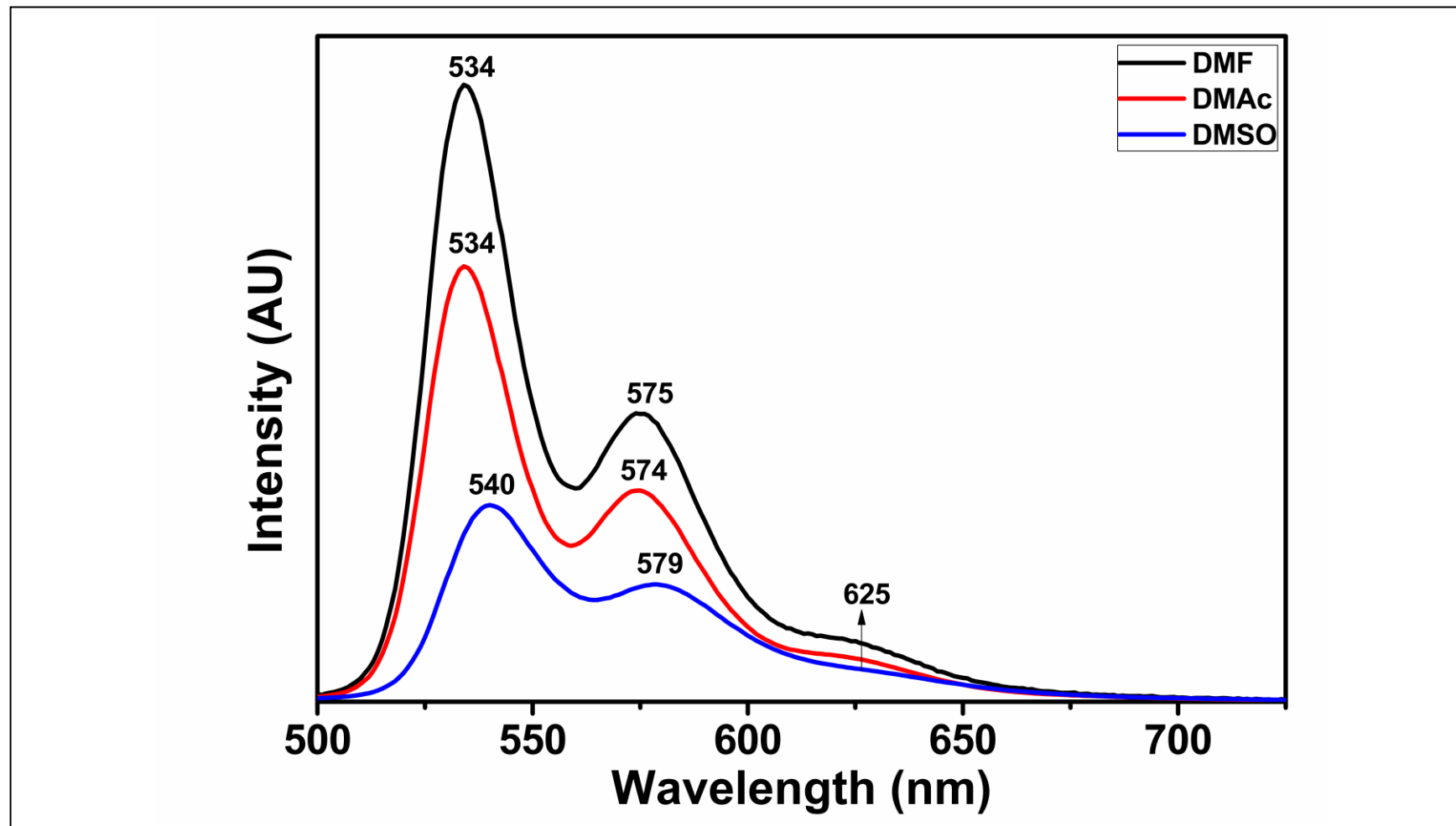


Figure 4.31: Emission Spectra of A3PCH in DMF, DMAc and DMSO

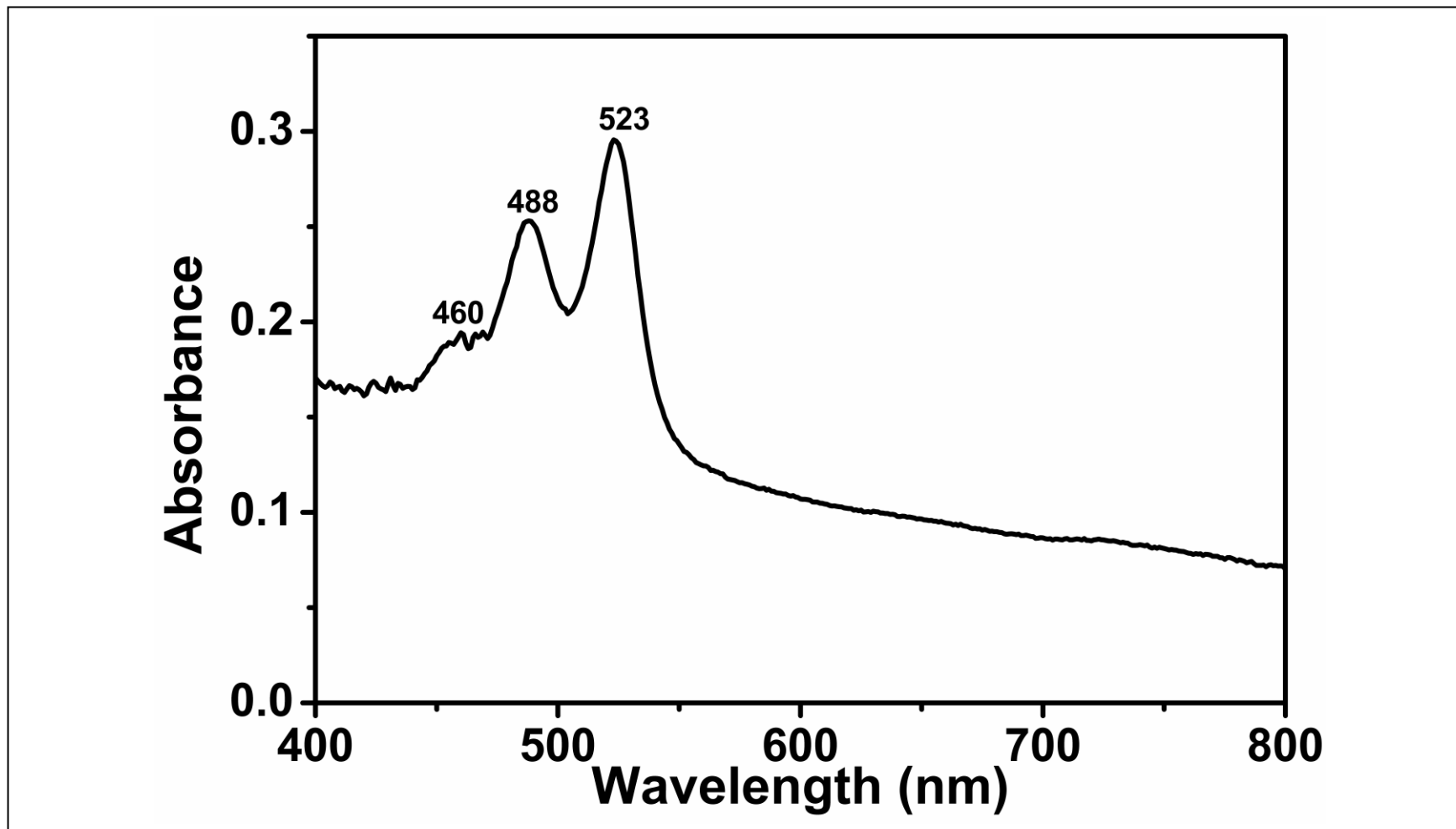


Figure 4.32: Absorption Spectrum of A4PCH in DMF

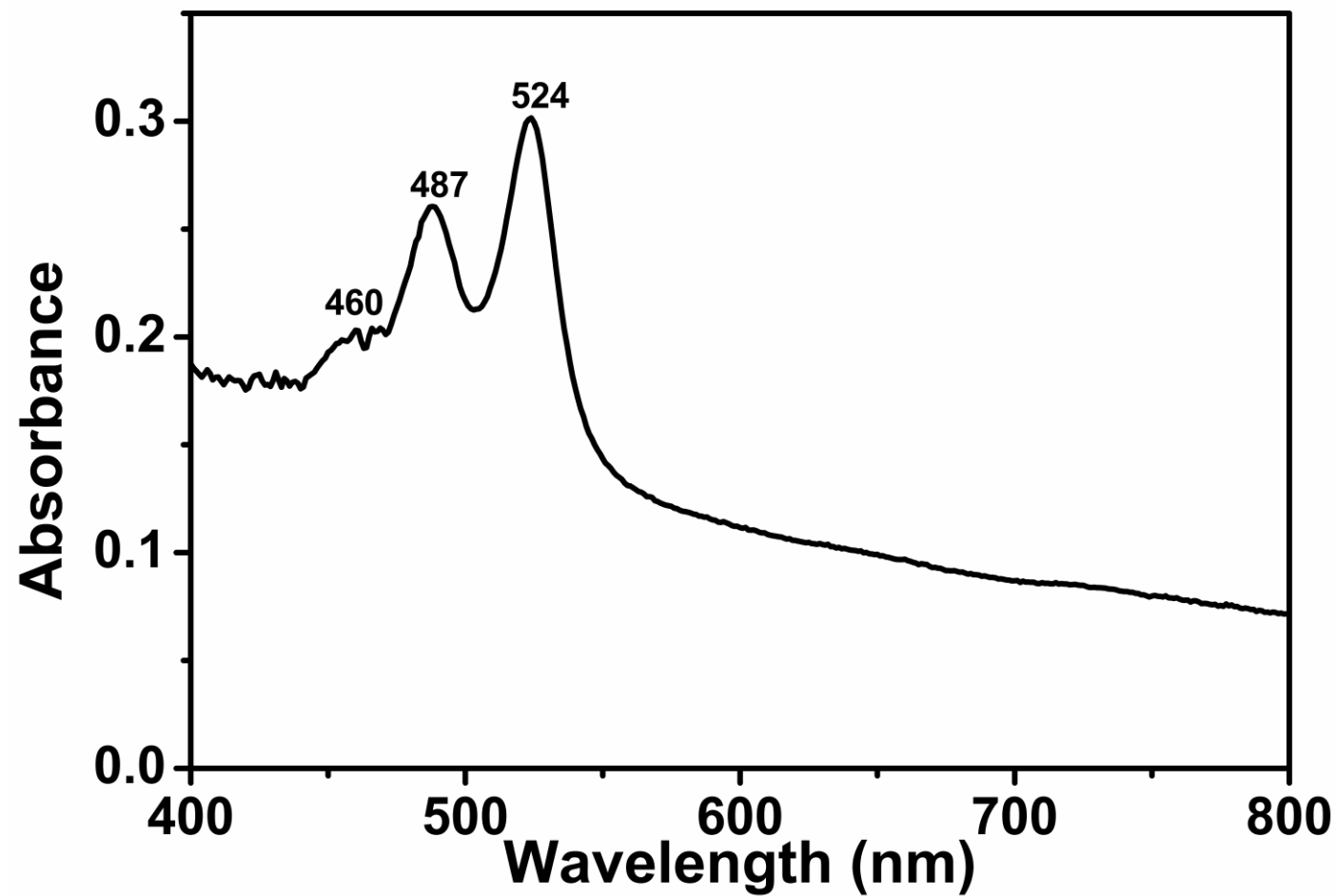


Figure 4.33: Absorption Spectrum of A4PCH in DMAc

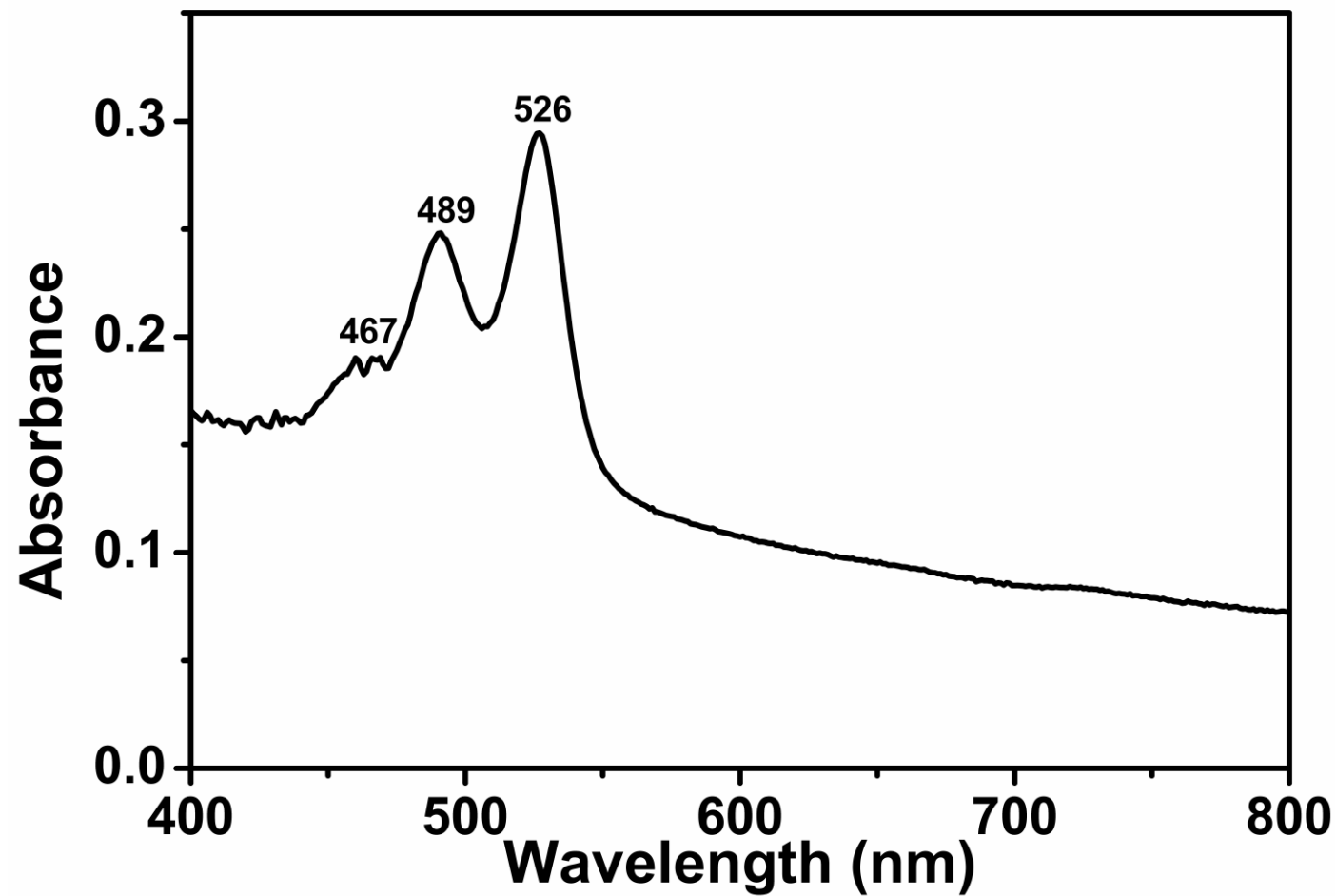


Figure 4.34: Absorbance Spectrum of A4PCH in DMSO

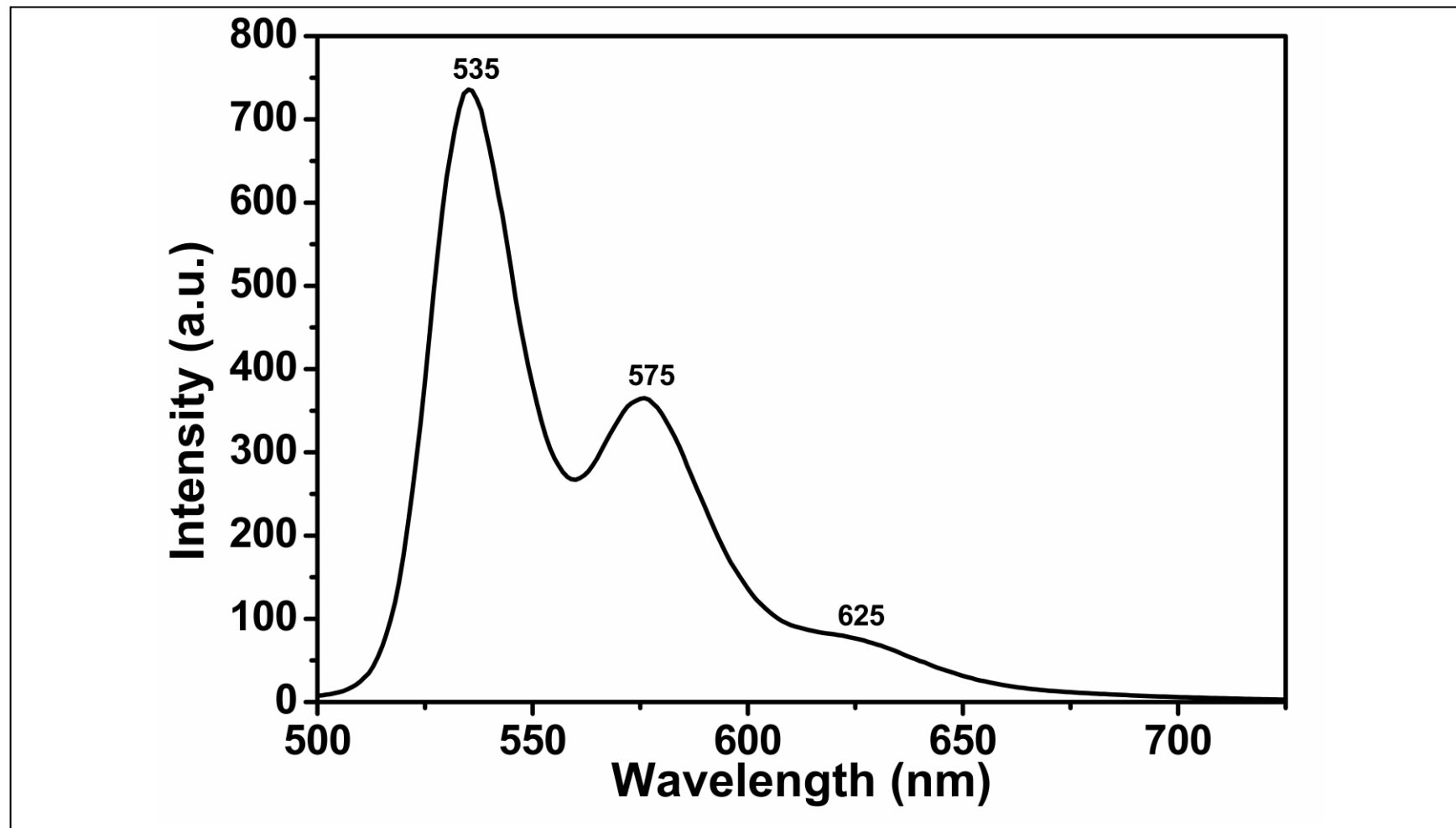


Figure 4.35: Emission Spectrum of A4PCH in DMF

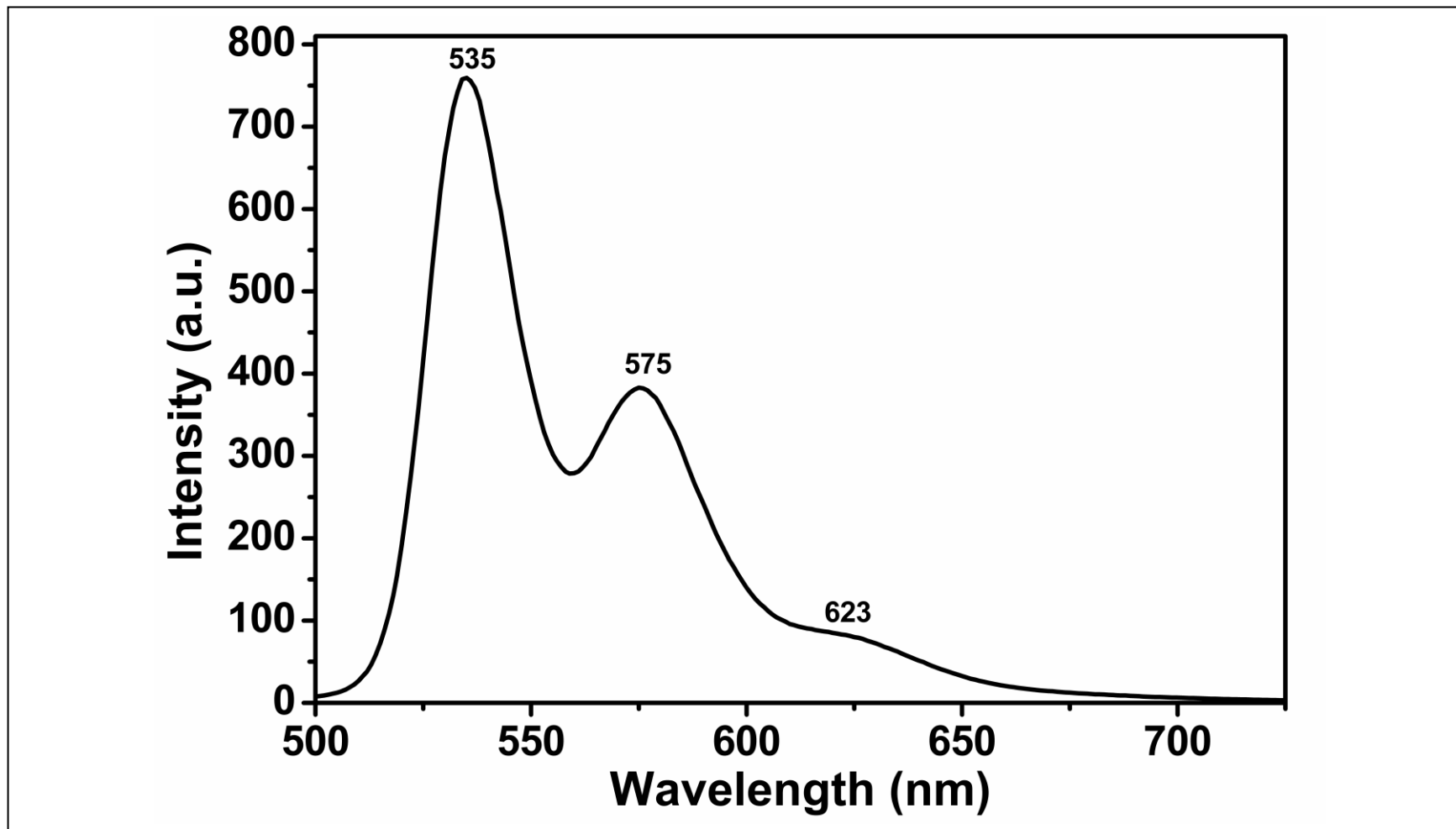


Figure 4.36: Emission Spectrum of A4PCH in DMAc



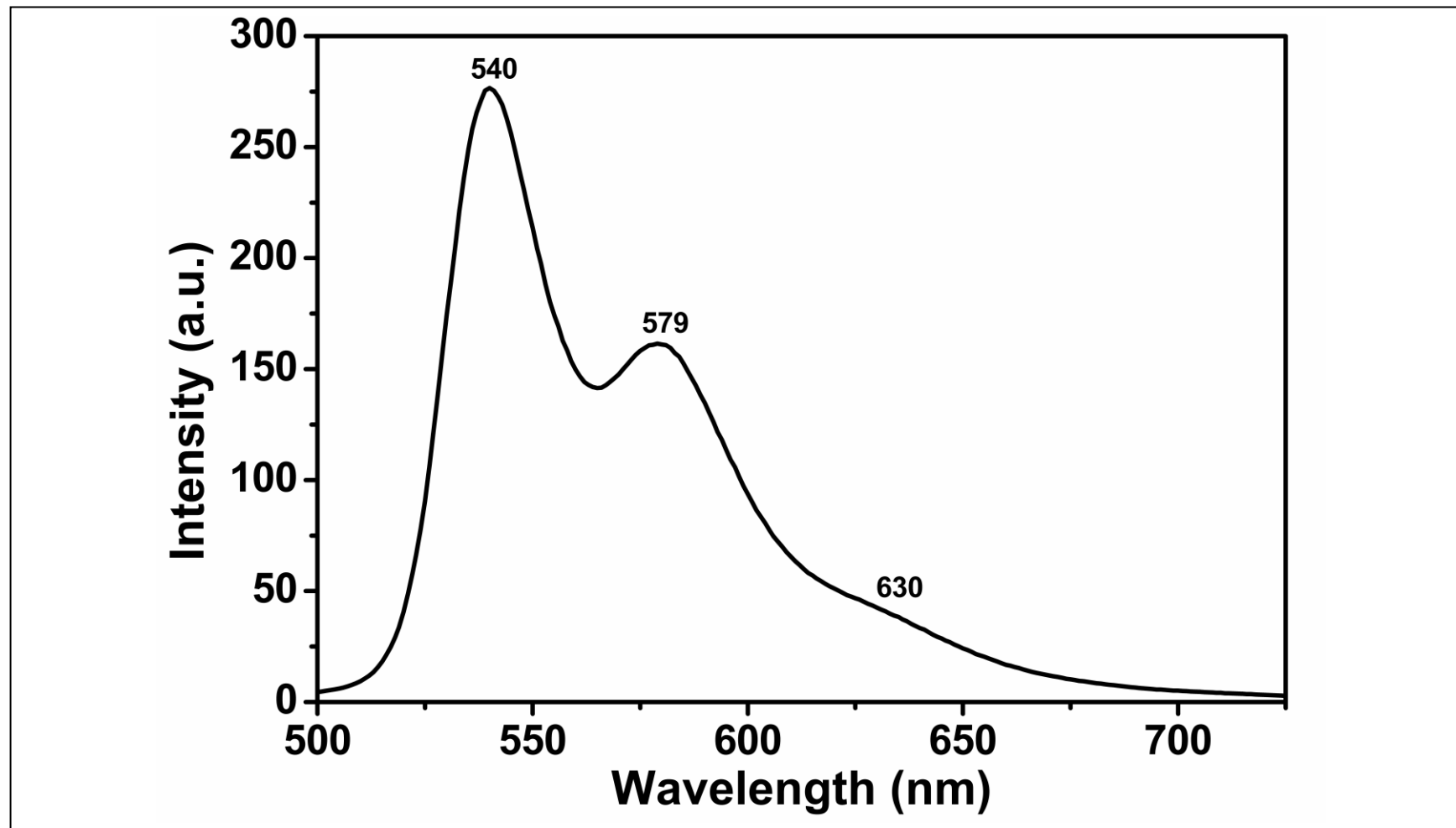


Figure 4.37: Emission Spectrum of A4PCH in DMSO

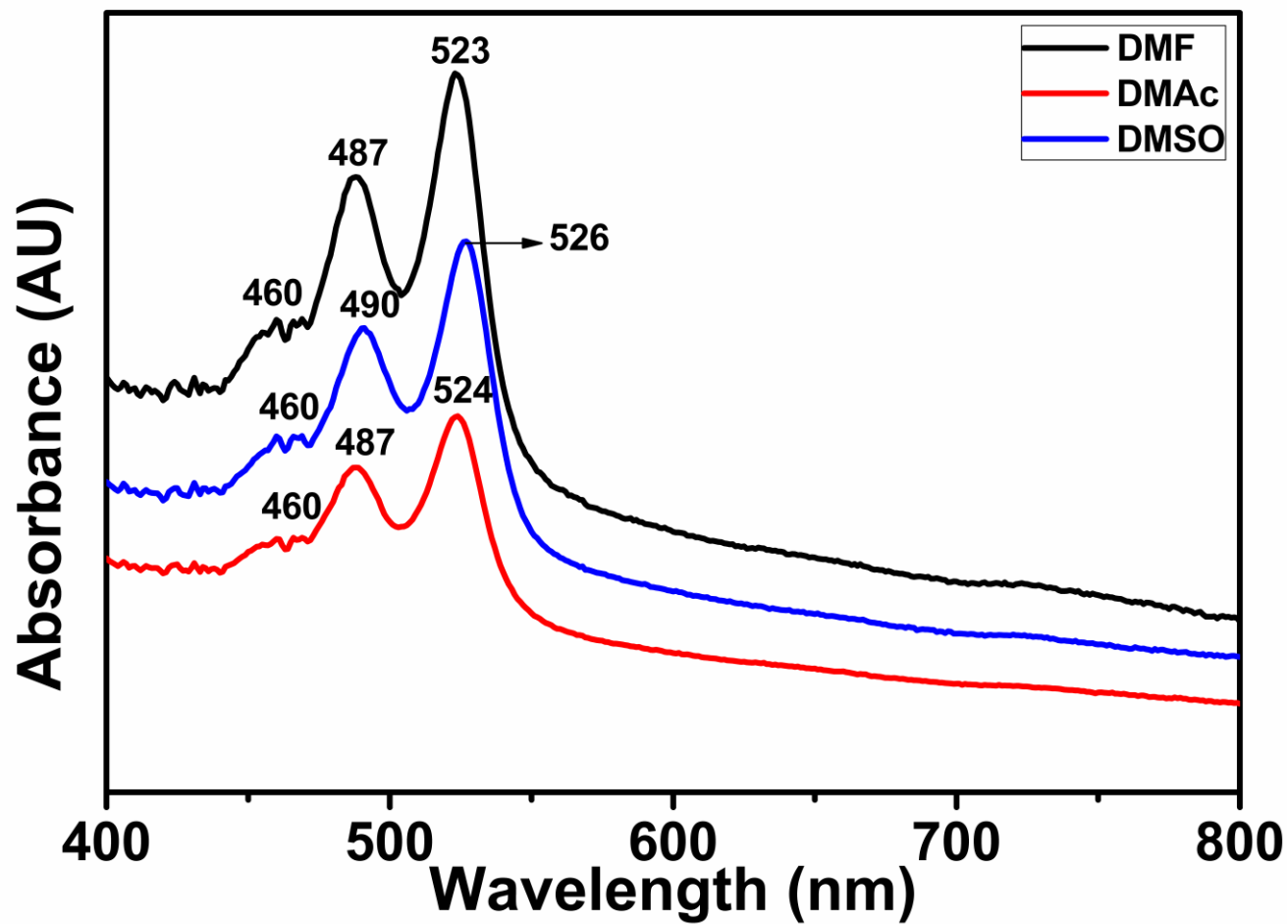


Figure 4.38: Absorption Spectra of A4PCH in DMF, DMAc and DMSO

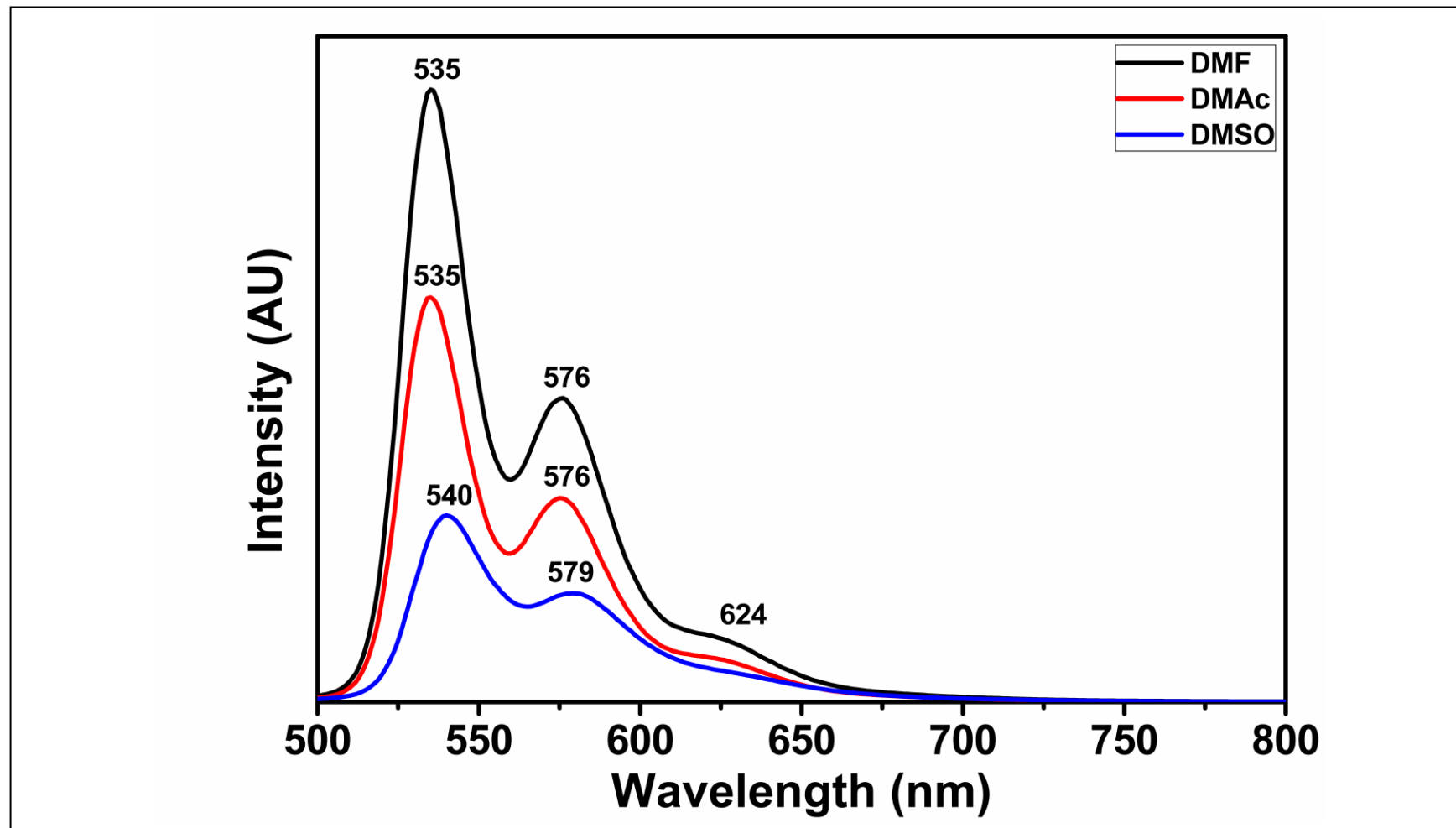


Figure 4.39: Emission Spectra of A4PCH in DMF, DMAc and DMSO

## Chapter 5

### RESULTS AND DISCUSSIONS

#### 5.1 Synthesis and Characterization

The PCH's synthetic route which is used for synthesis of new polyimides, is shown in Scheme 3.1. The synthesis of PCHs were achieved through polycondensation reaction between commercially existing Chitosan (CS) and industrial dye perylene dianhydride (PDA) under argon atmosphere. The anhydride groups of PDA were reacted with the primary amine groups of CS polymer. The synthesized products were accurately characterized by FTIR, UV-vis and emission spectrum.

#### 5.2 Solubility of PCHs

The solubility properties of PDA, CS, A1PCH, A2PCH, A3PCH and A4PCH are represented in Table 5.1 and Table 5.2. PDA is soluble in neither polar nor nonpolar organic solvents except  $\text{CHCl}_3$  and NaOH. As known, CS is only soluble in dilute acidic solutions like % 1 acetic acid. The amino groups of CS are protonated in acids below pH 6.0 and it becomes soluble.

Owing to combination of chitosan caused remarkable solubility of polyimides, the synthesized novel polyimides with chitosan have considerable solubility in most of well known organic solvents such as dimethyl sulfoxide (DMSO), N,N-dimethylformamide (DMF), dimethylacetamide (DMAc) and N-methylpyrrolidinone (NMP) at room temperature. On the other hand, solubility changes toward A1PCH to A4PCH. Significant efforts have been spent to improve solubility of polyimides by

designing their structures. The steric hindrance of perylene dye molecules could be prevented by imidization aromatic core of perylene dyes at imide position. Hence, solubility will be increased by loosening the rigid planarity.

Table 5.1: Solubility properties of PDA and CS

<b>Solubility / Color</b>		
<b>Solvent</b>	<b>PDA</b>	<b>CS</b>
<b>CHCl<sub>3</sub></b>	(+ -) / Orange	(- -) / Colorless
<b>EtAc</b>	(- -) / Colorless	(- -) / Colorless
<b>CH<sub>2</sub>Cl<sub>2</sub></b>	(- -) / Colorless	(- -) / Colorless
<b>Acetone</b>	(- -) / Colorless	(- -) / Colorless
<b>EtOH</b>	(- -) / Colorless	(- -) / Colorless
<b>MeOH</b>	(- -) / Colorless	(- -) / Colorless
<b>NMP</b>	(- -) / Colorless	(- -) / Colorless
<b>DMF</b>	(- -) / Colorless	(- -) / Colorless
<b>CH<sub>3</sub>CN</b>	(- -) / Colorless	(- -) / Colorless
<b>DMAc</b>	(- -) / Colorless	(- -) / Colorless
<b>DMSO</b>	(- -) / Colorless	(- -) / Colorless
<b>H<sub>2</sub>O</b>	(- -) / Colorless	(- -) / Colorless
<b>KOH</b>	(- -) / Colorless	(- -) / Colorless
<b>NaOH (5%)</b>	(+ +) / Green	(- -) / Colorless
<b>Acetic Acid(1%)</b>	(- -) / Colorless	(+ +) / Colorless

(+ +): soluble, (+ -): partially soluble, (- -): not soluble at room temperature

Table 5.2: Solubility test of A1PCH, A2PCH, A3PCH and A4PCH

<b>Solubility / Color</b>				
<b>Solvent</b>	<b>A1PCH</b>	<b>A2PCH</b>	<b>A3PCH</b>	<b>A4PCH</b>
<b>CHCl<sub>3</sub></b>	(+ -)* / Pale Orange	(+ -)* / Pale Orange	(+ -) / Pale Orange	(+ -) / Pale Orange
<b>EtAc</b>	_____	(+ -) / Pale Yellow	_____	_____
<b>CH<sub>2</sub>Cl<sub>2</sub></b>	(+ -) / Pale Orange	(+ -) / Pale Pink	(+ -) / Pale Orange	(+ -) / Pale Orange
<b>Acetone</b>	(+ -) / Pale Green	(+ -) / Pale Green	(+ -) / Pale Green	(+ -) / Pale Green
<b>EtOH</b>	(- -) / Colorless	(- -) / Colorless	(- -) / Colorless	(- -) / Colorless
<b>MeOH</b>	(+ -) / Colorless	(+ -) / Colorless	(+ -) / Pale Orange	(+ -) / Pale Orange
<b>NMP</b>	_____	(+ -) / Orange	_____	_____
<b>DMF</b>	(+ -) / Orange	(+ -) / Pink	(+ -) / Pink	(+ -) / Dark Pink
<b>CH<sub>3</sub>CN</b>	(+ -)* / Pale Orange	(+ -)* / Pale Orange	(+ -) / Pale Orange	(+ -) / Pale Orange
<b>DMAc</b>	(+ -) / Orange	(+ -) / Orange	(+ -) / Pink	(+ -) / Dark Pink
<b>DMSO</b>	(+ -) / Dark Orange	(+ -) / Pink	(+ -) / Pink	(+ -) / Dark Pink
<b>H<sub>2</sub>O</b>	(- -) / Colorless	(- -) / Colorless	(- -) / Colorless	(- -) / Colorless
<b>NaOH</b>	(- -) / Colorless	(+ -)* / Pale Yellow	(+ -) / Pale Yellow	(+ -) / Pale Yellow
<b>KOH</b>	(- -) / Colorless	(- -) / Colorless	(- -) / Colorless	(+ -)* / Pale Orange
<b>Acetic Acid(%1)</b>	(- -) / Colorless	(- -) / Colorless	(- -) / Colorless	(- -) / Colorless

Measured at a concentration 0.1 mg/ml in solvents. (+ +) is soluble at 25 °C, (+ -) is partially soluble at 25 °C, (+ -)\* is partially soluble on heating at 60 °C (- -): is not soluble.

### 5.3 Analysis of FTIR Spectra

Chemical structure of PDA and CS were confirmed and analyzed in terms of functional groups using IR spectroscopy. As shown in Fig. 4.2, the IR spectrum of PDA has distinctive bands at  $3118\text{ cm}^{-1}$  (aromatic C-H stretch);  $1772\text{ cm}^{-1}$  (anhydride C=O stretch);  $1594\text{ cm}^{-1}$  (conjugated C=C stretch) and  $1024\text{ cm}^{-1}$  (C-O-C stretch). Also, as given in Fig. 4.3, CS has unique peaks at  $3424\text{ cm}^{-1}$  ( $\text{NH}_2$  O-H stretch);  $2878\text{ cm}^{-1}$  (aliphatic C-H stretch);  $1657\text{ cm}^{-1}$  (Amide I, C=O stretch);  $1599\text{ cm}^{-1}$  (Amide II, N-H stretch);  $1378\text{ cm}^{-1}$  (C-N stretch);  $1155$  and  $1075\text{ cm}^{-1}$  (pyranose).

The covalent attachment of the perylene dyes to CS chains was proved by FTIR spectroscopy and it was shown from Figure 4.4 to Figure 4.7. While the new polyimides formed, some peaks retained. Besides, some of peaks lost and turn new bands. As shown in figure of PCH's infrared spectra, there are two significant characteristic change of band for perylene. First one, carbonyl stretching band around at  $1772\text{ cm}^{-1}$  had disappeared and instead of this carbonyl band, N-imide carbonyl stretching band nearly at  $1700\text{-}1650\text{ cm}^{-1}$  was formed. Second one, C-O-C stretching band around at  $1024\text{ cm}^{-1}$  had disappeared and replaced with C-N-C stretching band nearly at  $1350\text{ cm}^{-1}$ . At the same time, CS has characteristic O-H groups. So, the new polyimides conjugated chitosan have O-H stretch band nearly at  $3400\text{ cm}^{-1}$ .

## 5.4 Absorption and Fluorescence Properties

Photo-physical properties of PCHs were examined in different polar aprotic solvents such as DMSO, DMF and DMAc by UV-vis absorption and fluorescence emission. Obtained graphs for all of PCH polymers were depicted in Figure 4.8 – Figure 4.39.

The absorption peaks were shifted bathochromically in polar aprotic solvents as solvent polarity increases. The fluorescence spectra of organic dye molecules were matched with the mirror image their absorption spectra with small Stokes shifts. Fluorescence emission peaks were occurred at lower energy than the absorption peaks owing to the loss of vibrational excitation energy. So, different Stokes shifts were observed. Their absorption and emission bands, Stokes shifts and intensity ratio were shown in Table 5.3 - Table 5.6. The most important point to be considered here is to observed different absorption and emission spectrums due to different intermolecular interaction.

The excitation spectra of all of PCH polymers were measured at  $\lambda_{exc}= 485$  nm and the relative fluorescence quantum yields were designed in DMF using N,N- dodecyl-3,4,9,10-perylenebis (dicarboximide) in chloroform.  $\Phi_f$  of compounds are calculated and given in Table 4.3.



### 5.4.1 Absorption and Fluorescence Properties of A1PCH

Table 5.3: The UV-vis absorption and fluorescence maximum wavelengths of A1PCH

<b>SOLVENT</b>	<b>UV-Vis</b> <b>(<math>\lambda_{\max}</math>, nm)</b>	<b>Flu. Emis.</b> <b>(<math>\lambda_{\max}</math>, nm)</b>	<b>Stokes Shifts</b> <b>(<math>\Delta\lambda</math>, nm)</b>	<b>Intensity</b> <b>Ratio</b>
<b>DMF</b>	523, 487, 456	536, 576, 626	13	1.12
<b>DMAc</b>	522, 487, 460	534, 575, 627	12	1.14
<b>DMSO</b>	526, 490, 460	540, 580, 630	14	1.07

In the UV-vis absorption spectrum of A1PCH, 3 characteristic bands at 523 (0 $\rightarrow$ 0), 487 (0 $\rightarrow$ 1) and 456 nm (0 $\rightarrow$ 2) which are detected to the  $\pi$ - $\pi^*$  vibronic relaxation of perylene diimides core of electronic transition  $S_0\rightarrow S_1$  were observed in DMF with slightly aggregation as shown in the Figure 4.8. In the fluorescence spectra of A1PCH investigated in DMF, 2 characteristic distinct emission peaks were observed at 536 and 576 nm with a 13 nm Stokes shift, also 1 shoulder peak was seen at 626 nm as shown in Figure 4.11. ( $\lambda_{\text{exc.}}=485$  nm).

In the UV-vis absorption spectrum taken in DMAc, 3 peaks were obtained at 522, 487 and 460 nm with slightly aggregation as indicated Figure 4.9. In the fluorescence emission spectrum of A1PCH in DMAc, 2 peaks and 1 shoulder were got at 534, 575 and 627 nm as represented in Figure 4.12 with 12 nm Stokes shift.

In DMSO, the UV-vis absorption spectrum of A1PCH has 3 characteristic bands at 526, 490 and 460 nm with slightly aggregation as shown in Figure 4.10. The fluorescence spectra in DMSO, 2 peaks and 1 shoulder peak were observed at 540, 580 and 630 nm, respectively, as represented in Figure 4.13 with 14 nm Stoke shift.

The comparison of absorption and emission spectra and Stokes shift of A1PCH in DMF, DMAc and DMSO were demonstrated in Figure 4.14 and Figure 4.15.

#### 5.4.2 Absorption and Fluorescence Properties of A2PCH

Table 5.4: The UV-vis absorption and fluorescence maximum wavelengths of A2PCH

<b>SOLVENT</b>	<b>UV-Vis</b> ( $\lambda_{\max}$ , nm)	<b>Flu. Emis.</b> ( $\lambda_{\max}$ , nm)	<b>Stokes Shifts</b> ( $\Delta\lambda$ , nm)	<b>Intensity</b> <b>Ratio</b>
<b>DMF</b>	524, 488, 458	535, 575, 627	11	1.27
<b>DMAc</b>	523, 486, 457	534, 574, 626	11	1.21
<b>DMSO</b>	526, 490, 459	540, 579, 630	14	1.25

The Uv-vis absorbance spectrum of A2PCH in DMF has 3 absorption peaks at 524, 488 and 458 with weakly aggregation as given in Figure 4.16. The emission spectrum is obtained in DMF with the emission peaks at 535, 575 and 627nm. Stokes shift was found 11 nm as presented in Figure 4.19.

The UV-vis absorbance spectrum of A2PCH in DMSO has 3 distinct absorption peaks at 526, 490 and 459 with weakly aggregation as shown in Figure 4.17. In the emission spectrum, 3 peaks at 540, 579 and 630 nm were indicated with 14 nm Stokes shift in Figure 4.20.

In the UV-vis absorption spectrum of A2PCH taken in DMAc, 3 peaks were obtained at 523, 486 and 457 nm with weakly aggregation as indicated Figure 4.18. In the fluorescence emission spectrum of A2PCH in DMAc, 2 peaks and 1 shoulder were got at 534, 574 and 626 nm as represented in Figure 4.21 with 11 nm Stokes shift.

The comparison of absorption and emission spectra and Stokes shift of A2PCH in DMF, DMAc and DMSO were displayed in Figure 4.22 and Figure 4.23.

#### 5.4.3 Absorption and Fluorescence Properties of A3PCH

Table 5.5: The UV-vis absorption and fluorescence maximum wavelengths of A3PCH

<b>SOLVENT</b>	<b>UV-Vis</b> <b>(<math>\lambda_{\max}</math>, nm)</b>	<b>Flu. Emis.</b> <b>(<math>\lambda_{\max}</math>, nm)</b>	<b>Stokes Shifts</b> <b>(<math>\Delta\lambda</math>, nm)</b>	<b>Intensity</b> <b>Ratio</b>
<b>DMF</b>	523, 488, 460	534, 575, 625	11	1.12
<b>DMAc</b>	522, 486, 460	534, 575, 622	12	1.12
<b>DMSO</b>	525, 490, 460	540, 578, 623	15	1.17

The UV- vis absorption spectrum of A3PCH taken in DMF has shown 3 absorption peaks at 522, 488 and 460 nm with slightly aggregation as dedicated in Figure 4.24. The fluorescence spectrum of A3PCH in DMF showed mirror images of absorbance spectrum with small Stokes shift which is 11 nm as given in Figure 4.27 ( Emission peaks at: 534, 575 and 624 nm).

In DMAc, The absorption peaks at 522, 486 and 460 were observed with indistinctly aggregation as specified in Figure 4.25. The emission spectrum of A3PCH with 12 nm Stokes shift has 3 peaks at 534, 575 and 622 nm as defined in Figure 4.28.

In DMSO, the UV-vis absorption spectrum of A3PCH has 3 characteristic bands at 525, 490 and 460 nm with slightly aggregation as shown in Figure 4.26. The fluorescence spectra of A3PCH in DMSO, 2 peaks and 1 shoulder peak were observed at 540, 578 and 623 nm, respectively, as represented in Figure 4.29 with 15 nm Stokes shift.

The similarity of absorption and emission spectra and Stokes shift of A3PCH in DMF, DMAc and DMSO were shown in Figure 4.30 and Figure 4.31.

#### 5.4.4 Absorption and Fluorescence Properties of A4PCH

Table 5.6: The UV-vis absorption and fluorescence maximum wavelengths of A4PCH

<b>SOLVENT</b>	<b>UV-Vis</b> <b>(<math>\lambda_{\max}</math>, nm)</b>	<b>Flu. Emis.</b> <b>(<math>\lambda_{\max}</math>, nm)</b>	<b>Stokes Shifts</b> <b>(<math>\Delta\lambda</math>, nm)</b>	<b>Intensity</b> <b>Ratio</b>
<b>DMF</b>	523, 488, 460	535, 575, 625	12	1.20
<b>DMAc</b>	524, 487, 460	535, 575, 623	11	1.15
<b>DMSO</b>	526, 489, 467	540, 579, 630	14	1.16

In the UV-vis absorption spectrum of A4PCH in DMF, 3 characteristic bands at 523, 488 and 460 nm were observed with slightly aggregation as shown in the Figure 4.32. In the fluorescence spectra of A4PCH in DMF, 2 characteristic distinct emission peaks were observed at 535 and 575 nm with a 12 nm Stoke shift, also 1 shoulder peak was seen at 625 nm as shown in Figure 4.35.

In the UV-vis absorption spectrum of A4PCH taken in DMAc, 3 peaks were obtained at 524, 487 and 460 nm with slightly aggregation as indicated Figure 4.33. In the fluorescence emission spectrum of A4PCH in DMAc, 2 peaks and 1 shoulder were got at 535, 575 and 623 nm as represented in Figure 4.36 with 11 nm Stokes shift.

In DMSO, the UV-vis absorption spectrum of A4PCH has 3 characteristic bands at 526, 489 and 467 nm with slightly aggregation as shown in Figure 4.34. The fluorescence spectra in DMSO of A4PCH, 2 peaks and 1 shoulder peak were observed at 540, 579 and 630 nm as defined in Figure 4.37 with 14 nm Stoke shift.

Absorption and emission spectra and Stokes shift of A4PCH in DMF, DMAc and DMSO were demonstrated in Figure 4.38 and Figure 4.39.

On the other hand, maximum absorption wavelengths (nm), molar absorption coefficient ( $M^{-1} \cdot cm^{-1}$ ), fluorescence quantum yield ( $\lambda_{exc.}=485$  nm), half-width ( $cm^{-1}$ ), radiative lifetimes (ns), fluorescence lifetimes (ns), fluorescence rate constant ( $s^{-1}$ ), rate constant of radiation deactivation ( $s^{-1}$ ), oscillator strengths and singlet energy ( $kcal.mol^{-1}$ ) data were determined for all compounds in different solvents as shown in chapter 4 and are given in the Table 5.7, Table 5.8, Table 5.9 and Table 5.10.

Table 5.7: Optical and photochemical properties of A1PCH

<b>Solvent</b>	$\lambda_{max}$	$\epsilon_{max}$	$\Phi_f$	$\Delta\bar{\nu}_{1/2}$	$\tau_0$	$\tau_f$	$k_f$	$k_d$	$f$	$E_s$
<b>DMSO</b>	526	30900	--	1234.8	32.2	--	3.10	--	0.13	43.37
<b>DMAc</b>	522	15700	--	1136.5	53.4	--	1.87	--	0.08	54.79
<b>DMF</b>	523	55000	0.44	974.66	14.1	6.2	7.08	9.01	0.29	54.68

Table 5.8: Optical and photochemical properties of A2PCH

<b>Solvent</b>	$\lambda_{max}$	$\epsilon_{max}$	$\Phi_f$	$\Delta\bar{\nu}_{1/2}$	$\tau_0$	$\tau_f$	$k_f$	$k_d$	$f$	$E_s$
<b>DMSO</b>	526	49000	--	504.18	39.2	--	2.56	--	0.11	54.37
<b>DMAc</b>	523	29000	--	474.43	69.7	--	1.43	--	0.06	54.68
<b>DMF</b>	524	13900	0.76	440.45	157	119.32	0.64	0.2	0.03	54.58

Table 5.9: Optical and photochemical properties of A3PCH

<b>Solvent</b>	$\lambda_{\max}$	$\epsilon_{\max}$	$\Phi_f$	$\Delta\bar{\nu}_{1/2}$	$\tau_0$	$\tau_f$	$k_f$	$k_d$	$f$	$E_s$
<b>DMSO</b>	525	42700	--	997.49	21.4	--	4.42	--	0.18	54.78
<b>DMAc</b>	522	22000	--	943.89	45.9	--	2.18	--	0.09	54.79
<b>DMF</b>	523	47000	0.50	954.77	21.4	10.7	4.67	4.67	0.19	54.68

Table 5.10: Optical and photochemical properties of A4PCH

<b>Solvent</b>	$\lambda_{\max}$	$\epsilon_{\max}$	$\Phi_f$	$\Delta\bar{\nu}_{1/2}$	$\tau_0$	$\tau_f$	$k_f$	$k_d$	$f$	$E_s$
<b>DMSO</b>	526	30000	--	902.38	35.8	--	2.79	--	0.12	43.37
<b>DMAc</b>	524	30000	--	1020.48	31.4	--	3.18	--	0.13	54.58
<b>DMF</b>	523	30000	0.56	533.09	59.9	33.54	1.67	1.31	0.07	54.68

Additionally, the comparison of aggregation and fluorescence quantum yield in DMF of all products is given in Table 5.11. As shown in table, while fluorescence quantum yield was directly proportional with intensity ratio, intensity ratio was inversely proportional with aggregation. The best fluorescence process was observed at the lowest aggregation.

**Table 5.11: The comparison of aggregation and fluorescence quantum yield in DMF**

Products	Intensity Ratio	$\Phi_f$
A1PCH	1.07	0.44
A3PCH	1.12	0.50
A4PCH	1.2	0.56
A2PCH	1.27	0.76



## Chapter 6

### CONCLUSION

In conclusion, four novel comb shaped amphiphilic polymers were synthesized by polycondensation reaction of Low Molecular Weight Chitosan (LMWC) with different amounts of Perylene-3,4,9,10- tetracarboxylic dianhydride (PDA). The structure of the four fluorescent Perylene conjugated Chitosan polymers (PCH) have been characterized and the photophysical and also optical properties have been examined using FTIR, UV-vis and Fluorescence Spectroscopy.

Unlike Chitosan and PDA, each synthesized fluorescent amphiphilic polymers (A1PCH, A2PCH, A3PCH and A4PCH) have a moderately good solubility in most of well known organic solvents such as DMF, DMSO, DMAc and so on. Because of their solubility properties, products having amphiphilic features can be used as drug delivery system in the field of biotechnology.

The structure of the products for the determination of their photophysical and optical properties have a great importance. As a result of combination of hydrophobic perylene with hydrophilic Chitosan, amphiphilic polymers which have network structure have extension of  $\pi$ - $\pi$  conjugation. In general, the absorbance spectra of perylene substituted Chitosan polymers have 3 characteristic peaks with slightly aggregation in polar aprotic solvents such as DMSO, DMAc and DMF. Absorption bands were shifted bathochromically as solvent polarity increases. Also, the emission

spectra of products showed mirror image of their absorbance spectra with small Stokes shifts.

The emission spectra of all of PCH products were taken  $\lambda_{exc.} = 485$  nm. Thus, their fluorescence quantum yields were found in DMF using standart N-N'-didodecyl-3,4,9,10-perylenebis(dicarboximide) in  $CHCl_3$ .

The relationships between solubility, aggregation and fluorescence quantum yield of each synthesized PCH polymers have been investigated and consequently, it was observed the differences between the polymers due to different intermolecular interaction. While A2PCH has the highest solubility and fluorescence properties, it has the lowest aggregation.

In summary, four novel comb shaped amphiphilic perylene conjugated Chitosan polymers having fluorescent properties can be used in drug delivery system.

## REFERENCES

- [1] Kozma, E., & Catellani, M. (2013). Perylene Diimides Based Materials for Organic Solar Cell. *Dyes and Pigments*. 98, 160-179.
- [2] Ma, Y., Li, X., Wei, X., Jiang, T., Wu, J., & Ren, H. (2015). Synthesis and Properties of Amini Acid Functionalized Water-Soluble Perylene Diimides. *Korean J. Chem. Eng.* 32(7), 1427-1433.
- [3] Liav, D., Wang, K., Huang, Y., Lee, K., Lai, J., & Ha, C. (2012). Advanced Polyimide Materials: Syntheses, Physical Properties and Applications. *Progress in Polymer Science*. 37, 907-974.
- [4] Bacosca, I., Hamciuc, E., & Bruma, M. (2010). Study of Aromatic Polyimides Containing Cyano Groups. *High Performance Polymers*. 22, 703-714.
- [5] Bodapati, J., & Icil, H. (2008). Highly Soluble Perylene Diimide and Oligomeric Diimide Dyes Combining Perylene and Hexa(ethylene glycol) Units: Synthesis, Characterization, Optical and Electrochemical Properties. *Dyes and Pigments*. 79, 224-235.
- [6] Dinleyici, M. Ms. Thesis (2015). Eastern Mediterranean University.
- [7] Icil, H., Uzun, D., & Arslan, E. (2001). Synthesis and Spectroscopic Characterization of Water-Soluble Perylene Tetracarboxylic Diimide Derivatives. *Spectroscopy Letters*. 34(5), 605-614.

- [8] Açıkgöz, S., Demir, M., Yapasan, E., Kiraz, A., Unal, A., & Inci, M. (2014). Investigation of Spontaneous Emission Rate of Perylene Dye Molecules Encapsulated into Three-Dimensional Nanofibers Via FLIM Method. *Applied Physics A*. 339, 14- 8346.
- [9] Yang, S., & Zimmerman, S. (2012). Polyglycerol-Dendronized Perylenediimides as Stable, Water-Soluble Fluorophores. *Adv. Funct. Mater.* 22, 3023-3028.
- [10] Yen, M., Yang, J., & Mau, J. (2008). Antioxidant Properties of Chitosan from Crab Shells. *Carbohydrate Polymers*. 74, 840-844.
- [11]Caner, H. PhD. Thesis (2002). Eastern Mediterranean University.
- [12] Pillai, C., Paul, W., & Sharma, C. (2009). Chitin and Chitosan Polymers: Chemistry, Solubility and Fiber Formation. *Progress in Polymer Science*. 34, 641-678.
- [13] Weiping, S., Changqing, Y., Yanjing, C., Zhiguo, Z., & Xiangzheng, K. (2006). Self-Assembly of an Amphiphilic Derivative of Chitosan and Micellar Solubilization of Puerarin. *Colloids and Surfaces B: Biointerfaces*. 48, 13-16.
- [14] Li, W., Peng, H., Ning, F., Yao, L., Luo, M., Zhao, Q., Zhu, X., & Xiong, H. (2014). Amphiphilic Chitosan Derivative- Based Core-Shell Micelles: Synthesis, Characterisation and Properties for Sustained Release of Vitamin D<sub>3</sub>. *Food Chemistry*. 152, 307-315.

- [15] Liu, Y., Kong, M., Cheng, X., Wang, Q., Jiang, L., & Chen, X. (2013). Self-Assembled Nanoparticles Based on Amphiphilic Chitosan Derivative and Hyaluronic Acid for Gene Delivery. *Carbohydrate Polymers*. 94, 309-316.
- [16] Dutta, P., Tripathi, S., Mehrotra, G., & Dutta, J. (2009). Perspectives for Chitosan Based Antimicrobial Films in Food Applications. *Food Chemistry*. 114, 1173-1182.
- [17] Ntoukam, D., Jiworrawathanakul, S., Hoven, V., Luinstra, G., & Theato, P. (2015). 1,1-Disubstituted-2-Vinylcyclopropanes for The Synthesis of Amphiphilic Polymers. *European Polymer Journal*. 66, 319-327.
- [18] Shelma, R., & Sharma, C. (2011). Submicroparticles Composed of Amphiphilic Chitosan Derivative for Oral Insulin and Curcumin Release Applications. *Colloids and Surfaces B: Biointerfaces*. 88, 722-728.
- [19] Wu, Y., Zheng, Y., Yang, W., Wang, C., Hu, J., & Fu, S. (2005). Synthesis and Characterization of a Novel Amphiphilic Chitosan-Polylactide Graft Copolymer. *Carbohydrate Polymers*. 59, 165-171.
- [20] Ji, Y., Kang, W., Liu, S., Yang, R., Fan, H. (2015). The Relationship Between Rheological Rules and Cohesive Energy of Amphiphilic Polymers With Different Hydrophobic Groups. *J. Polym. Res.* 22-26.

- [21] Kang, W., Ji, Y., Xu, B., Hu, L., Meng, L., Fan, H., & Bai, B. (2014). Research on Association Between Multi-Sticker Amphiphilic Polymer and Water-Soluble  $\beta$ -Cyclodextrin Polymer. *Colloid Polymer Science*. 292, 895-903.
- [22] Dech, S., Wruk, V., Fik, C., & Tiller, J. (2012). Amphiphilic Polymer Conetworks Derived from Aqueous Solutions for Biocatalyst in Organic Solvents. *Polymer*. 53, 701-707.
- [23] Xu, B., Kang, W., Meng, L., Yang, R., Liu, S., & Zhang, L. (2013). Synthesis, Aggregation Behavior and Emulsification Characteristic of a Multi-Sticker Amphiphilic Polymer. *Journal of Macromolecular Science, Part A: Pure and Applied Chemistry*. 50, 302-309.
- [24] Yasuda, M., Kasahara, H., Kawahara, K., Ogino, H., & Ishikawa H. (2001). Synthesis of Amphiphilic Polymer Particles for Lipase Immobilization. *Macromol. Chem. Phys.* 202, 3189-3197.
- [25] Bruns, N., Hanko, M., Dech, S., Ladisch, R., Tobis, J., & Tiller, J. (2010). Amphiphilic Polymer Conetworks as Matrices for Phase Transfer Reactions. *Macromol. Symp.* 291-292, 293-301.
- [26] Korshak, V. (1982). Catalysis in Polycondensation Reactions. *Russian Chemical Reviews*. 51, 2096-2111.
- [27] Allcock, H. R., & Lampe, W. F. *Contemporary Polymer Chemistry*, Second edition (Prentice Hall, Englewood Cliffs, New Jersey, 1990), 35.

- [28] Damaceanu, M., Rusu, R., & Bruma, M. (2012). Copolyimides Containing Perylene and Hexafluoroisopropylidene Moieties. *High Performance Polymers*. 24(I), 50-57.
- [29] Rusu, R., Damaceanu, M., & Bruma, M. (2010). Aromatic Copolyimides Containing Perylene Units. *Macromol Symp*. 296, 399-406.
- [30] Refiker, H. PhD Thesis (2011). Eastern Mediterranean University.
- [31] Kus, M., Hakli, O., Zafer, C., Varlikli, C., Demic, S., Ozcelik, S., & Icli, S. (2008). Optical and Electrochemical Properties of Polyether Derivatives of Perylenediimides Adsorbed on Nanocrystalline Metal Oxide Films. *Organic Electronics*. 9, 757-766.
- [32] Asir, S., Zaanardi, C., Seeber, R., & Icil, H. (2016). A Novel Unsymmetrically Substituted Chiral Amphiphilic Perylene Diimide: Synthesis, Photophysical and Electrochemical Properties Both in Solution and Solid State. *Journal Photochemistry and Photobiology A: Chemistry*. 318, 104-113.
- [33] Singh, R., et. all. (2014). On The Role of Aggregation Effects in the Performance of Perylene-Diimide Based Solar Cells. *Organic Electronics*. 15, 1347-1361.
- [34] Material Science Product / Structure of a Bilayer Organic Photovoltaic Device. <http://www.sigmaaldrich.com/materials-science/organic-electronics/opv-tutorial>

- [35] Alishai, A., & Aider, M. (2012). Applications of Chitosan in the Sea Food Industry and Aquaculture: A Review. *Food Bioprocess Technol.* 5, 817-830.
- [36] Vakili, M. et. all. (2014). Application of Chitosan and Its Derivatives as Adsorbents for Dye Removal from Water and Wastewater: A Review. *Carbohydrate Polymers.* 113, 115-130.
- [37] Scheme of N-Deacetylation of Chitin into Chitosan through Hydrolysis by Sodium. (2016, May 13).  
<https://www.researchgate.net>
- [38] Franca, E., Freitas, L., & Lins, R. (2011). Chitosan Molecular Structure as a Function of N-Acetylation. *Wiley Periodicals, Inc. Biopolymers.* 95, 448-460.
- [39] Taghizadeh, S., & Davari, G. (2006). Preparation, Characterization and Swelling Behavior of N-Acetylated and Deacetylated Chitosans. *Carbohydrate Polymers.* 64, 9-15.
- [40] Hasipoglu, H., Yilmaz, E., Yilmaz, O., & Caner, H. (2005). Preparation and Characterization of Maleic Acid Grafted Chitosan. *International Journal of Polymer Anal. Charact.* 10, 313-327.
- [41] Thirungnanasambandham, K., Sivakumar, V., & Maran, J. (2013). Application of Chitosan as an Adsorbent to Treat Rice Mill Wastewater: Mechanism, Modelling and Optimization. *Carbohydrate Polymers.* 97, 451-457.



- [42] Yücekan, I. PhD. Thesis (2013). Eastern Mediterranean University.
- [43] Ozdal, D. Ms. Thesis (2009). Eastern Mediterranean University.
- [44] Thompson, C., J., et. all. (2008). The Effect of Polymer Architecture on the Nano Self-Assemblies Based on Novel Comb-Shaped Amphiphilic Poly(allylamine). *Colloid Polymer Science*. 286, 1511-1526.
- [45] Shiau, L. (2002). Molecular Weight Distribution of Step-Growth Comb-Branched Polymers. *Polymer*. 43, 2835-2843.
- [46] Uzun, K. (2014). Ms. Thesis. Fatih University.
- [47] Kadam, Y., Yerramilli, U., & Bahadur, A. (2009). Solubilization of Poorly Water-Soluble Drug Carbamezapine in Pluronic Micelles: Effect of Molecular Characteristics, Temperature and Added Salt on the Solubilizing Capacity. *Colloids and Surfaces B: Biointerfaces*. 72, 141-147.
- [48] Parmar, A., Yerramilli, U., & Bahadur, P. (2012). Effect of Hydrophobicity of PEO-PPO-PEO Block Copolymers on Micellization and Solubilization of a Model Drug Nimesulide. *J. Surfact. Deterg.* 15, 367-375
- [49] Zhang, Y., Huo, M., Zhou, J., & Wu, Y. (2009). Potential of Amphiphilically Modified Low Molecular Weight Chitosan as a Novel Carrier for Hydrophobic Anticancer Drug: Synthesis, Characterization, Micellization and Cytotoxicity Evaluation. *Carbohydrate Polymers*. 77, 231-238.

- [50] Yagui, C., Pessoa, A., & Tavares, L. (2005). Micellar Solubilization of Drugs. *J. Pharm. Pharmaceut Sci.* 8(2), 147-163.
- [51] Sui, W., Song, G., Chen, G., & Xu, G. (2005). Aggregate Formation and Surface Activity Property of an Amphiphilic Derivative of Chitosan. *Colloids and Surfaces A: Physicochem. Eng. Aspects.* 256, 29-33.
- [52] Ogata, Y., Makita, Y., & Okaniwa, M. (2008). Aggregation Behavior of New Cyclic Saturated Copolymers Synthesized Via Ring-Opening Metathesis Polymerization. *Polymer.* 49, 4819-4825.
- [53] Hadgiivanova, R. (2009). PhD. Thesis. Tel Aviv University.
- [54] Li, J., Garg, M., Shah, D., & Rajagopalan, R. (2010). Solubilization of Aromatic and Hydrophobic Moieties by Arginine in Aqueous Solutions. *The Journal of Chemical Physics.* 153, 054902.
- [55] Yan, M., Li, B., & Zhao, X. (2010). Determination of Critical Aggregation Concentration and Aggregation Number of Acid-Soluble Collogen from Walleye Pollock (*Theragra Chalcogramma*) Skin Using the Fluorescence Probe Pyrene. *Food Chemistry.* 122, 1333-1337.
- [56] Wang, Y. Et. all. (2015). Mesoscopic Simulation Studies on the Formation Mechanism of Drug Loaded Polymeric Micelles. *Colloids and Surfaces B: Biointerfaces.* 136, 536-544.

- [57] Kulthe, S., Choudhari, Yogesh., Inamdar, N., & Mourya, V. (2012). Polymeric Micelles: Authoritative Aspects for Drug Delivery. Designed Monomers and Polymers. 465-521.
- [58] Rapoport, N. (2007). Physical Stimuli-Responsive Polymeric Micelles for Anti-Cancer Drug Delivery. *Prog. Polym. Sci.* 32, 962-990.
- [59] Perrin, D. D., & Armarego, W. L. F. (1980). *Purification of Laboratory Chemicals*.
- [60] Valeur, B. & Berbaran- Santos, N. M. *Molecular Fluorescence Principles and Applications*. Second edition. (Wiley: VCH, 2013), 508-56.
- [61] Williams A., Winfield S. & Miller J. (1983). Relative Fluorescence Quantum Yields Using a Computer – Controlled Luminescence Spectrometer. *Analyst*. 108, 1067-1071.
- [62] Icli, S., Icil. H.(1996). A Thermal and Photostable Reference Probe for Qf Measurements: Chloroform Soluble Perylene-3,4,9,10- tetracarboxylic acid-bis- N-N'-dodecyl dimide. *Spectroscopy Letters*.29, 1253-1257.
- [63] Turro, N. J. (1965). *Molecular photochemistry*, Benjamin, London, 44-64.

## **APPENDIX**

## **Appendix A: Curriculum Vitae**

### **Personel Information**

Name	Selin
Surname	Temürlü
Adress	Leventler Öğrenci Yurdu Famagusta- TRNC Mersin 10 Turkey
Phone	Office: +90 0392 630 40 15 Mobile: 0533 834 81 52
e- mail	selintemurlu@gmail.com
Date of Birth	07/06/1989
Citizenship	T. C.
Marital Single	Single
Driver's license	Class B

### **Education**

1999- 2003	Şile 75. Yıl İlkokulu Şile-Istanbul/ Turkey
2003- 2007	Beykoz Fevzi Çakmak Super Lisesi, Istanbul/ Turkey
2008- 2013	Balıkesir University Faculty of Education Department of Secondary School Chemistry Education Balıkesir / Turkey
2014 – present	Eastern Mediterranean University Faculty of Arts & Science Department of Chemistry / Organic Chemistry(Ms)

## **Work Experience**

2010- 2011	Atakule Dershanesi /Chemistry Teacher
2012- 2013	Rahmi Kula Anadolu Lisesi Stajyer Chemistry Teacher
2012- 2013	Fatma Emin Kutvar Anadolu Lisesi Stajyer Chemistry Teacher
2013- 2014	Bahçeşehir Fen ve Teknoloji Lisesi Stajyer Chemistry Teacher
2015- present	Eastern Mediterranean University Department of Education (Research Assistant)

## **Skills**

Language	Turkish, English
Computer	Microsoft Applications